Università degli Studi di Cagliari

PhD DEGREE

Earth and Environmental Sciences and Technologies

32nd cycle

TITLE OF THE PhD THESIS

Study of innovative materials for the removal of high concentrations of fluoride from water for drinking and domestic use

Disciplinary Scientific Sector

Environmental Mineralogy GEO/09

PhD Student	Alfredo Idini
Coordinator of the PhD Programme	Prof. Giorgio Ghiglieri
Supervisor	Prof. Franco Frau
Co-supervisor	Dr. Elisabetta Dore
Co-supervisor	M.Eng. Marco Trevisan
Co-supervisor	Dr. Revocatus Machunda

Final exam. Academic Year 2018 – 2019

Thesis defence: June - July 2020 Session

Table of content

Defluoridation of water through the transformation of octacalcium phosphate into fluorapatite paper.

Published 8 August 2019 by Heliyon - Elsevier Ltd

Preface

The title of the PhD thesis here presented is "Study of innovative materials for the removal of high concentrations of fluoride from water for drinking and domestic use", and the main goal of the research is to find an innovative defluoridation method that can be applied at household scale in the rural areas of the East African Rift Valley, where the endemic fluorosis is a health emergency.

This PhD project was carried out in the frame of the Italian National Program PON R&I 2014-2020 "Innovative doctorates with industrial characterization". The activity period of the PhD project was subdivided in 23 months at the Department of Chemical and Geological Sciences of the University of Cagliari (tutor Prof. Franco Frau, co-tutor PhD Elisabetta Dore), in 6 months at the industrial partner Hydro Technical Engineering (HTE S.r.l., Peschiera del Garda, VR, Italy; co-tutor MSc Marco Trevisan) and in 7 months at the foreign partner Nelson Mandela African Institution of Science and Technology (NM-AIST, Arusha, Tanzania; co-tutor PhD Revocatus Machunda).

The PhD project has been developed parallel to the Horizon2020 FLOWERED Project (coordinator Prof. Giorgio Ghiglieri, University of Cagliari). The FLOWERED objective was to contribute to the development of a sustainable water management system in areas affected by fluoride contamination of water, soils and food in the East African Rift Valley countries (Ethiopia, Kenya, Tanzania), with the aim of improving the living standards (environmental, health and food security) of rural populations (www.floweredproject.org).

The thesis here presented is based on scientific articles published on or submitted to peer-reviewed journals, and it is composed of 3 chapters. After a general introduction on the fluoride contamination of groundwater, the first chapter consists of a published paper that describes the innovative use of octacalcium phosphate in removing dissolved fluoride from aqueous solutions. In the second chapter, a submitted paper presents some mineralogical and geochemical features of the octacalcium phosphate connected to its efficiency in fluoride uptake. The third chapter consists of another published paper that presents the application of the octacalcium phosphate with an innovative defluoridator device in the rural areas of Tanzania. Finally, the thesis ends with the conclusions.

Abstract

Natural fluoride contamination of drinking water is a serious issue that affects several countries of the world. The consumption of water with fluoride concentration higher than 1.5 mg/L (WHO recommended limit) is recognized to cause serious diseases, and fluoride removal from natural contaminated waters is a health priority for more than 200 million people worldwide. The octacalcium phosphate (OCP), a mineralogical precursor of bio-apatite, is here tested as a fluoride remover. Fluoride removal experiments are performed in batch-mode using different initial concentrations of fluoride (from 40 to 140 mg/L) and reaction times. Most of fluoride is removed within the first two hours of all experiments, and the drinkable limit of 1.5 mg/L is reached within a minimum of 3 hours for an initial fluoride concentration of 40 mg/L. The experimental fluoride removal capacity of OCP is 25.7 mg/g, and 4 g of OCP can effectively treat 1 L of water with fluoride concentration up to 50 times higher than the drinking limit of 1.5 mg/L. XRD and chemical characterization of the solid phases, before and after the removal experiments, indicate that OCP transforms into fluorapatite (FAP) uptaking fluoride from solution. The property of OCP to be the crystalline precursor of apatite has been also investigated using equal molar amounts of fluoride, chloride, hydroxyl and carbonate anions dissolved in aqueous solution, in order to asses if and how the anionic competition can influence the formation of the different apatite end-members. The investigation, conducted through XRD, SEM and ICP-OES analyses, shows that fluoride is the main anion removed from solution during the OCP transformation, and consequently fluorapatite is the main resulting apatitic phase, followed by hydroxyapatite.

With the aim to perform the field trial, a new device based on the application of OCP has been developed. The prototype (FLOWERED Defluoridator Device [FDD]) essentially is composed of a 20-L tank and a recirculating pump that guarantees the interaction between water and OCP. The device is powered by a car battery for a fixed pumping working time using a fixed amount of OCP for every defluoridation cycle. The results of tests performed in the rural areas of Tanzania show that a standardized use of the prototype can lower the dissolved fluoride from an initial concentration of 21 mg/L to below the World Health Organization (WHO) drinkable limit of 1.5 mg/L in 2 h without secondary negative effects on water quality. The approximate cost of this device is around US$220, whereas that of OCP is about $0.03/L of treated water. As with any device, acceptance requires a behavioural change on behalf of rural communities that needed to be investigated. To this end, we piloted a survey to explore how psychological and socioeconomic factors influence the consumption of fluoride-free water. Results show that the adoption of FDD and OCP is more appealing to members of the rural communities who are willing to pay more and have a high consumption of water. Moreover, we suggest that given the low level of knowledge about fluorosis diseases, the government should introduce educational programs to make rural communities aware of the negative health consequences.

Introduction

Fluorine (F) is the ninth element in the periodic table of elements and its atomic weight is 18.998 u, it is the lightest halogen and the most electronegative element of the periodic table. Fluorine is the 13th most abundant element and constitutes about 0.06–0.09% in the earth crust, it is present in the ionic form as fluoride (F^-) both in solid and liquid phases and can occur in a large variety of natural environments [1].

Fluorine is an essential element for life in low quantity, but excessive intake can cause several adverse effects on human health [2]. Because of that, the European Food Safety Authority (EFSA) has established a Tolerable Upper Intake Level (UL) of F^- at 0.1 mg/kg body weight per day, or 1.5 mg/day and 2.5 mg/day for children aged 1-3 and 4-8 years, respectively [3]. The UL for older children and adults was set at 0.12 mg/kg body weight per day, or 5 mg/day and 7 mg/day for children and adolescents aged 9-14 and 15 years and older, respectively [3]. The UL proposed by US Institution of Medicine (IOM) recommends 10 mg per day for adults and children 9 years older, while for younger children the UL values decrease to 2.2, 1.3, 0.9 and 0.7 mg depending on the age [4]. The adverse effects on human health caused by excessive F^- intake has been investigated from 1944 [5]. In the last decade several clinics and epidemiologic studies have described and clarified the different toxic effects. Among them, the most well-known pathologies are the dental and skeletal fluorosis. In the fluorosis pathologies the F^- replaces the hydroxyl ion (OH^-) in the apatitic mineral structure of bones and teeth, and this leads to physical damage of teeth, and deformity and fragility effects on the bones [6]. Recently, the adverse effect of F^- toxicity affecting the neurological and cognitive functions have been investigated by some authors [7], and the effect on children's intelligence has been also documented [8], even though more evidence on the brain damage effect is requested by the scientific community [7]. Others adverse effects that can be mentioned concern the gastrointestinal tract, renal and hepatic disorder and the augmented carcinogenic risk [9].

One of the most important dietary sources of F^- is from water, and because of F^- toxicity, the World Health Organization (WHO) recommends a drinkable limit at 1.5 mg F^- per litre [10]. The relationship of high concentration of F^- in groundwater and endemic fluorosis has been reported in several areas worldwide, in which the water-rock interaction is the common geogenic source of F^- in groundwater. After several types of research carried out in the field of geology, geochemistry and hydrology, five "fluoride-belts" have been globally recognized [11] across on any populated continent. Interestingly, the occurrence of F^- in groundwater is often related to volcanic rocks [12] where the resulting water-rock interaction often generates a sodium-bicarbonate water composition. As a consequence, the hydrochemical sodium-bicarbonate *facies* is a common global feature in most of the areas where the fluorosis is endemic [13].

The review papers about the geogenic contamination of F$^-$ show that over 200 million people in 35 countries are exposed to excessive intake of F$^-$ from drinking water, and thus are vulnerable to fluorosis and related pathologies, especially, but not only, in some parts of China, India, Pakistan, Sri Lanka, Thailand, Mexico, Ethiopia, Kenya and Tanzania where people, both in rural and metropolitan areas, do not have access to fluoride-free water [14,15].

An attempt to estimate the global burden of diseases due to fluoride excess in drinking water, published by Fewtrell et alii (2006) [16], indicates that at least 23.5 and 10.8 million people are affected by dental and skeletal fluorosis, respectively. The data may be underestimated especially in the rural areas of the underdeveloped and developing countries [16].

In order to avoid the risk of fluorosis, and their related pathologies, the removal of F$^-$ from groundwater is one of the key points. As well, the removal of F$^-$ from groundwater (i.e. defluoridation of groundwater) meets the Sustainable Development Goal n.6: "*Ensure availability and sustainable management of water and sanitation for all*" established by United Nations in the 2030 Agenda for Sustainable Development [17].

In recent decades, the scientific community has made a great effort with the purpose to fight the diffusion of fluorosis, and it is worth mentioning the 1100 papers on the topic of "water defluoridation", of which 400 in the last 4 years (data updated to 02/11/2018).

On a global scale, the most common defluoridation methods for household application are based on the use of hydroxyapatite (HAp) and activated alumina (AA) [18]. The HAp is produced trough a well-known synthesis method charring the bones of different mammals, e.g. cattle bones, to obtain the so-called bone char (BC). A deepened discussion on the use of AA, HAp and BC is contained in Chapter 3 of the dissertation here presented.

A general literature overview of the defluoridation methods can be useful to understand which characteristics should be taken into account for the water treatment in a rural context.

In agreement with the most recent review, an innovative defluoridation method targeted for the rural areas of the developing countries, in order to be feasible and reliable, should be [19,20]:

i) *Effective on F$^-$ removal using natural groundwater*
ii) *Free of collateral effects*
iii) *Affordable and cost-effective*
iv) *Easy to use directly by people at home.*

We used the mentioned above four criteria as lenses for a rational reading of the literature on defluoridation. Among the plethora of defluoridation methods, the most used ones can be summarized as follows [9,20,19,21,22,23,24,25,26,27,28,29,30].

Coagulation-Precipitation

In the coagulation-precipitation methods, the addition of aluminium (Al) sulphate or calcium (Ca) salts is used to bind the dissolved F^- into solid phases, e.g. $Al(OH)_{3-x}F_x$ or CaF_2. In this methods, there is an effective reduction of F^- in solution, the limitations reside in the correct dosage of the chemicals depending on the amount of F^- that must be removed. Moreover, as a consequence of the treatment through Al-salt, an excessive concentration of sulphate and aluminium can be released into the water. On the other hand, the use of Ca-salts can reduce the F^- concentration until 8 mg/L, through the precipitation of CaF_2. For these reasons, coagulation-precipitation using Ca and Al salts fails at the criterion "*Effective on F^- removal using natural groundwater*" and *"Free of collateral effects"*.

Another precipitation method involves the addition to Ca-salt and phosphoric compound to form fluorapatite $Ca_5(PO_4)_3OH$ [18]. This method has been applied at pilot scale in a small community and in various schools in Tanzania and Kenya producing excellent results according to the first 3 criteria, but the operation requires centralized management with a trained worker, because of that the method fails the criterion "*Easy to use directly by people at home*".

Reverse Osmosis (RO)

In the RO process the hydraulic pressure of water is used to force the water through a semi-permeable membrane, leaving the F^- and other ions in the resulting brine. The RO effectiveness on defluoridation allows to have drinkable water regardless of the F^- concentration in the untreated starting water. However, the management of the brine, the power consumption of the pump and the cost of the membrane fail the criteria *"Affordable and cost-effective"* and "*Easy to use directly by people at home*".

Nano-Filtration (NF)

The NF process is similar to RO, but it uses a different membrane that requires a less pressure of water. The results of defluoridation treatment of the pilot plant installed in Tanzania are good [31], but the capital cost and maintenance appear not to meet the criterion *"Affordable and cost-effective"*. The same problem in terms of the capital cost involves the electro-dialysis and electro-coagulation methods [9].

Adsorption

Adsorption is a microscale surface phenomenon where atoms, ions or molecules (adsorbate) adhere to the surface of a phase (adsorbent). Some authors include in the F^- adsorption process also all the physical, chemical and ion-exchange processes [32], but we prefer to maintain the differentiation among these processes.

The number of adsorbents (sensu latu) tested successfully in laboratory experiments for the removal of dissolved F^- is vast [28]: approximately more than 600 different materials (e.g. synthetic phases containing Al, Mg, Fe, REE, Zr, Ti, Ca, P, etc..; natural minerals and soils such as bauxite, kaolinite, red soils, chalk, calcite, gypsum, struvite, quartz, etc..; biomaterials such as eggshells, bird feathers, rice husk, coffee husk, natural sugarcane bagasse) [33], and usually the data reported show a really encouraging F^- removal capacity, cost-effectiveness, easy availability and inexpensive procedure for regeneration. However, in many cases the technology transfer of these adsorbents is lacking.

It is worth mentioning the study of Lunge et alii [34], where lanthanum-treated chitosan granules were used successfully at household scale in some Indian rural communities. In that case, a complete technology transfer has been achieved, bringing the experimental results to a real application of the method. Unfortunately, the cost of the adsorbent is not reported.

In conclusion, despite the large number of promising results of the researches about the remediation of F^- contaminated groundwater, the challenge is still open. As evidence of that, during the World Water Challenge organized in the frame of Korean International Water Week 2018 (www.kiww.org), the environmental and health problem of water contamination by F^- has been selected as one of the most harmful global water issues that need to be solved. As a matter of fact, in 2019 the WHO claimed that "*inadequate or excess of fluoride is a global major public health concern*" [35].

The reason behind the gap between scientific research and the actual unsolved problem of F^- contamination of groundwater is unclear. It is reasonable that a multidisciplinary approach including engineering, economic, social and educational researches could disentangle this issue. Because of that, part of Chapter 3 of the dissertation is dedicated to the socio-economic analysis of the problem of F^- contaminated groundwater and of the solution proposed by us in some rural contexts of Tanzania.

References

1. Singh, G. *et al.* Fluoride distribution and contamination in the water, soil and plants continuum and its remedial technologies, an Indian perspective– a review. *Environ. Pollut.* **239**, 95–108 (2018).
2. World Health Organization (WHO). Guidelines for drinking-water quality. *WHO Chron.* **38**, 564 (2008).
3. Panel, E. & Nda, A. Scientific Opinion on Dietary Reference Values for fluoride. *EFSA J.* **11**, 1–46 (2013).
4. Institute of Medicine, U.S. National Academy of Science. *Dietary DRI Reference Intakes*. (2006). doi:10.17226/11537
5. Grech, P. & Latham, M. C. Fluorosis in the Northern Region of Tanganyika. *Trans. R. Soc. Trop. Med. Hyg.* **58**, 566–574 (1964).
6. Patil, M. M., Lakhkar, B. B. & Patil, S. S. Curse of Fluorosis. **85**, 375–383 (2018).
7. Agalakova, N. I. & Nadei, O. V. Inorganic fluoride and functions of brain. *Crit. Rev. Toxicol.* **50**, 28–46 (2020).
8. Xiang, Q. *et al.* Effect of fluoride in drinking water on children’s intelligence. *Fluoride* **36**, 84–94 (2003).
9. Kabir, H., Gupta, A. K. & Tripathy, S. Fluoride and human health: Systematic appraisal of sources, exposures, metabolism, and toxicity. *Crit. Rev. Environ. Sci. Technol.* **50**, 1116–1193 (2020).
10. Gorchev, H. G. & Ozolins, G. *WHO guidelines for drinking-water quality. WHO chronicle* **38**, (2011).
11. Chowdhury, A., Adak, M. K., Mukherjee, A., Dhak, P. & Khatun, J. Review papers A critical review on geochemical and geological aspects of fluoride belts, fluorosis and natural materials and other sources for alternatives to fluoride exposure. *J. Hydrol.* **574**, 333–359 (2019).
12. D’Alessandro, W. Human fluorosis related to volcanic activity: A review. *WIT Trans. Biomed. Heal.* **10**, 21–30 (2006).
13. Ali, S., Thakur, S. K., Sarkar, A. & Shekhar, S. Worldwide contamination of water by fluoride. *Environ. Chem. Lett.* **14**, 291–315 (2016).
14. Vithanage, M. & Bhattacharya, P. Fluoride in the environment: sources, distribution and defluoridation. *Environ. Chem. Lett.* **13**, 131–147 (2015).
15. Ayoob, S. & Gupta, A. K. Fluoride in Drinking Water : A Review on the Status and Stress Effects Fluoride in Drinking Water : A Review. *Crit. Rev. Environ. Sci. Technol.* **36**, 433–487 (2006).
16. Fewtrell, L., Smith, S., Kay, D. & Bartram, J. An attempt to estimate the global burden of disease due to fluoride in drinking water. *J. Water Health* **4**, 533–542 (2006).

17. 2030 Agenda for sustainable development. (https://sustainabledevelopment.un.org/)

18. Fawell J, Bailey K, Chilton J, Dahi E, Fewtrell L, Magara Y. 2006. Fluoride in drinking-water. Geneva (CH): World Health Organization. 144 p. https://apps.who.int/iris/handle/10665/43514

19. Meenakshi & Maheshwari, R. C. Fluoride in drinking water and its removal. *J. Hazard. Mater.* **137**, 456–463 (2006).

20. Yadav, K. K., Gupta, N., Kumar, V., Khan, S. A. & Kumar, A. A review of emerging adsorbents and current demand for defluoridation of water: Bright future in water sustainability. *Environ. Int.* **111**, 80–108 (2018).

21. Suneetha, M., Syama Sundar, B. & Ravindhranath, K. Studies on defluoridation techniques: A critical review. *Int. J. ChemTech Res.* **8**, 295–309 (2015).

22. Kumar, P. S. *et al.* Treatment of fluoride-contaminated water. A review. *Environ. Chem. Lett.* **17**, 1707–1726 (2019).

23. Mohapatra, M., Anand, S., Mishra, B. K., Giles, D. E. & Singh, P. Review of fluoride removal from drinking water. *J. Environ. Manage.* **91**, 67–77 (2009).

24. Sakhare, N. *et al.* Defluoridation of water using calcium aluminate material. *Chem. Eng. J.* **203**, 406–414 (2012).

25. Ayoob, S., Gupta, A. K. & Bhat, V. T. A conceptual overview on sustainable technologies for the defluoridation of drinking water. *Critical Reviews in Environmental Science and Technology* **38**, (2008).

26. Fan, X., Parker, D. J. & Smith, M. D. Adsorption kinetics of fluoride on low cost materials. *Water Res.* **37**, 4929–4937 (2003).

27. Rojas, R. Layered double hydroxides applications as sorbents for environmental remediation. *Hydroxides: Synthesis, Types and Applications* (2012)

28. Bhatnagar, A., Kumar, E. & Sillanpää, M. Fluoride removal from water by adsorption-A review. *Chem. Eng. J.* **171**, 811–840 (2011).

29. Fantin, A. C. An evaluation of defluoridation technologies in the context of decision-making strategies. (2009). *Theses and dissertations*. Paper 1024

30. Barathi, M., Kumar, A. S. K. & Rajesh, N. Impact of fluoride in potable water – An outlook on the existing defluoridation strategies and the road ahead. *Coord. Chem. Rev.* **387**, 121–128 (2019).

31. Bouhadjar, S. I. *et al.* Solar powered nanofiltration for drinking water production from fluoride-containing groundwater – A pilot study towards developing a sustainable and low-cost treatment plant. *J. Environ. Manage.* **231**, 1263–1269 (2019).

32. Loganathan, P., Vigneswaran, S., Kandasamy, J. & Naidu, R. Defluoridation of drinking water using adsorption processes. *J. Hazard. Mater.* **248**–**249**, 1–19 (2013).

33. Mukherjee, S. & Halder, G. A review on the sorptive elimination of fluoride from

contaminated wastewater. *J. Environ. Chem. Eng.* **6**, 1257–1270 (2018).

34. Lunge, S., Biniwale, R., Labhsetwar, N. & Rayalu, S. S. User perception study for performance evaluation of domestic defluoridation techniques for its application in rural areas. *J. Hazard. Mater.* **191**, 325–332 (2011).

35. WHO. Inadequate or Excess Flouride: a major public health concern. https://apps.who.int/iris/bitstream/handle/10665/329484/WHO-CED-PHE-EPE-19.4.5-eng.pdf?ua=1

CHAPTER I

Defluoridation of water through the transformation of octacalcium phosphate into fluorapatite

Alfredo Idini, Elisabetta Dore, Dario Fancello, Franco Frau *

Department of Chemical and Geological Sciences, University of Cagliari, 09042, Monserrato (CA), Italy

Published 8 August 2019

by Heliyon - Elsevier Ltd

Heliyon 5 (2019) e02288

Contents lists available at ScienceDirect

Heliyon

journal homepage: www.heliyon.com

Defluoridation of water through the transformation of octacalcium phosphate into fluorapatite

Alfredo Idini, Elisabetta Dore, Dario Fancello, Franco Frau [*]

Department of Chemical and Geological Sciences, University of Cagliari, 09042, Monserrato (CA), Italy

ARTICLE INFO

Keywords:
Materials science
Materials synthesis
Environmental science
Environmental geochemistry
Environmental pollution
Water pollution
Water quality
Earth sciences
Water defluoridation method
OCP synthesis
OCP-FAP transformation
Dissolved fluoride removal

ABSTRACT

The consumption of water with fluoride concentration higher than 1.5 mg/L (WHO recommended limit) is recognized to cause serious diseases, and fluoride removal from natural contaminated waters is a health priority for more than 260 million people worldwide. The octacalcium phosphate (OCP), a mineralogical precursor of bio-apatite, is here tested as a fluoride remover. A new two-step method for the synthesis of OCP is proposed: 1) synthesis of brushite from calcium carbonate and phosphoric acid; 2) subsequent hydrolysis of brushite. Fluoride removal experiments are performed in batch-mode using different initial concentrations of fluoride (from 40 to 140 mg/L) and reaction times. Most of fluoride is removed within the first 2 h of all experiments, and the drinkable limit of 1.5 mg/L is reached within a minimum of 3 h for an initial fluoride concentration of 40 mg/L. The experimental fluoride removal capacity of OCP is 25.7 mg/g, and 4 g of OCP can effectively treat 1 L of water with fluoride concentration up to 50 times higher than the drinking limit of 1.5 mg/L. XRD and chemical characterization of the solid phases, before and after the removal experiments, indicate that OCP transforms into fluorapatite (FAP) uptaking fluoride from solution.

1. Introduction

Fluorine is an essential micronutrient for human health but the World Health Organization (WHO) recommends a maximum concentration of fluoride (F^-) in drinking water equal to 1.5 mg/L (WHO, 2011) because higher F^- concentrations are known to cause many diseases, such as skeletal fluorosis and neurological issues (Ozsvath, 2009; Tewari and Dubey, 2009). Geogenic contamination of F^- in groundwater is one of the major problems of the water crisis of the 21st century, affecting more than 260 million people over 24 countries worldwide. For instance, high concentrations of F^- in in sodium-bicarbonate groundwaters with average pH in the range of 8.0–8.5 have been reported in several rural areas along the East African Rift Valley (Ethiopia, Kenya, Tanzania) (Tekle-Haimanot et al., 2006; Ghiglieri et al., 2012; Olaka et al., 2016) and in different areas of Pakistan, India and China (Farooqi et al., 2007; Gao et al., 2007; Singh et al., 2018). This is the reason why the online databases Scopus and Web of Science together report more than 1100 papers on the topic “water defluoridation”, of which 400 in the last 4 years (data updated to 02/11/2018) (Fig. 1). The most recent reviews (Ayoob and Gupta, 2006; Mohapatra et al., 2009; Bhatnagar et al., 2011; Renuka and Pushpanji, 2013; Vithanage and Bhattacharya, 2015; Singh et al., 2016; Yadav et al., 2018) indicate that several materials, both synthetic and natural, and technologies have been tested and proposed for the removal of F^- from water, and the mechanisms involved mainly are: ion exchange, precipitation, Donnan dialysis, electrodialysis, reverse osmosis, nanofiltration and adsorption. However, in agreement with Yadav et al. (2018), the removal of excess amounts of F^- from groundwater is still to be solved in rural areas of developing countries where people have insufficient access to drinking water and a defluoridation technique should be as much as possible: (i) simple; (ii) effective; (iii) based on cheap materials and devices; (iv) easy to use; (v) free of collateral effects on water quality.

This study, as a part of the *FLOWERED* project (a Horizon 2020 European funded project) aimed at developing a defluoridation method for drinking water suitable for rural areas of the East African Rift Valley (EARV) and with the above-mentioned features, presents a new method for water defluoridation through the use of octacalcium phosphate (OCP; $Ca_8(HPO_4)_2(PO_4)_4 \cdot 5H_2O$), based on the same mineralogical principle of accumulation of F^- into the hard tissues of human body. In fact, the inorganic part of animal and human bones and teeth consists of non-stoichiometric calcium-deficient carbonate hydroxyapatite, also called bio-apatite (Sakae et al., 2015), whose crystallization is subsequent to the

---

[*] Corresponding author.
E-mail address: frauf@unica.it (F. Frau).

https://doi.org/10.1016/j.heliyon.2019.e02288
Received 20 May 2019; Received in revised form 17 June 2019; Accepted 8 August 2019

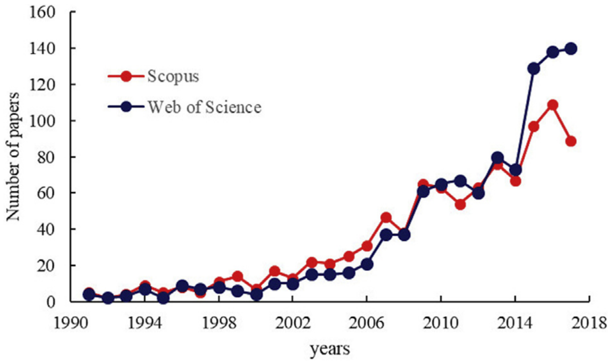

Fig. 1. The diagram shows the trend of papers published in indexed journals from 1991 to 2108 in the topic of defluoridation of water. Sources: www.scopus.com (Scopus); www.webofknowledge.com (Web of Science).

formation of its natural precursor OCP (Suzuki, 2013; Lu et al., 2015). In case of long-term high F^- exposure, the F^- ion can be accumulated into the hard tissue by means of the formation of fluorapatite (FAP; $Ca_5(PO_4)_3F$) instead of bio-apatite (Inoue et al., 2011).

The use of calcium phosphates, such as brushite (also known as dicalcium phosphate dihydrate – DCPD; $CaHPO_4 \cdot 2H_2O$) and hydroxyapatite (HAP; $Ca_5(PO_4)_3(OH)$), for water defluoridation is widely studied, but information about the use of OCP is lacking. In fact, synthetic OCP is extensively used in biomedical applications for bone regeneration (Markovic and Chow, 2010; Suzuki, 2013) but at the best of our knowledge only Yang et al. (2012) investigated the F^- uptake capacity from water by OCP.

In this work the OCP effectiveness as F^- remover is tested through laboratory sorption experiments conducted at circum-neutral pH and room conditions, using synthetic aqueous solutions and varying some parameters such as the contact time and the initial F^- concentration, as well as using a natural aqueous matrix with addition of F^-.

This work does not claim to be all-encompassing, and focuses exclusively on laboratory experiments aimed at understanding the F^- removal mechanism using OCP. Future studies will be more applicative and mainly devoted to: (i) test the removal capacity of OCP in presence of coexisting anions other than F^-, also using different starting pH values; (ii) test OCP with natural fluoride-rich groundwaters from the EARV in order to obtain important information about the real application of OCP in water defluoridation.

2. Materials and methods

All the reagents used for the synthesis and the removal experiments were of analytical grade (Carlo Erba reagents ACS-for analysis) and without further purification; ultrapure water (Millipore, Milli-Q©, 18.2 MΩ cm) was used to dissolve the salts and to dilute the solutions.

2.1. Synthesis

The OCP was synthesized in two steps. Firstly, synthetic DCPD was synthesized at room temperature adding 0.366 mol of both H_3PO_4 and $CaCO_3$ in 2 L of ultrapure water acidified at pH 1.5 with HCl. After precipitation, the DCPD was recovered through filtration, and dried at 40 °C. During the second step the OCP was obtained from the DCPD hydrolysis: 1.2 g of DCPD was added to 500 mL of ultrapure water with starting pH = 7.2; the solution was then heated in a stove at 60 °C for 65 h; the solid was recovered through filtration and dried at room temperature.

2.2. Fluoride removal experiments

Fluoride removal experiments were performed in batch-mode using 50 mL conical flasks agitated through a rotor system (40 rpm), at room temperature: 200 mg of OCP were added to 50 mL solutions (solid/solution ratio = 4 g/L) with different initial F^- concentrations (40, 60, 80, 120, 140 mg/L), for different times of reaction (from 0.5 to 21 h). Fluoride-bearing solutions were obtained dissolving NaF in ultrapure water stabilized at pH 8 using NaOH.

A test with a natural aqueous matrix was performed using 8 L of a low calcium, sodium-bicarbonate commercial bottled water, whose composition very well simulates fluoride-rich groundwaters from the EARV (Tekle-Haimanot et al., 2006). An adequate amount of NaF was added to the bottled water in order to have an initial F^- concentration of 30 mg/L. Before starting the experiment, 32 g of OCP were added to the solution reaching a solid/solution ratio of 4 g/L. The solution was kept under stirring at 500 rpm at room temperature (25 ± 3 °C) for 12 h inside a PE container with a capacity of 10 L.

All experiments were replicated twice or more. The solution pH of each experiment was measured before the addition of OCP and at the end of the reaction time. At the end of the experiments the solids and solutions were separated through filtration and recovered to carry out the mineralogical characterization and chemical analyses.

2.3. Chemical analyses and mineralogical characterization

The concentration of F^- in solution before and after the experiments was determined by a potentiometer (sensION TM + MM340, *HACH* LANGE) with Ion Selective Fluoride Electrode (ISE F^- 9655C, *HACH* LANGE) and adding the TISAB III (*HACH*) solution to avoid interference of metallic complexes during the analysis. A portion of OCP and the solid recovered after each experiment was dissolved in 5% v/v HNO_3 and then diluted with ultrapure water for the chemical analyses. The concentrations of Ca and P in both solids and solutions were determined by inductively coupled plasma optical emission spectroscopy (ICP-OES, ARL Fisons 3520).

The cationic and anionic chemical composition of bottled water, before and after the F^- removal experiment, was analyzed by ion chromatography (IC); only P was measured by ICP-OES. The initial bicarbonate concentration was calculated by alkalinity determined with the Gran method; to obtain the final bicarbonate concentration the contribution of phosphate was subtracted from alkalinity.

The mineralogical characterization of DCPD, OCP and the solid recovered after each experiment was performed collecting XRD patterns in the 3.5–55 °2θ angular range on an automated PANalytical X'pert Pro diffractometer, with Ni-filtered Cu-$K_{\alpha 1}$ radiation (λ = 1.54060 Å), operating at 40 kV and 40 mA, using the X'Celerator detector.

3. Results

3.1. Synthesis

The XRD pattern of the phase obtained from the first step of the synthesis reaction (Fig. 2a) shows that all the peaks are ascribable to DCPD (reference ICSD pattern n. 00-009-0077). The pattern of the product of DCPD hydrolysis after 40 h (Fig. 2b) still shows the presence of DCPD peaks and new peaks at 4.75, 9.41 and 9.73 °2θ corresponding to the (010), (110) and (020) characteristic reflections of OCP (reference ICSD pattern n. 00-026-1056), indicating that the hydrolysis reaction is in progress. The pattern of the solid recovered after 65 h (Fig. 2c) shows only the characteristic peaks of OCP, suggesting that the hydrolysis reaction has gone to completeness. Peaks of undesired phases were never detected.

The reaction of DCPD precipitation from aqueous solution and its hydrolysis into OCP can be summarized, respectively, by the reactions (1) and (2):

$$CaCO_3 + H_3PO_4 + 2\ H_2O \rightarrow CaHPO_4 \cdot 2H_2O_{(DCPD)} + CO_{2\ (g)} + H_2O \quad (1)$$

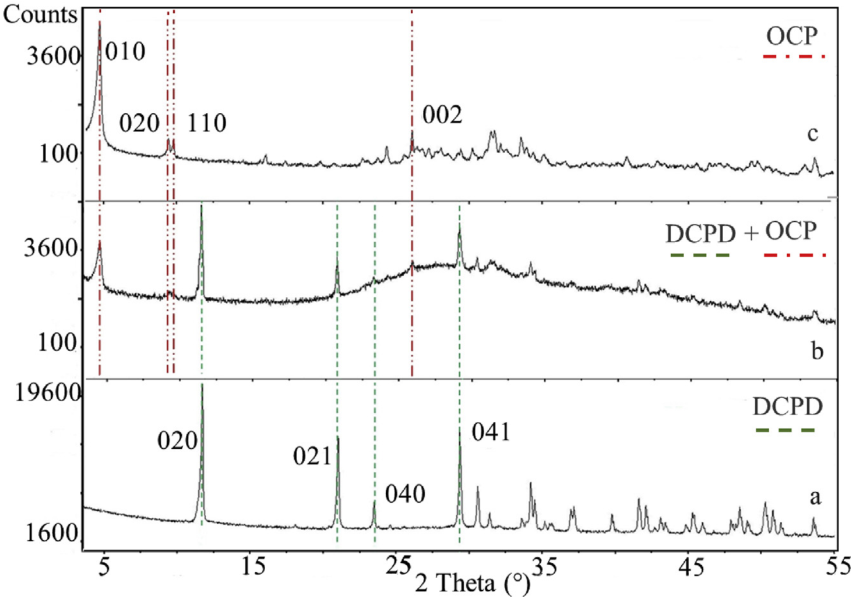

Fig. 2. XRD patterns and labelled representative peaks of (a) DCPD, (b) its hydrolysis product after 40 h with initial appearance of OCP and (c) final transformation in OCP after 65 h at 60 °C. Reference ICSD patterns used for phase identification are n. 00-009-0077 for DCPD and n. 00-026-1056 for OCP.

$$CaHPO_4 \cdot 2H_2O_{(DCPD)} \leftrightarrow 0.125\ Ca_8(HPO_4)_2(PO_4)_4 \cdot 5H_2O_{(OCP)} + 0.25\ HPO_4^{2-} + 1.375\ H_2O + 0.5\ H^+ \quad (2)$$

3.2. *Sorption experiments*

3.2.1. *Solutions*

The results of all sorption experiments show that most of F^- is removed from solution during the first hours after the addition of OCP, and the equilibrium is reached more o less quickly depending on the initial F^- concentration (F^- i.c.) (Fig. 3). The time required to reach the F^- equilibrium in solution varies from 3 h (F^- i.c. = 40 mg/L) to 10 h (F^- i.c. = 140 mg/L). More than 99% of F^- is removed in the experiments with F^- i.c. of 40, 60 and 80 mg/L, whereas the removal reaches 76% and 73% for F^- i.c. of 120 and 140 mg/L, respectively (Table 1). At the end of all experiments, an increase of dissolved P^{5+} (up to 72.4 mg/L) and Ca^{2+} (up to 0.26 mg/L) was observed, as well as a pH decrease from 8.0 to 6.5–7.0 (Table 1).

The results of the experiment with the bottled water (Table 2) show that dissolved F^- decreases from 30.4 to 0.18 mg/L, well below the drinking limit of 1.5 mg/L; other compositional differences before and after the treatment with OCP regard the decrease of dissolved Ca^{2+}, Mg^{2+} and HCO_3^-, and the increase of P^{5+}.

Table 1
Chemical parameters measured before (0 h) and at the end (21 h) of F^- removal batch experiments performed with 200 mg of OCP in 50 mL of solution. F^- i.c. = initial fluoride concentration in solution.

Experiment	F^- i.c. (0 h)	F^- (21 h)	F^- removed	Ca^{2+} (21 h)	total P^{5+} (21 h)	pH	
	mg/L	mg/L	%	mg/L	mg/L	0 h	21 h
Exp1	40	0.03	99.9	0.24	42.5	8	6.52
Exp2	60	0.53	99.1	0.26	44.6	8	6.62
Exp3	80	0.71	99.1	0.19	69.0	8	6.72
Exp4	120	28.5	76.2	0.16	72.4	8	6.92
Exp5	140	37.3	73.4	0.18	70.8	8	6.96

3.2.2. *Solids*

The XRD patterns of synthetic OCP and solids recovered at the end of

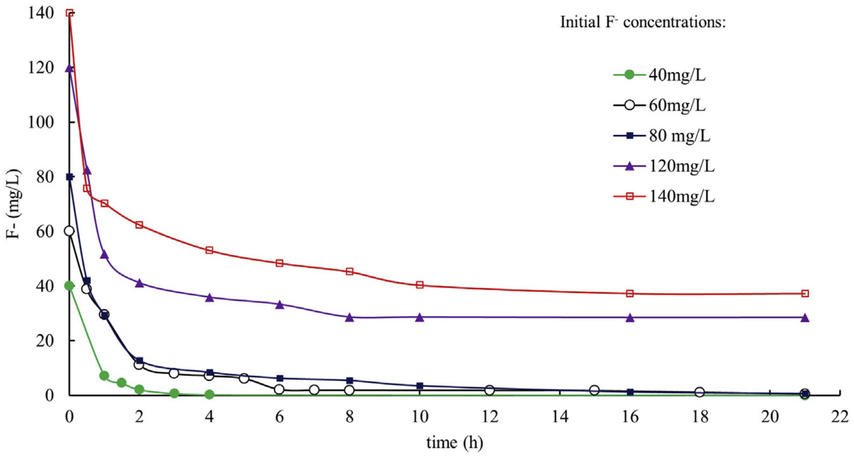

Fig. 3. The diagram shows the removal trend of dissolved F^- by 200 mg of OCP in 50 mL of solution at different step times and different initial F^- concentrations.

Table 2
Compositional differences of the bottled water before and after the F^- removal experiment.

	pH	Conductivity	T	Na^+	K^+	Mg^{2+}	Ca^{2+}	P^{5+}_{tot}	F^-	Cl^-	NO_3^-	SO_4^{2-}	HCO_3^-
		μS/cm	°C	mg/L	mg/L	mg/L	mg/L	mg/L	mg/L	mg/L	mg/L	mg/L	mg/L
Initial composition	8.3	596	25.2	123	1.6	3.9	12.2	0	30.4	79	5.0	16.1	126
Final composition	7.4	506	24.6	122	1.7	0.1	0.20	46.2	0.18	79	2.4	15.8	28.2

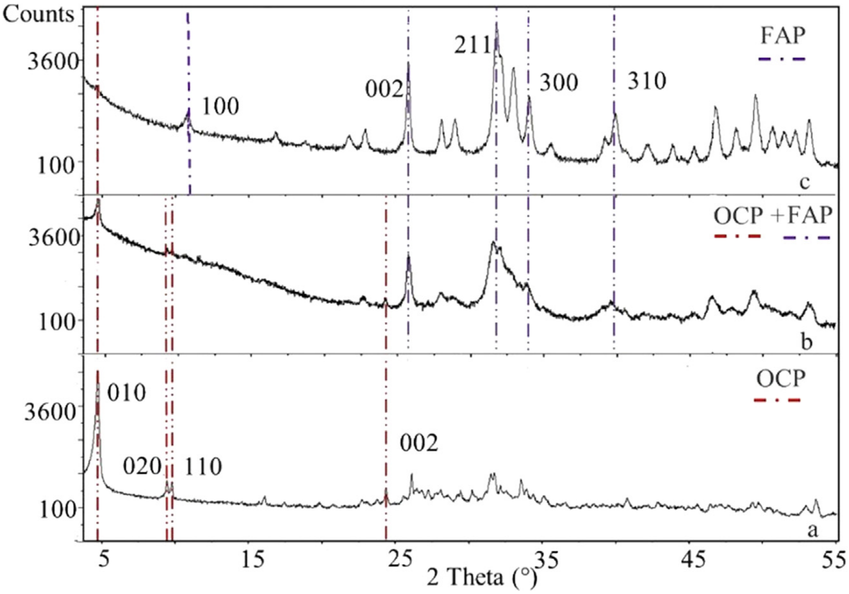

Fig. 4. XRD patterns of a) OCP that is the initial phase before F^- removal experiments; b) solid phase recovered after the experiment with F^- i.c. (initial fluoride concentration in solution) = 40 mg/L; c) solid phase recovered after the experiment with F^- i.c. = 140 mg/L. Phases shown in XRD patterns b) and c) were collected after 21 h of contact time with F^- solutions. Reference ICSD pattern used for identification of FAP is n. 00-015-0876.

the experiments with F^- i.c. of 40 and 140 mg/L are shown in Fig. 4. The solid phases after F^- uptake point out the transformation of OCP into FAP. The transformation is partial for the experiment with the lowest F^- i.c. (40 mg/L) whose XRD pattern shows the peaks of both phases, whereas the transformation appears to be complete for the experiment with the highest F^- i.c. (140 mg/L) when only the characteristic peaks of FAP are visible in the corresponding XRD pattern (Fig. 4). The XRD patterns of the experiments with intermediate F^- i.c. (not reported in Fig. 4) mainly show the presence of FAP, with OCP barely detectable.

The certain presence of FAP, that cannot be only assessed on the basis of XRD analysis due to the very similar XRD patterns of all end-members of the apatite series, is confirmed by the results of chemical analyses performed on the solid phases recovered after the sorption experiments. In fact, the amount of F^- in the solids increases as F^- i.c. increases (Table 3). Moreover, the molar Ca/P ratio of the phases recovered after the experiments with F^- i.c. of 80, 120 and 140 mg/L (Ca/P = 1.62, 1.62 and 1.64, respectively) is very close to the theoretical one for FAP (Ca/P = 1.67), whereas it is significantly lower when OCP is still detectable (Fig. 4b) at the end of the experiments with F^- i.c. of 40 and 60 mg/L (Ca/P = 0.93 and 1.14, respectively) (Table 3).

4. Discussion

4.1. *Water defluoridation*

The experimental data show that 200 mg of OCP in 50 mL of deionized water can reduce the F^- content from initial concentrations of 40, 60 and 80 mg/L to concentrations lower than the WHO limit for drinking water of 1.5 mg/L (Table 1). This result means that 4 g of OCP can effectively treat 1 L of water with F^- concentration up to 50 times higher than the drinking limit of 1.5 mg/L. Importantly, no deleterious collateral effects on the quality of the treated water are produced during the defluoridation process: the solution pH slightly decreases, however remaining in the range suggested by WHO for drinking water (pH = 6.5–9.5), and the increase of dissolved phosphorus (Table 1) can be considered a positive effect as phosphorus is an essential element for life

Table 3
Chemical composition of solid phases recovered after F^- removal experiments.

Experiment	F^- i.c. (0 h)	Detected phases	Ca^{2+}	total P^{5+}	F^-	Ca^{2+}/P^{5+}	
	mg/L		wt.%	wt.%	wt.%	mass ratio	molar ratio
Exp1	40	OCP + FAP	29.6	24.6	0.8	1.20	0.93
Exp2	60	OCP + FAP	31.5	21.3	1.1	1.48	1.14
Exp3	80	FAP + OCP	37.6	17.9	1.6	2.10	1.62
Exp4	120	FAP	37.2	17.8	3.1	2.09	1.62
Exp5	140	FAP	38.3	18.1	3.4	2.12	1.64
OCP theoretical			35.9	20.8	0	1.73	1.33
FAP theoretical			39.7	18.4	3.77	2.16	1.67

(U.S National Academy of Science, 1997) not subject to limitations for drinking water (WHO, 2011).

The effectiveness of the method in removing F^- from water is confirmed also using a natural aqueous matrix (Table 2), where the observed compositional variations are related to the F^- removal mechanism.

Furthermore, both physical (pH, conductivity, etc.) and organoleptic (taste, turbidity, etc.) features of the water defluoridated with the proposed method meet the WHO requirements.

4.2. *Removal mechanism*

The chemical and mineralogical results indicate that the F^- removal from aqueous solution takes place by means of the transformation of OCP into FAP. This reaction can be schematized as follows:

$$Ca_8(HPO_4)_2(PO_4)_4 \cdot 5H_2O_{(OCP)} + 1.6\ F^- \rightarrow 1.6\ Ca_5(PO_4)_3F_{(FAP)} + 1.2\ HPO_4^{2-} + 5\ H_2O + 0.8\ H^+ \quad (3)$$

It is known that the transformation of OCP into HAP is controlled by hydrolysis and subsequent epitaxial growth of HAP on OCP (Zhan et al., 2005; Arellano-Jiménez et al., 2009; Carino et al., 2018), with a minor contribution from OCP dissolution and HAP precipitation that must be taken into account. Considering that FAP and HAP have a complete anion solid solution (i.e. $F^- \leftrightarrow OH^-$) (Hughes and Rakovan, 2002), we assume the same mechanism of transformation from OCP into FAP.

The contribution of both reactions (i.e. OCP hydrolysis and FAP growth) can be evaluated monitoring the concentrations of Ca^{2+}, P^{5+} and F^- in solution during the experiments. The concentrations in solution of these elements as a function of time, during the representative experiment with F^- i.c. = 140 mg/L, are shown in Fig. 5. The sharp increase of P^{5+} and partly of Ca^{2+} in solution, occurring within the first hour simultaneously with the sharp decrease of F^-, is related to the solubility of OCP, that is about 8 mg/L (Dorozhkin, 2012), and the consequent oversaturation and precipitation of FAP which has a solubility of about 0.2 mg/L (Dorozhkin, 2012). After about 1.5 h, the concentration of Ca^{2+} in solution decreases below 0.2 mg/L, while P^{5+} continues to increase; this can be explained with transformation of OCP into FAP that has a molar Ca/P ratio (1.67) higher than that of OCP (1.33), with consequent release of phosphate to solution.

In the solid phases recovered after the experiments with F^- i.c. of 120 and 140 mg/L, where the transformation OCP → FAP appears to be complete, the molar Ca/P ratio is lower than the stoichiometric value of theoretical FAP (Table 3). The deficiency of Ca in the minerals of the apatite series often occurs in natural apatites and can be explained with the substitution of PO_4^{3-} by HPO_4^{2-} (Hutchens et al., 2006) and/or CO_3^{2-} (Vallet-Regí and González-Calbet, 2004). These substitutions cause the decrease of the negative charge, and therefore the amount of Ca necessary to counterbalance can decrease too. The chemical analyses confirm that in every experiment the formed apatite is mainly FAP and that its formation depends on the initial F^- concentration available in solution. In fact, the apatite obtained at the end of the experiments could be defined as a calcium-deficient fluoro-hydroxyl-apatite.

The F^- removal mechanism is confirmed also in the experiment with the bottled water (Table 2). In fact, the increase of P^{5+} and the decrease of Ca^{2+} in solution are explainable by the higher molar Ca/P ratio in FAP (1.67) with respect to the starting molar Ca/P ratio in OCP (1.33), whereas the decrease of HCO_3^- can be explained by (i) lowering of pH from 8.3 to 7.4, and (ii) replacement of PO_4^{3-} with carbonate species into the FAP structure.

4.3. *Modeling*

The empirical F^- removal capacity has been calculated with the formula:

$$Q_t = (C_i - C_t)\ V / W \quad (4)$$

where the removal capacity Q_t is the F^- removed per unit of sorbent (mg/g) at the t time (h), C_i and C_t are, respectively, the initial F^- concentration and the F^- concentration at t time in solution (mg/L), V is the volume of solution (L) and W is the weight of sorbent (g).

The experimental removal capacity of OCP calculated at the equilibrium (Q_{exp}) (Table 4) increases as the initial F^- concentration increases, and reaches 25.7 mg/g in the experiment with F^- i.c. = 140 mg/L. This value is lower than the stoichiometric theoretical F^- uptake capacity of reaction (3) (34.0 mg/g) calculated considering that 1 mol of OCP (molar mass 892.468 g/mol) reacts with 1.6 mol of F^- (molar mass 18.998 g/mol) to form FAP. The lower value of measured F^- uptake can be explained considering: (i) the partial ingress of OH^- instead of F^- in the FAP lattice; (ii) the Ca-deficiency of FAP (Table 3); the slight solubility of FAP (Dorozhkin, 2012).

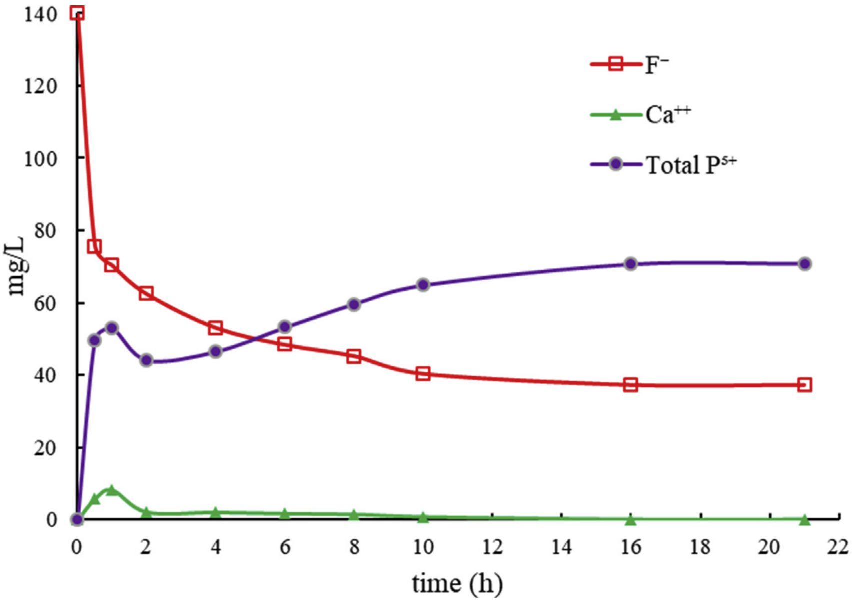

Fig. 5. The diagram shows the concentrations of calcium, total phosphorus and fluoride as a function of time, during the F^- removal experiment with OCP and F^- i.c. = 140 mg/L.

Table 4

Fluoride sorption capacity of OCP determined at equilibrium from the experimental data (Q_{exp}) and calculated from the pseudo-second order kinetic model (Q_e), and the sorption Langmuir isotherm parameters calculated using experimental data at equilibrium (21 h).

Experiment	F^- i.c. (0 h)	F^- (21 h)	Experimental	Pseudo-second order kinetics			Langmuir isotherm		
			Q_{exp}	Q_e	k	R^2	Q_{max}	K_L	R^2
	mg/L	mg/L	mg/g	mg/g	g/mg h		mg/g	L/mg	
Exp1	40	0.03	9.99	10.1	0.0138	0.9999			
Exp2	60	0.53	14.9	15.2	0.0577	0.9989			
Exp3	80	0.71	19.8	19.6	0.0241	0.9998			
Exp4	120	28.5	22.9	23.5	0.0192	0.9995			
Exp5	140	37.3	25.7	26.6	0.0260	0.9987			
							26.8	0.7645	0.9953

Although the removal mechanism of F^- from solution by using OCP has been demonstrated not to be adsorption but precipitation and epitaxial growth of FAP at the expense of dissolving OCP, the application of the Langmuir isotherm to our results can be useful as a simple interpolation model to compare stoichiometric and empirical removal capacity values with calculated one (i.e., Q_{max}). The theoretical maximum sorption capacity (Q_{max}) has been calculated through the linear form of the Langmuir isotherm equation expressed as follows:

$$C_e / Q_{exp} = (1/K_L\, Q_{max}) + (1/Q_{max})\, C_e \tag{5}$$

where C_e is the F^- concentration in solution at equilibrium (mg/L), Q_{max} is the maximum theoretical sorption capacity (mg/g), and K_L is the Langmuir constant (L/mg).

The plot of C_e/Q_{exp} vs C_e shows a good linearity (Fig. 6a), therefore the maximum sorption capacity (Q_{max}) and the Langmuir constant K_L can be calculated from the slope ($1/Q_{max}$) and from the intercept ($1/K_L\, Q_{max}$) of the straight line in the plot of Fig. 6a. The Q_{max} value is 26.8 mg/g, that is rather close to the Q_{exp} (25.7 mg/g) obtained with F^- i.c. of 140 mg/L (Table 4).

The effect of contact time has been studied through the pseudo-second order kinetic equation (Ho and McKay, 1999) expressed as:

$$dQ_t / dt = k(Q_e - Q_t)^2 \tag{6}$$

where k is the rate constant of pseudo-second order sorption (g/mg h) and Q_e is the calculated F^- removal capacity at equilibrium ($Q_e = Q_{exp}$). The integration of Eq. (6) written in linear form is:

$$t/Q_t = (1/kQ_e^2) + (1/Q_e)\ t \tag{7}$$

The applicability of the pseudo-second order kinetic model on the sorption system is indicated by the linear relationship of the plot of t/Q_t vs t (Fig. 6b), that can be used to calculate the F^- removal capacity at equilibrium (Q_e) and k from the straight line slope ($1/Q_e$) and the intercept ($1/kQ_e^2$), respectively (Table 4). The Q_e values are very close to the corresponding Q_{exp}, and in particular the Q_e value obtained with F^- i.c. of 140 mg/L (26.6 mg/g) is almost identical to Q_{max} (Table 4).

The Standard Gibbs free energy of formation ($\Delta G°$) of reaction OCP → FAP can be calculated from the isotherm and is used to determine whether the reaction is spontaneous or not. The $\Delta G°$ is calculated from the following equation:

$$\Delta G° = -RT \ln K_o \tag{8}$$

where R is the universal gas constant (8.134 J/mol K), T is the temperature in Kelvin (293.15 K = 20 °C) and K_o is the dimensionless equilibrium constant of the reaction defined as:

$$K_o = a_s / a_e = (v_s\, Q_{exp}) / (v_e\, C_e) \tag{9}$$

where a_s is the activity of F^- in the solid, a_e is the activity of F^- in the aqueous solution at equilibrium, and v_s and v_e are their relative activity coefficients. If the F^- concentration in solution decreases and approaches to zero, the activity coefficient v approaches to the unit and Eq. (9) can be written as follows:

$$\lim_{Q_{exp} \to 0} = a_s / a_e = Q_{exp}/C_e = K_o \tag{10}$$

According to the method used by various authors (Khan and Singh, 1987; Gunay et al., 2007), K_o can be determined also by plotting $\ln(Q_{exp}/C_e)$ vs. Q_{exp} (Fig. 6c). The value of Y-axis of C_e interpolated at zero corresponds at $\ln K_o = 9.76$, and therefore the value of $\Delta G°$ at 293 K is -23.3 kJ/mol. The calculated value of $\Delta G°$ is in agreement with that reported for the formation of apatite (Drouet, 2015), and indicates that the reaction of transformation of OCP into FAP is spontaneous at room conditions.

4.4. *Comparison with other methods based on calcium phosphates*

One of the most studied and used defluoridation methods is based on the $OH^- \leftrightarrow F^-$ ion exchange through HAP that, in presence of F^- in solution, forms FAP (Waghmare and Arfin, 2015). The use of HAP has some advantages, given that the method does not produce negative effects on treated water and its application is cheap and low-tech compared with other defluoridation methods. HAP can be obtained via different processes: (i) synthesis, but this method increases the cost of production; (ii) extraction from calcium phosphate-bearing rocks, but these source-rocks commonly host FAP and undesired elements for human health, such as uranium and other heavy metals (Abouzeid, 2008); (iii) calcination of animal bones (bone char), but this method requires a large amount of bones and a correct calcination temperature. Furthermore, the latter method, which is by far the most widely used, requires: (i) a control on the size of bone char particles and relative filter pores to avoid the release of very fine bone char particles into the treated water; (ii) a sanification process to avoid the bad taste and smell of water after the treatment, as well as the proliferation of bacteria inside the filter (Smittakorn et al., 2010).

In relatively recent years, other synthetic calcium phosphate compounds have been tested for defluoridation of water. The comparison of the different materials is a hard task to deal with because they were tested in different experimental conditions (e.g., initial F^- concentration, pH, solid/liquid ratio, etc.). For this reason, the different materials and their F^- removal capacity reported in Table 5 were selected according to the following criteria: (i) no pH buffering during the F^- removal experiment, and initial and final pH values in the range of drinking water (pH = 6.5–9.5); (ii) the lowest initial F^- concentration higher than 5 mg/L; (iii) absence or minimization of negative effects on the overall quality of treated water; (iv) experimental temperature close to 20–30 °C. The aim of these criteria is not only to compare the F^- removal capacity of different calcium phosphate materials, but also to compare their possible applicability.

As far as we know, the only paper that explores the uptake of F^- from water by OCP is the work of Yang et al. (2012) that compares the different kinetics of F^- uptake (and not the removal capacity at equilibrium) by different calcium phosphate materials (HAP, DCPD and OCP), both in absence and in presence of polymeric additives. In that

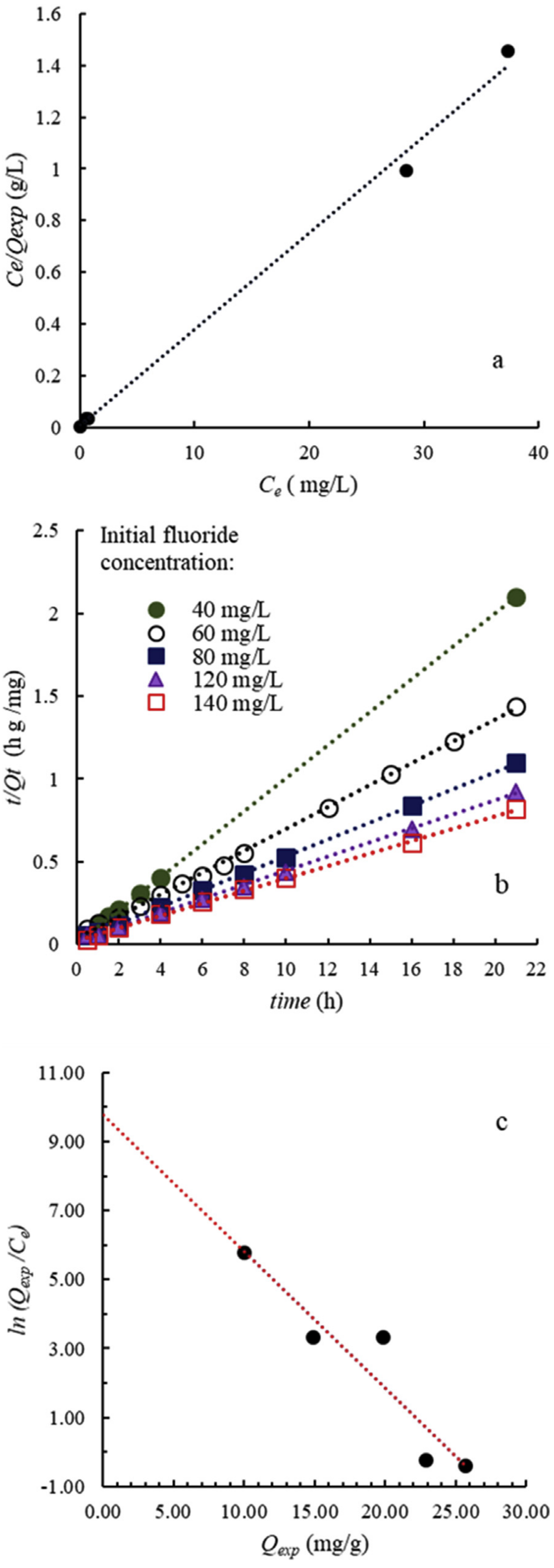

Fig. 6. Diagrams of a) plot of the linearized Langmuir isotherm applied to F^- removal from solution by OCP, calculated using experimental data at equilibrium (21 h); b) plot of the linearized pseudo-second order kinetic model for experiments performed with different initial F^- concentrations (60, 80, 120, 140 mg/L); c) plot of *ln*(Q_{exp}/C_e) vs Q_{exp} for F^- removed from solution by the hydrolysis reaction OCP → FAP.

Table 5
Comparison of the F^- removal capacities of various calcium phosphate materials.

Materials	Abbreviation in the cited paper	Q_{exp} mg/g	Q_{max} mg/g	Reference
Hydroxyapatite	HAP	13.2	16.4	(Nie et al., 2012)
Hydroxyapatite	HAP	19.0		(Badillo-Almaraz et al., 2007)
Hydroxyapatite-nanowire	HAP	6.28	25.5	(He et al., 2016)
Hydroxyapatite	PHA	11.5		(Wagutu et al., 2018)
Brushite	DCPD	18.1		(Yang et al., 2012)
Brushite	DCPD	2.85	6.59	(Mourabet et al., 2011)
Brushite	CHA	18.2		(Wagutu et al., 2018)
Apatitic tricalcium phosphate	TCP	7.8	13.9	(Mourabet et al., 2012)
Octacalcium phosphate	OCP	22.7		(Yang et al., 2012)
Bone char	BC 400°	3	3.51	(Mbabaye et al., 2017)
Bone char	–	4.1	5.44	(Medellin-Castillo et al., 2007)
Monetite	DCP	26	66.7	(Yang et al., 2018)
Monetite	MONs@CS	2.87	50.0	(Shen et al., 2016)
Monetite	–	56.6	120	(Shen et al., 2018)
Octacalcium phosphate	OCP	25.7	26.8	Present study

work the reaction kinetics of F^- removal is in the following order: DCPD > OCP > HAP. The experiments were performed using only one initial F^- concentration of 50 mg/L in 20 mL of water and only one dosage of sorbent, that is different for each material (26.4 mg of HAP, 35.2 mg of OCP and 45.3 mg of DCPD). The value of removal capacity (mg/g), neither empirical nor calculated, is not discussed but we extrapolated it from the plots included in the paper (22.7 mg/g in Table 5).

5. Conclusions

The use of octacalcium phosphate (OCP) has been tested for the removal of fluoride (F^-) from water in order to subsequently develop a simple, effective and low-cost defluoridation method suitable for rural communities affected by fluorosis in the East African Rift Valley (EARV) and in other parts of the world.

The synthesis method of OCP has been successfully realized using calcium carbonate and phosphoric acid, in order to lower the production costs using non-expensive reagents and avoid any possible negative secondary effect in terms of water drinkability. The results of experiments indicate that OCP can act as an effective remover of F^- from water via transformation into fluorapatite (FAP), obtaining experimental and calculated removal capacity of $Q_{exp} = 25.7$ mg/g and $Q_{max} = 26.8$ mg/g, respectively. Moreover, the release of some phosphorus to water during the transformation of OCP into FAP may result in an improvement of the quality of water after the treatment, because the minimum intake of phosphorus is 100 mg/die for infants, 700 mg/die for pregnant women, and 1250 mg/die for children and adults (U.S. National Academy of Science, 1997). Thus, drinking 2 L/day of water defluoridated with OCP can provide a significant percentage of phosphorus RDA (Recommended Dietary Allowance) to people living in rural areas in developing countries.

Further studies will be devoted to test the defluoridation performance of the OCP transformation into FAP in presence of different concentrations of other anions, such as Cl^- and HCO_3^-, and with different starting pH values. Testing OCP with natural fluoride-rich waters from the EARV will provide important information about the real application of OCP in water defluoridation in terms of appropriate dose of OCP and defluoridation time required. Finally, a defluoridator device based on OCP will be designed with low-cost and low-tech features in order to be easily applicable and usable in rural areas of the EARV.

Declarations

Author contribution statement

Alfredo Idini: Conceived and designed the experiments; Performed the experiments; Analyzed and interpreted the data; Contributed reagents, materials, analysis tools or data; Wrote the paper.

Elisabetta Dore: Performed the experiments; Analyzed and interpreted the data; Contributed reagents, materials, analysis tools or data.

Dario Fancello: Performed the experiments.

Franco Frau: Conceived and designed the experiments; Analyzed and interpreted the data; Wrote the paper.

Funding statement

This work is a part of the Ph.D. project of Idini Alfredo Idini, supported by MIUR (Italian Ministry of Education, University and Research) in the frame of the Italian National Program PON R&I 2014–2020 “Innovative doctorates with industrial characterization”. This work is also supported by the FLOWERED project (Coordinator G. Ghiglieri), a Horizon 2020 European funded project (Grant Agreement - N. 690378) (www.floweredproject.org).

Competing interest statement

The authors declare no conflict of interest.

Additional information

No additional information is available for this paper.

Acknowledgements

We wish to thank Prof. Giorgio Ghiglieri (University of Cagliari, Italy) for his continuous support and encouragement.

References

Abouzeid, A.Z.M., 2008. Physical and thermal treatment of phosphate ores - an overview. Int. J. Miner. Process. 85, 59–84.

Arellano-Jiménez, M.J., García-García, R., Reyes-Gasga, J., 2009. Synthesis and hydrolysis of octacalcium phosphate and its characterization by electron microscopy and X-ray diffraction. J. Phys. Chem. Solids 70, 390–395.

Ayoob, S., Gupta, A.K., 2006. Fluoride in drinking Water : a review on the status and stress effects fluoride in drinking Water : a review. Crit. Rev. Environ. Sci. Technol. 36, 433–487.

Badillo-Almaraz, V.E., Armando Flores, J., Arriola, H., López, F.A., Ruiz-Ramirez, L., 2007. Elimination of fluoride ions in water for human consumption using hydroxyapatite as an adsorbent. J. Radioanal. Nucl. Chem. 271, 741–744.

Bhatnagar, A., Kumar, E., Sillanpää, M., 2011. Fluoride removal from water by adsorption-A review. Chem. Eng. J. [Internet] 171, 811–840.

Carino, A., Ludwig, C., Cervellino, A., Müller, E., Testino, A., 2018. Formation and transformation of calcium phosphate phases under biologically relevant conditions : experiments and modelling. Acta Biomater. [Internet] 74, 478–488.

Dorozhkin, V.S., 2012. Amorphous calcium orthophosphates: nature, chemistry and biomedical applications. Int. J. Mater. Chem. [Internet] 2, 19–46. Available from: http://article.sapub.org/10.5923.j.ijmc.20120201.04.html.

Drouet, C., 2015. A comprehensive guide to experimental and predicted thermodynamic properties of phosphate apatite minerals in view of applicative purposes. J. Chem. Thermodyn. 81, 143–159.

Farooqi, A., Masuda, H., Firdous, N., 2007. Toxic fluoride and arsenic contaminated groundwater in the Lahore and Kasur districts, Punjab, Pakistan and possible contaminant sources. Environ. Pollut. 145, 839–849.

Gao, X., Wang, Y., Li, Y., Guo, Q., 2007. Enrichment of fluoride in groundwater under the impact of saline water intrusion at the salt lake area of Yuncheng basin, northern China. Environ. Geol. 53, 795–803.

Ghiglieri, G., Pittalis, D., Cerri, G., Oggiano, G., 2012. Hydrogeology and hydrogeochemistry of an alkaline volcanic area: the NE Mt. Meru slope (East African Rift-Northern Tanzania). Hydrol. Earth Syst. Sci. 16, 529–541.

Gunay, A., Arslankaya, E., Tosun, I., 2007. Lead removal from aqeous solutions by natural and pretreated clinoptilolite: adsorption equation and kinetics. J. Hazard Mater. 146, 362–371.

He, J., Zhang, K., Wu, S., Cai, X., Chen, K., Li, Y., Sun, B., Jia, Y., Meng, F., Jin, Z., et al., 2016. Performance of novel hydroxyapatite nanowires in treatment of fluoride contaminated water. J. Hazard Mater. [Internet] 303, 119–130.

Ho, Y.S., McKay, G., 1999. Pseudo-second order model for sorption processes. Process Biochem. 34, 451–465.

Hughes, J.M., Rakovan, J., 2002. The crystal structure of apatite, $Ca_5(PO_4)_3(F,OH,Cl)$. Rev. Mineral. Geochem. [Internet] 48, 1–12.

Hutchens, S.A., Benson, R.S., Evans, B.R., O'Neill, H.M., Rawn, C.J., 2006. Biomimetic synthesis of calcium-deficient hydroxyapatite in a natural hydrogel. Biomaterials 27, 4661–4670.

Inoue, M., Rodriguez, A.P., Nagai, N., Nagatsuka, H., Legeros, R.Z., Tsujigiwa, H., Inoue, M., Kishimoto, E., Takagi, S., 2011. Effect of fluoride-substituted apatite on in vivo bone formation. J. Biomater. Appl. 25, 811–824.

Khan, A.A., Singh, R.P., 1987. Adsorption thermodynamics of carbofuran on Sn (IV) arsenosilicate in H^+, Na^+ and Ca^{2+} forms. Colloids Surface. 24, 33–42.

Lu, X., Leng, Y., Johnsson, M.S.-A., Nancollas, G.H., House, W.A., Tung, M.S.S., Tomazic, B., Brown, W.E.W.E., Effect, T., Valletregi, M., 2015. The role of brushite and octacalcium phosphate in apatite formation. Rev. Mineral. Geochem. [Internet] 48, 61–82.

Markovic, M., Chow, L.C., 2010. An octacalcium phosphate forming cement. J. Res. Natl. Inst. Stand Technol. [Internet] 115, 257–265. Available from: http://www.pubmedcentral.nih.gov/articlerender.fcgi?artid=2957834&tool=pmcentrez&rendertype=abstract.

Mbabaye, G.K., Mtalo, F., Minja, R.J.A., Legonda, I., 2017. Standardizing defluoridation of community waters using bone char. J. Water Supply Res. Technol. - Aqua 66, 131–139.

Medellin-Castillo, N.A., Leyva-Ramos, R., Ocampo-Perez, R., De La Cruz, R.F.G., Aragon-Piña, A., Martinez-Rosales, J.M., Guerrero-Coronado, R.M., Fuentes-Rubio, L., 2007. Adsorption of fluoride from water solution on bone char. Ind. Eng. Chem. Res. 46, 9205–9212.

Mohapatra, M., Anand, S., Mishra, B.K., Giles, D.E., Singh, P., 2009. Review of fluoride removal from drinking water. J Environ. Manage [Internet] 91, 67–77.

Mourabet, M., El Boujaady, H., El Rhilassi, A., Ramdane, H., Bennani-Ziatni, M., El Hamri, R., Taitai, A., 2011. Defluoridation of water using Brushite: equilibrium, kinetic and thermodynamic studies. Desalination [Internet] 278, 1–9.

Mourabet, M., El Rhilassi, A., El Boujaady, H., Bennani-Ziatni, M., El Hamri, R., Taitai, A., 2012. Removal of fluoride from aqueous solution by adsorption on Apatitic tricalcium phosphate using Box-Behnken design and desirability function. Appl. Surf. Sci. [Internet] 258, 4402–4410.

Nie, Y., Hu, C., Kong, C., 2012. Enhanced fluoride adsorption using Al (III) modified calcium hydroxyapatite. J. Hazard Mater. [Internet] 233–234, 194–199.

Olaka, L.A., Wilke, F.D.H., Olago, D.O., Odada, E.O., Mulch, A., Musolff, A., 2016. Groundwater fluoride enrichment in an active rift setting: Central Kenya Rift case study. Sci. Total Environ. [Internet] 545–546, 641–653.

Ozsvath, D.L., 2009. Fluoride and environmental health: a review. Rev. Environ. Sci. Biotechnol. 8, 59–79.

Renuka, P., Pushpanji, K., 2013. Review on defluoridation techniques of water. Int. J. Eng. Sci. 2, 86–94.

Sakae, T., Nakada, H., LeGeros, J.P., 2015. Historical review of biological apatite crystallography. J. Hard. Tissue Biol. [Internet] 24, 111–122. Available from: https://www.jstage.jst.go.jp/article/jhtb/24/2/24_111/_article.

Shen, C., Wu, L., Chen, Y., Li, S., Rashid, S., Gao, Y., Liu, J., 2016. Efficient removal of fluoride from drinking water using well-dispersed monetite bundles inlaid in chitosan beads. Chem. Eng. J. 303, 391–400.

Shen, J., Evangelista, M.F., Mkongo, G., Wen, H., Langford, R., Rosair, G., McCoustra, M.R.S., Arrighi, V., 2018. Efficient defluoridation of water by Monetite nanorods. Adsorption 24, 135.

Singh, G., Kumari, B., Sinam, G., Kriti, Kumar N., Mallick, S., 2018. Fluoride distribution and contamination in the water, soil and plants continuum and its remedial technologies, an Indian perspective– a review. Environ. Pollut. [Internet] 239, 95–108.

Singh, J., Singh, P., Singh, A., 2016. Fluoride ions vs removal technologies: a study. Arab. J. Chem. [Internet] 9, 815–824.

Smittakorn, S., Jirawongboonrod, N., Mongkolnchai-Arunya, S., Durnford, D., 2010. Homemade bone charcoal adsorbent for defluoridation of groundwater in Thailand. J. Water Health 8, 826–836.

Suzuki, O., 2013. Octacalcium phosphate (OCP)-based bone substitute materials. Jpn. Dent. Sci. Rev. [Internet] 49, 58–71.

Tekle-Haimanot, R., Melaku, Z., Kloos, H., Reimann, C., Fantaye, W., Zerihun, L., Bjorvatn, K., 2006. The geographic distribution of fluoride in surface and groundwater in Ethiopia with an emphasis on the Rift Valley. Sci. Total Environ. 367, 182–190.

Tewari, A., Dubey, A., 2009. Defluoridation of drinking water: efficacy and need. J. Chem. Pharm. Res. 1, 31–37.

U.S. National Academy of Science, 1997. Dietary Reference Intakes, pp. 319–326.

Vallet-Regí, M., González-Calbet, J.M., 2004. Calcium phosphates as substitution of bone tissues. Prog. Solid State Chem. 32, 1–31.

Vithanage, M., Bhattacharya, P., 2015. Fluoride in the environment: sources, distribution and defluoridation. Environ. Chem. Lett. [Internet] 13, 131–147.

Waghmare, S., Arfin, T., 2015. Fluoride removal from water by calcium materials: a state-of-the-art review. Int. J. Innov. Res. Sci. Eng. Technol. [Internet] 4, 8090–8102. Available from: http://ijirset.com/upload/2015/september/13_Fluoride.pdf.

Wagutu, A.W., Machunda, R., Jande, Y.A.C., 2018. Crustacean derived calcium phosphate systems: application in defluoridation of drinking water in East African rift valley. J. Hazard Mater. [Internet] 347, 95–105.

WHO, 2011. Guidelines for Drinking-Water Quality, fourth ed. World Health Organization, Geneva.

Yadav, K.K., Gupta, N., Kumar, V., Khan, S.A., Kumar, A., 2018. A review of emerging adsorbents and current demand for defluoridation of water: bright future in water sustainability. Environ. Int. [Internet] 111, 80–108.

Yang, C., Guan, L., Wang, J., Yang, X., Lin, M., Tan, S., Yu, X., Ge, M., 2018. Enhanced fluoride removal behaviour and mechanism by dicalcium phosphate from aqueous solution. Environ. Technol. [Internet] 0, 1–10.

Yang, T., Kim, C., Jho, J., Kim, I.W., 2012. Regulating fluoride uptake by calcium phosphate minerals with polymeric additives. Colloids Surfaces Physicochem. Eng. Asp. [Internet] 401, 126–136.

Zhan, J., Tseng, Y.H., Chan, J.C.C., Mou, C.Y., 2005. Biomimetic formation of hydroxyapatite nanorods by a single-crystal-to- single-crystal transformation. Adv. Funct. Mater. 15, 2005–2010.

CHAPTER II

Mineralogical-geochemical study of the anionic competition effect on the octacalcium phosphate reaction into apatite: implications on water defluoridation

Alfredo Idini and Franco Frau *

Department of Chemical and Geological Sciences, University of Cagliari, 09042, Monserrato (CA), Italy

Submitted 3 May 2020

Heliyon - Elsevier Ltd

Mineralogical-geochemical study of the anionic competition effect on the octacalcium phosphate reaction into apatite: implications on water defluoridation

Alfredo Idini, Franco Frau*

Department of Chemical and Geological Sciences, University of Cagliari, 09042, Monserrato (CA), Italy

* Corresponding author: frauf@unica.it

Abstract

The octacalcium phosphate (OCP) is an unstable compound extensively studied due to its use as bone&tooth-substitute material. The main feature of OCP is its tendency to react into apatite depending on the media conditions; this peculiarity has been exploited also for environmental concerns, e.g. against the fluoride contamination of groundwater through the OCP transformation into fluorapatite. The property of OCP to be the crystalline precursor of apatite has been here investigated using equal molar amounts of fluoride, chloride, hydroxyl and carbonate anions dissolved in aqueous solution, in order to asses if and how the anionic competition can influence the formation of the different apatite end-members. The investigation, conducted through XRD, SEM and ICP-OES analyses, shows that fluoride is the main anion removed from solution during the OCP transformation, and consequently fluorapatite is the main resulting apatitic phase, followed by hydroxyapatite. These results are of significant importance in better defining the possible environmental role of OCP in the treatment of fluoride-polluted waters.

Keywords: octacalcium phosphate; anionic competition; fluorapatite formation; fluoride removal implications.

1. Introduction

The apatite supergroup is composed of 43 minerals (formally divided into five groups: apatite, hedyphane, belovite, britholite and ellestadite) which have general chemical formula $M1_2M2_3(TO_4)_3X$ (Z = 2). The M sites (M1 in coordination IX, M2 in coordination VII) host mainly calcium (Ca^{2+}) and lead (Pb^{2+}) and a large number of other cations, the T site (coordination IV) can host mainly phosphorous (P^{5+}), arsenic (As^{5+}), vanadium (V^{5+}), and the X site is occupied by fluoride (F^-), chloride (Cl^-) and hydroxyl (OH^-) anions (Fig. 1) [1].

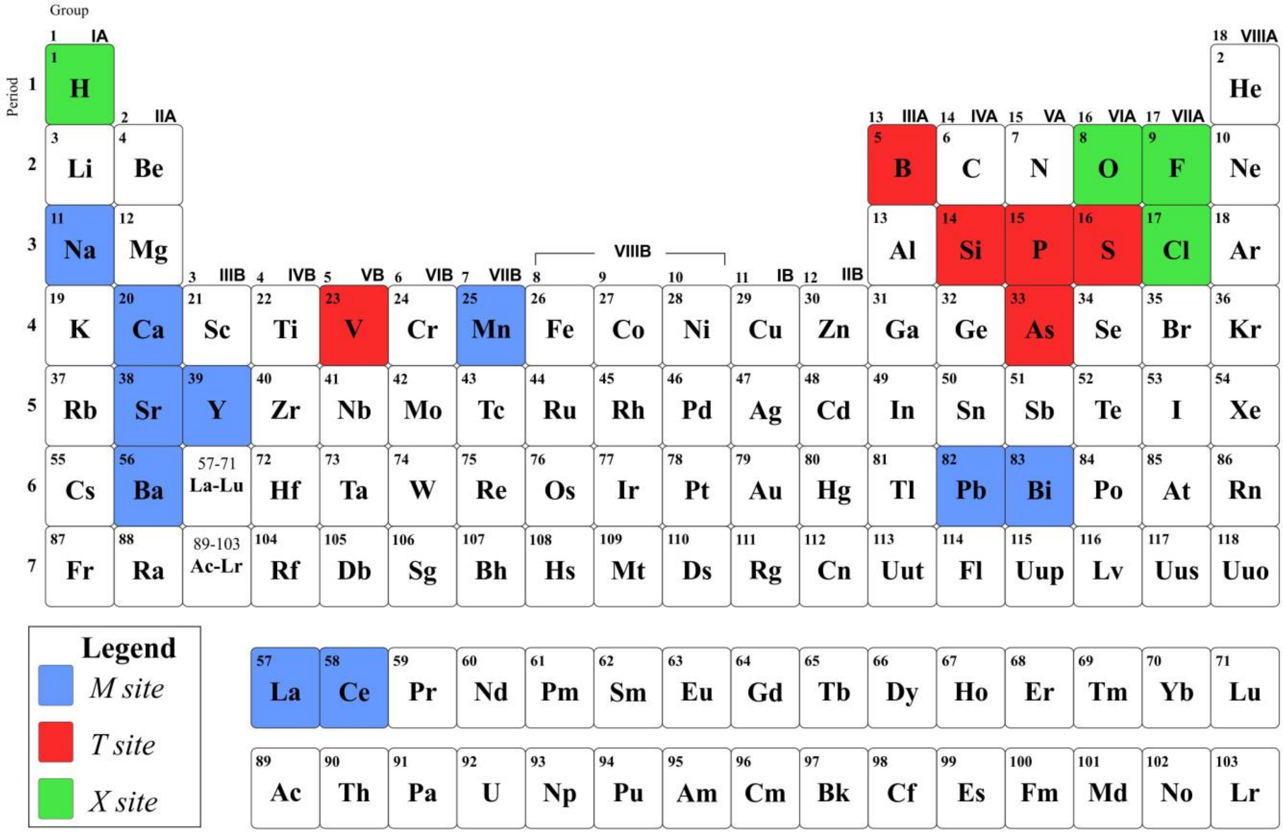

Fig. 1. The end-member forming elements of the apatite supergroup highlighted by crystallographic site occupancy.

In the apatite group, hydroxyapatite (HAp, $Ca_5(PO_4)_3OH$), fluorapatite (FAp, $Ca_5(PO_4)_3F$) and chlorapatite (ClAp, $Ca_5(PO_4)_3Cl$) are the ideal end-members of a complete solid solution. The natural apatite is mostly fluorapatite where F^- can be partially replaced by OH^- and Cl^- in the X site [2]. Moreover, several studies report that many different substitutions in the M and T sites can occur both in natural and synthetic samples, one of which is the entrance of the carbonate anion (CO_3^{2-}) in partial substitution of phosphate, which is geologically well documented in the sedimentary phosphorite deposits, composed primarily of francolite, the carbonate-rich variety of FAp [3]. In addition to the great importance of apatite in the geological ambit [4], the related compound called calcium orthophosphate [5] is extensively studied in medicine and biology because the inorganic part of mammal hard tissues is composed of bioapatite, a calcium-phosphate mineral with apatitic structure [6]. Common chemical features of bioapatite include: (i) the presence of hydrogen phosphate (HPO_4^{2-}) and/or carbonate instead of phosphate, both substitutions causing a calcium deficiency in the structure (i.e. a calcium-deficient apatite); (ii) the OH^- depletion in the anionic X site [7]. However, the bioapatite can show very different Ca/P and OH/F ratios, depending on the type of biological hard tissue. Among the calcium orthophosphate compounds, the octacalcium phosphate (OCP, $Ca_8(HPO_4)_2(PO_4)_4 \cdot 5H_2O$, 892.468 g/mol) has been extensively studied, exploiting its biomedical properties as bone&tooth-substitute material in various forms as OCP is one of the mineralogical precursors of apatite [8] and bioapatite [9]. In fact, in alkaline aqueous solution, OCP tends to transform into HAp or, depending on medium conditions, into bioapatite. The mechanism of mineralogical transformation has been debated in several studies, but the articles of Xin et al. and Carino et al. [10-11] clarified that the solid-state transformation and then the epitaxial growth of HAp onto OCP are the main mechanisms involved.

Recent studies have shown that OCP reacts in presence of fluoride in solution to form FAp [12], and this reaction occurs also in biological conditions. The formation of FAp, instead of bioapatite, in mammal hard tissues causes different pathologies called skeletal and dental fluorosis [13]. Skeletal and non-skeletal fluorosis [14] pathologies are a well-known issue in many countries around the globe that affect more than two hundred million people [15]. The World Health Organization (WHO) indicates the fluoride-rich groundwaters as the main source of the excessive intake of fluorine by people, and the WHO guidelines for drinking-water quality (GDWQ) adopt a fluoride concentration of 1.5 mg/L as the permissible limit for human consumption [16]. In the frame of the FLOWERED project (www.floweredproject.org, Horizon2020 program funded by the European Commission), one of the main goals was to develop an innovative, frugal and feasible method capable of removing the geogenic contamination of fluoride from groundwater used for drinking purposes by the rural communities of the East African Rift Valley (EARV). The results of the research have shown that

OCP can effectively uptake dissolved fluoride from groundwater through the mineralogical transformation into FAp, both in laboratory and field trials using natural fluoride-rich waters [17-18].

The aim of the work here presented is (i) to understand how OCP reacts in the presence of equivalent molar concentrations of F^-, Cl^-, OH^- and carbonate species (HCO_3^- + CO_3^{2-}); (ii) to assess the effect of the anionic competition and, consequently, determine which one of the apatite end-members is favoured in the OCP transformation reaction; (iii) to indicate the possible environmental implications on the treatment of fluoride-polluted waters.

2. Materials and methods

All the reagents used for the synthesis and the anionic competition experiments were of analytical grade (Carlo Erba reagents ACS-for analysis) and without further purification; ultrapure water (Millipore, Milli-Q©, 18.2 MΩ cm) was used to dissolve the salts and to dilute the solutions.

2.1 Synthesis of OCP

The OCP was synthesized in two steps. Firstly, dicalcium phosphate dihydrate (DCPD, $CaHPO_4 \cdot 2H_2O$) was synthesized at room temperature adding 0.366 mol of both H_3PO_4 and $CaCO_3$ in 2 L of ultrapure water acidified at pH 1.5 with HCl. After precipitation, the DCPD was recovered through filtration, and dried at 40 °C. During the second step the OCP was obtained from the DCPD hydrolysis: 1.2 g of DCPD was added to 500 mL of ultrapure water with starting pH 7.2; the solution was then heated in a stove at 60 °C for 65 h; the solid was recovered through filtration and dried at room temperature. The OCP synthesized is a white powder with particle size in the range of 14-125 µm, determined using mesh sieves.

2.2 Anionic competition experiments

The anionic competition experiments were performed at room conditions in batch-mode using 50 mL conical flasks agitated through a rotor system at 40 rpm; 200 mg (0.223 mmol) of OCP were added to 50 mL solutions (solid/solution ratio = 4 g/L) with same molar concentrations of F^-, Cl^-, OH and carbonate species (HCO_3^- + CO_3^{2-}). The choice of the anionic concentrations in solution was based on the reaction of OCP into FAp:

$$Ca_8(HPO_4)_2(PO_4)_4 \cdot 5H_2O_{(OCP)} + 1.6F^- \rightarrow 1.6Ca_5(PO_4)_3F_{(FAp)} + 1.2HPO_4^{2-} + 5H_2O + 0.8H^+ \quad (1).$$

Considering reaction (1) and the experimental setting, the F^- stoichiometric amount needed is 0.357 mmol for 0.223 mmol of OCP in 50 mL of solution, that is 7.14 mmol /L, but, in order to favour the kinetics of reaction (1), a slightly higher F^- amount was used (0.368 mmol in 50 mL, that is 7.37 mmol/L corresponding to 140 mg/L), and the molarity of the other competing anions in solution was set up to that value. The time required because the OCP → FAp reaction goes close to completion in such conditions is less than 16 h, therefore every experiment was checked after 16, 20 and 24 h [17]. The salts used to provide the anions into solution were NaF, KOH, $NaHCO_3$ and NaCl. In order to have an exact amount of OH^-, the solution pH of each experiment was measured before the addition of OCP and after adding the other salts, and then KOH was added till the expected OH^- value was reached. The experiments were labelled as follows: No_Comp (absence of competitors; only F^- present in solution); Cl_Comp (F^- and Cl^- present together); OH_Comp (F^- and OH^- present together); Alk_Comp (F^- and carbonate species ($HCO_3^- + CO_3^{2-}$) present together); Tot_Comp (F^- and all anionic competitors simultaneously present in solution).

At the end of the experiments, the solids and solutions were separated through filtration and recovered to carry out the mineralogical characterization and chemical analysis.

2.3 Mineralogical and chemical analyses

The concentration of F^- in both solids (after their dissolution) and solutions was determined by a potentiometer (sensION TM + MM340, *HACH* LANGE) with Ion Selective Fluoride Electrode (ISE F^- 9655C, *HACH* LANGE) and adding the TISAB III (*HACH*) solution to avoid interference of metallic complexes during the analysis. A portion of OCP before and after the experiments was dissolved in 67% v/v HNO_3 and then diluted with ultrapure water for elemental analyses. The concentration of Na, Ca and P in solids was determined by inductively coupled plasma optical emission spectroscopy (ICP-OES, ARL Fisons 3520), while Cl^- was analysed by Ion Chromatography (IC, Dionex ICS3000). The initial bicarbonate concentration was calculated from alkalinity determined with the Gran method; in order to obtain the final bicarbonate concentration the contribution of phosphate was subtracted from alkalinity. The mineralogical characterization of solid phases, before and after the experiments, was performed collecting X-ray diffraction (XRD) patterns in the 3.5-55 °2θ angular range on an automated PANalytical X'Pert Pro diffractometer, with Ni-filtered Cu-$K_{\alpha 1}$ radiation (λ = 1.54060 Å), operating at 40 kV and 40 mA, using the X'Celerator detector. The XRD data were interpreted for phase identification with the X'Pert HighScore Plus software. Microphotographs and semi-quantitative chemical analyses of solids were collected with an environmental scanning electron microscope (ESEM, FEI Quanta 200) equipped with an energy dispersive X-ray spectrometer (EDS) and elaborated with the Pathfinder software (Thermo Fisher Scientific).

3. Results

3.1 Characterization of OCP

The XRD analysis of the synthesized compound identified it as OCP (Fig. 2) in agreement with the two patterns of OCP listed in the Inorganic Crystal Structure Database (ICSD reference codes 00-026-1056 and 00-044-0778). All the peaks can be attributed to the OCP pattern, especially the OCP characteristic reflections at 4.74, 9.44 and 9.76 °2θ.

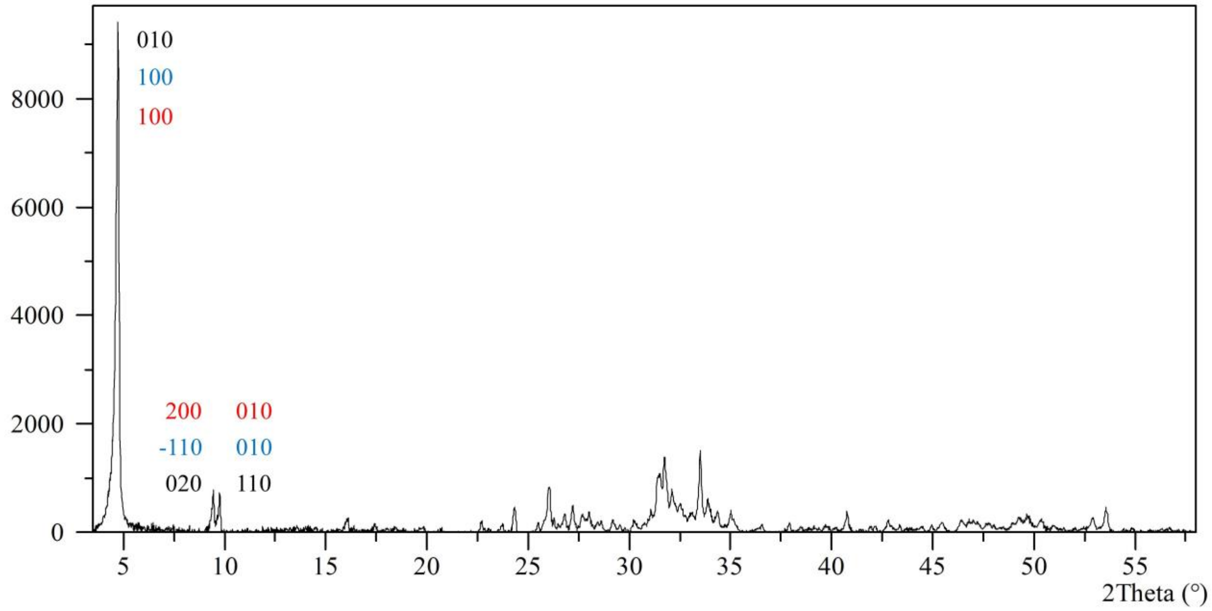

Fig. 2. XRD pattern of the OCP used in the experiments. The indexed reflections written in black font are from [19], those in blue are from [20] and those in red are from the present study.

The crystallographic parameters, calculated with the DICVOL software [21], converge towards the Triclinic system (P-1): a = 20.37, b = 9.78, c = 4.76 (Å); α = 90.7°, β = 92.9°, γ = 113.2°; V = 868.4 · 10^6 pm^3. The calculation was performed using 24 reflections with 3% minimum relative intensities without unindexed peaks in the output. The agreement of the refinement, according to [22], shows a Figure of Merit of 23.6.

It is worth saying that other authors have published OCP crystallographic refinement and reflections indexing (Table 1, Fig. 2 and Table SD1 in the supplemental data), and there is an overall agreement about the belonging of OCP to the Triclinic system.

Table 1. Crystallographic parameters of OCP for a Triclinic system.

a	b	c	α	β	γ	V	Reference
	Å			(°)		10^6 pm^3	
9.259	18.994	6.855	92.33	90.13	79.93	1220.57	[19]
19.87	9.63	6.875	89.28	92.22	108.95	1243.29	[20]
19.70	9.50	6.85	90.03	92.48	108.3	n.r.	[8]
20.37	9.78	4.76	90.70	92.90	113.2	868.4	present study

n.r. = not reported

The ESEM images of OCP crystal aggregates (Fig. 3) reveal that the synthesized OCP has a prismatic bladed habitus with an elongated axis (the a axis, according to our refinement). The crystals occur in radial aggregates (Fig. 3).

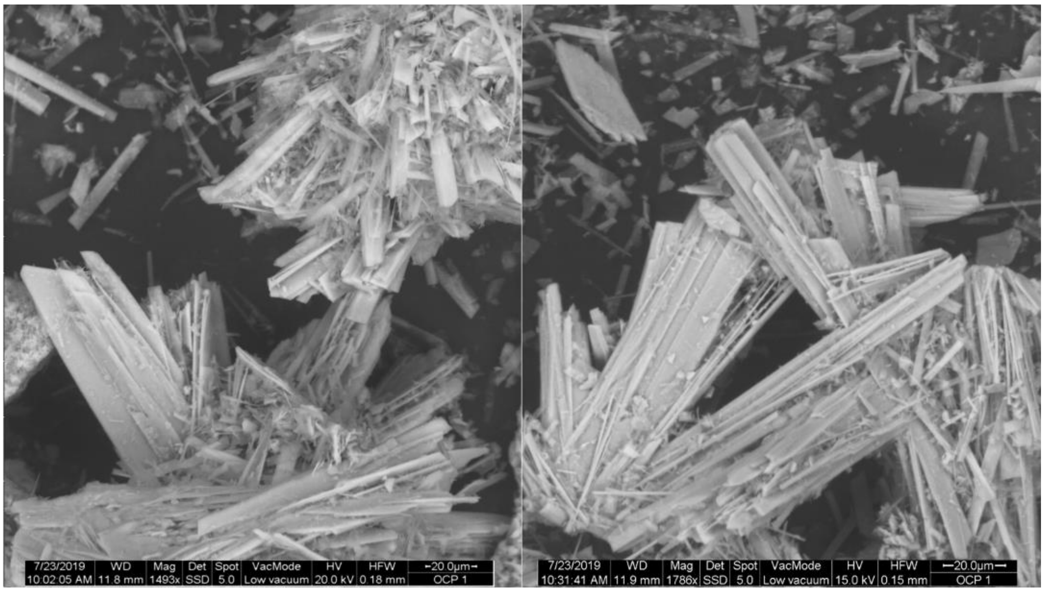

Fig. 3. ESEM images of the synthesized OCP used for the anionic competition experiments.

The OCP spectra collected from different crystals show homogeneous elemental composition (Figure SD2), and the quantitative ICP-OES chemical analysis, performed after dissolution of 1 g of OCP, shows a Ca concentration of 8.16 mmol/L and P concentration of 6.22 mmol/L, equivalent to a Ca/P molar ratio of 1.31 that is very close to the stoichiometric value of 1.33 in OCP.

3.2 OCP reaction into apatite: effect of anionic competition on aqueous solutions

The results of the anionic competition experiments are reported in Table 2. For convenience, due to the change of dissolved carbonate species as a function of pH, the carbonate species ($HCO_3^{-} + CO_3^{2-}$) are indicated with the general term "Alk" for alkalinity, and the corresponding experiment is Alk_Comp.

Table 2. Initial and final pH and dissolved anionic concentrations in the competition experiments of OCP transformation into apatite.

	pH		OH^- (mmol/L)		F^- (mmol/L)		Cl^- (mmol/L)		Alk (mmol/L)	
Experiment	initial	final	initial	final	initial	final	initial	final	initial	final
No_Comp	7.00	7.08	$1\cdot10^{-4}$	$1.20\cdot10^{-4}$	7.37	1.43	0	0	0	0
Cl_Comp	7.00	6.91	$1\cdot10^{-4}$	$8.13\cdot10^{-5}$	7.37	1.77	7.37	7.02	0	0
OH_Comp	11.87	7.26	7.37	$1.82\cdot10^{-4}$	7.37	2.34	0	0	0	0
Alk_Comp	8.80	7.79	$6.31\cdot10^{-3}$	$6.17\cdot10^{-4}$	7.37	1.57	0	0	7.37	7.22
Tot_Comp	11.87	7.84	7.37	$6.92\cdot10^{-4}$	7.37	2.09	7.37	7.07	7.37	7.18

Alk = $HCO_3^{-} + CO_3^{2-}$

The main variations of anionic concentration in solution concern the decrease of F^- and OH^-, while Cl^- and ($HCO_3^- + CO_3^{2-}$) shown a slight decrease (Table 2). The pH tends to the neutrality in every competition experiment regardless of the anionic species in solution. Similar results are observed in the "Tot_Comp" experiment, where the coexistence of all anions in solution is tested.

In order to compare the reduction of dissolved F^- in the different experiments, the removal of F^- from solution can be expressed as an empirical removal capacity (q_e) calculated through the formula:

$$q_e = (C_i - C_f)\, V/w \qquad (2)$$

where q_e is the molar mass of F^- removed by mol of OCP (mol/mol), C_i and C_f are respectively the initial and final F^- concentrations (mol/L), V is the volume of solution (L) and w is the molar mass of OCP (Table 3). The maximum value of $q_e = 1.33$ is reached in the No_Comp experiment, that is 17% lower than the stoichiometric theoretical value of 1.6 in the OCP → FAp reaction (1). The No_Comp experiment is taken as a reference for the other experiments, and therefore a percentage value of F^- removed equal to 100% is attributed to it (Table 3, Fig. 4).

Table 3. Measured amounts of F^- removed, P^{5+} and Ca^{2+} dissolved, and F^- empirical removal capacity (q_e) in the anionic competition experiments, compared with the theoretical values of the OCP transformation into FAp (reaction (1) in the text). The No_Comp experiment is taken as a reference (100% F^- removed) for the other experiments, and the relative percentages (%) are reported.

Experiment	F^- removed		q_e	P^{5+} dissolved	Ca^{2+} dissolved
	mmol	*%*	*mol/mol*	*mmol*	*mmol*
No_Comp	0.30	100	1.33	0.30	0.03
Cl_Comp	0.28	93	1.24	0.31	0.04
OH_Comp	0.25	83	1.10	0.32	0.03
Alk_Comp	0.29	97	1.29	0.31	0.03
Tot_Comp	0.24	80	1.06	0.33	0.04
OCP → FAp reaction	0.357		1.6	0.267	0

The competition effect of Cl^- (Cl_Comp experiment) and (HCO_3^- + CO_3^{2-}) (Alk_Comp experiment) on F^- removal is very limited (respectively, q_e = 1.24, 93% F^- removed; q_e = 1.29, 97% of F^- removed), while the OH^- competition (OH_Comp experiment) is more evident (q_e = 1.10, 83% F^- removed). When all anions are simultaneously present in solution (Tot_Comp experiment), the competition effect on F^- removal is even more noticeable (q_e = 1.06, 80% F^- removed) (Table 3, Fig. 4).

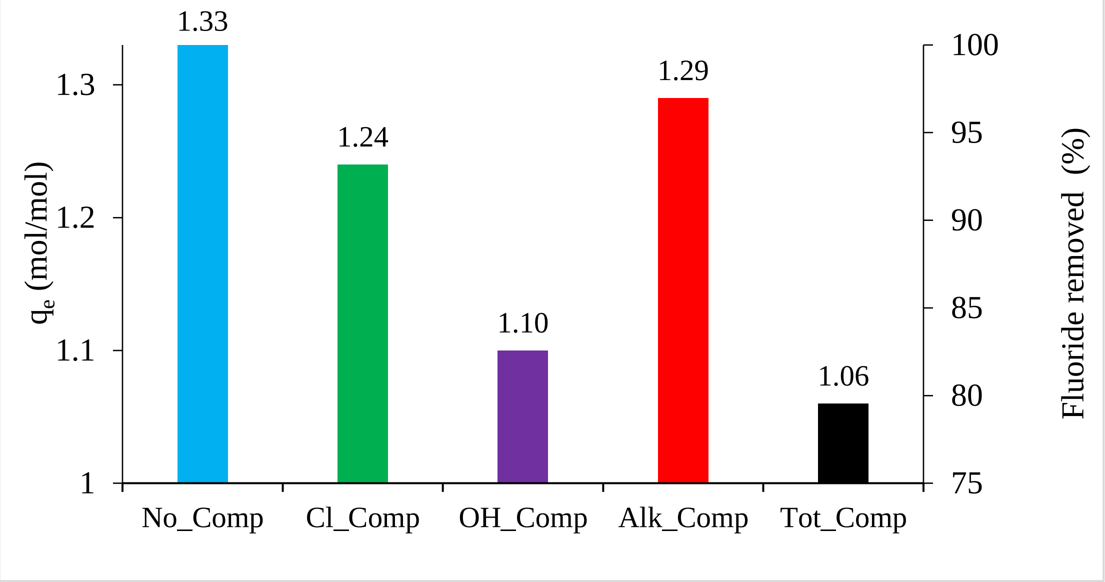

Fig. 4. Plot of the fluoride empirical removal capacity (q_e) and percentage of fluoride removed for each anionic competition experiment. The No_Comp experiment is taken as a reference (100% fluoride removed) for the other experiments.

In every anionic competition experiment, as predicted by the OCP → FAp reaction (1), some phosphorous is released into solution, while dissolved calcium should be nil. However, we have measured dissolved concentrations of P^{5+} and Ca^{2+} that are slightly higher than the stoichiometric values according to reaction (1) (Table 3).

3.3 OCP reaction into apatite: effect of anionic competition on solid phases

The XRD analysis of the solid phases collected after the anionic competition experiments shows very similar patterns (Fig. 5 and Figure SD3) that can be completely assigned, by means of peaks and whole diffraction profile fitting, to the apatite group minerals. Moreover, the OCP immersed in a deionized water solution (initial pH = 7.00, final pH = 5.62, absence of any of the competing anions) tends to retrocede to DCPD without apatite neo-formation (Figure SD4). Another phase that should be considered, taking into account the overall elemental composition of the experiments, is fluorite (CaF_2). In fact, due to the complete overlap of the fluorite XRD peaks with those of apatite in the investigated °2θ range, the minor precipitation of fluorite during the competition experiments cannot be excluded only considering the XRD data. The presence, or not, of fluorite will be later discussed according to the ESEM and chemical analyses.

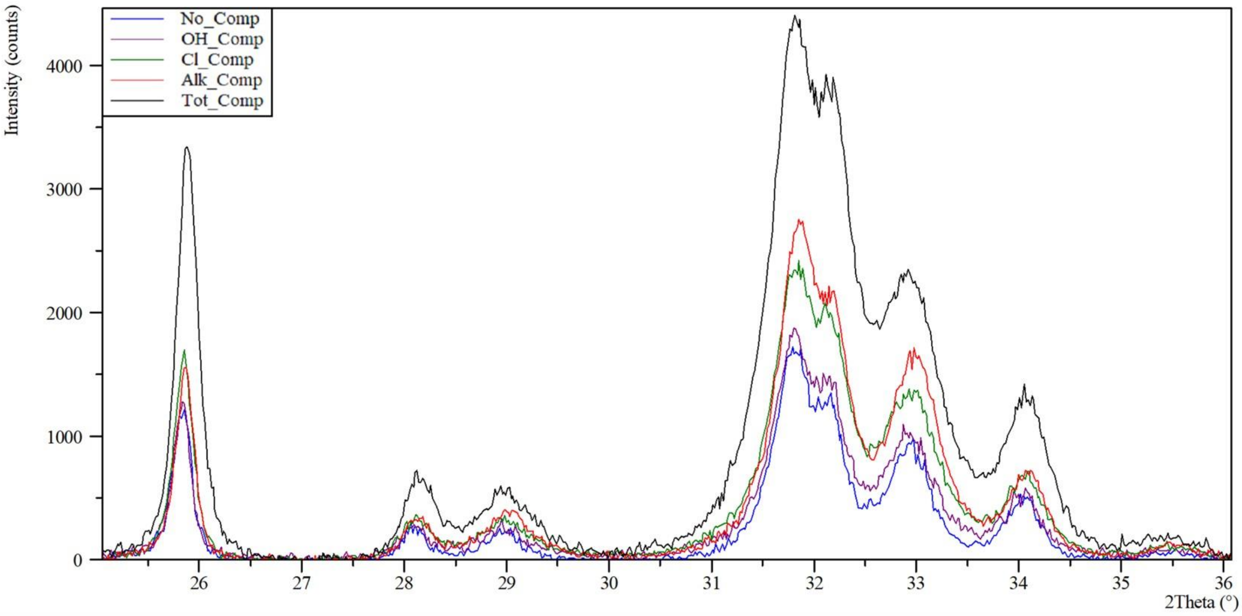

Fig. 5. Selected portion of X-ray diffraction patterns of the solid phases collected at the end of the anionic competition experiments.

Moreover, the OCP immersed in a deionized water solution (initial pH = 7.00, final pH = 5.62, absence of any of the competing anions) tends to retrocede to DCPD without apatite neo-formation (Figure SD4). Another phase that should be considered, taking into account the overall elemental composition of the experiments, is fluorite (CaF_2). In fact, due to the complete overlap of the fluorite XRD peaks with those of apatite in the investigated °2θ range, the minor precipitation of fluorite during the competition experiments cannot be excluded only considering the XRD data. The presence, or not, of fluorite will be later discussed according to the ESEM and chemical analyses.

Due to the strong similarity of the XRD patterns of the apatite group members (Figure SD5), the choice of the reference patterns for the phase identification should be carefully considered. For this purpose, the following ICDD patterns of HAp (PDF code 00-009-0432), FAp (PDF code 00-015-0876), ClAp (PDF code 00-033-0271) and carbonate-apatite (CarbAp, PDF code 00-019-0272) have been selected because they were collected from synthetic samples and match the Star quality mark (i.e. well characterized chemically and crystallographically pattern, no unindexed lines, $\Delta 2\theta \leq 0.03°$). The phase identification was carried out using the Rietveld algorithm that adopts the following agreement parameters [23]:

$$R_{exp} = \sqrt{(N-P)/\sum_{i=1}^{N} w_i\,(y_j - b_i)^2}$$

$$R_{wp} = \sqrt{\sum_{i=1}^{N}[w_i\,(y_i - M_i)^2]/\sum_{i=1}^{N} w_i\,(y_j - b_i)^2}$$

$$GoF = \left(\frac{R_{wp}}{R_{exp}}\right)^2$$

where R_{exp} is the statistical expected value of the dataset and represents the maximum possible agreement value; R_{wp} is the weighted profile, which is the statistical square root difference of the quantity minimized, scaled by the weighted intensities; *GoF* (Goodness of Fit) is the numerical evaluation of the fit, and its minimum value should be 1; N is the number of points and P the number of varied parameters; w, y, M and b are respectively the weight, the intensity, the calculated intensity and the background intensity at step i [23].

The results of the Rietveld method applied for the phase identification are listed in Table 4 and indicate that FAp is the phase that better fits all the experimental patterns, followed by HAp, while CarbAp and ClAp show a worse agreement. The good fit for HAp can be related to the co-occupancy of OH^- and F^- in the X site of apatite in all the experiments, while the co-occupancy seems to be more difficult for Cl^-. About the CarbAp poor fit, the entry of the carbonate anion in place of the phosphate one, and the consequent formation of carbonate-apatite, could also be inhibited by an excess of dissolved phosphate. It is worth saying that the aim of the Rietveld calculations here presented is just to compare the different fits for the apatite group end-members and not a refinement of their structures, since in the latter case better R_{wp} (< 10) and *GoF* (~2) values would be required.

Table 4. Results of the Rietveld method applied for the identification of the solid phases collected at the end of the anionic competition experiments. See the text for the meaning of the tabulated parameters and labels.

Phase	No_Comp			OH_Comp			Cl_Comp			Alk_Comp			Tot_Comp		
	R_{wp}	R_{exp}	*GoF*	R_{wp}	R_{exp}	*GoF*	R_{wp}	R_{exp}	*GoF*	R_{wp}	R_{exp}	*GoF*	R_{wp}	R_{exp}	*GoF*
FAp	10.394	5.148	*4.076*	9.232	4.273	*4.668*	10.295	5.181	*6.747*	9.156	4.31	*4.51*	9.542	3.070	*9.355*
HAp	10.788	5.148	*4.391*	9.477	4.273	*4.918*	13.562	5.181	*6.853*	9.520	4.31	*4.87*	9.763	3.070	*9.986*
ClAp	-	-	-	-	-	-	15.258	5.181	*9.894*	-	-	-	9.815	3.070	*10.219*
CarbAp	-	-	-	-	-	-	-	-	-	11.62	4.23	*7.55*	14.094	3.089	*20.814*

The cell parameters, calculated using the McMaille algorithm [24], show that all the solid phases can be solved in the Hexagonal system (space group $P\ 6_3/m$); the values show small differences among them (Table 5) and are close to the cell parameters of the apatite group end-members (e.g. fluorapatite from MinDat https://www.mindat.org/min-1572.html has a = 9.3973 Å, c = 6.8782 Å, V = 526.03 · 10^6 pm^3).

Table 5. Cell parameters calculated for the solid phases collected at the end of the anionic competition experiments. At least 22 XRD reflections with 2% minimum relative intensity were used for calculations. The cell parameters refer to the Hexagonal system (space group P 6_3/m).

Experiment	a	c	α	β	γ	V	Indexed reflections
	Å			(°)		10^6 pm^3	(unindexed)
No_Comp	9.401	6.889	90	90	120	527.33	24 (0)
Cl_Comp	9.415	6.895	90	90	120	529.37	22 (0)
OH_Comp	9.405	6.889	90	90	120	527.81	32 (0)
Alk_Comp	9.402	6.887	90	90	120	527.30	29 (0)
Tot_Comp	9.416	6.884	90	90	120	528.36	28 (0)

The ESEM images of the solid phases collected at the end of all the anionic competition experiments show aggregates of acicular crystals (Fig. 6a,b,c), indicating a clear morphological change with respect to the OCP crystals shown in Figure 3. Moreover, the EDS analyses (Fig. 6d and Figure SD6) indicate that, in addition to O, the only elements identified are Ca, P and F, and their intensity ratios are constant along the points analysed, confirming that the phase formed through OCP transformation in the presence of various dissolved anions (F^-, Cl^-, OH^-, HCO_3^- + CO_3^{2-}) is mainly a fluorapatite (FAp).

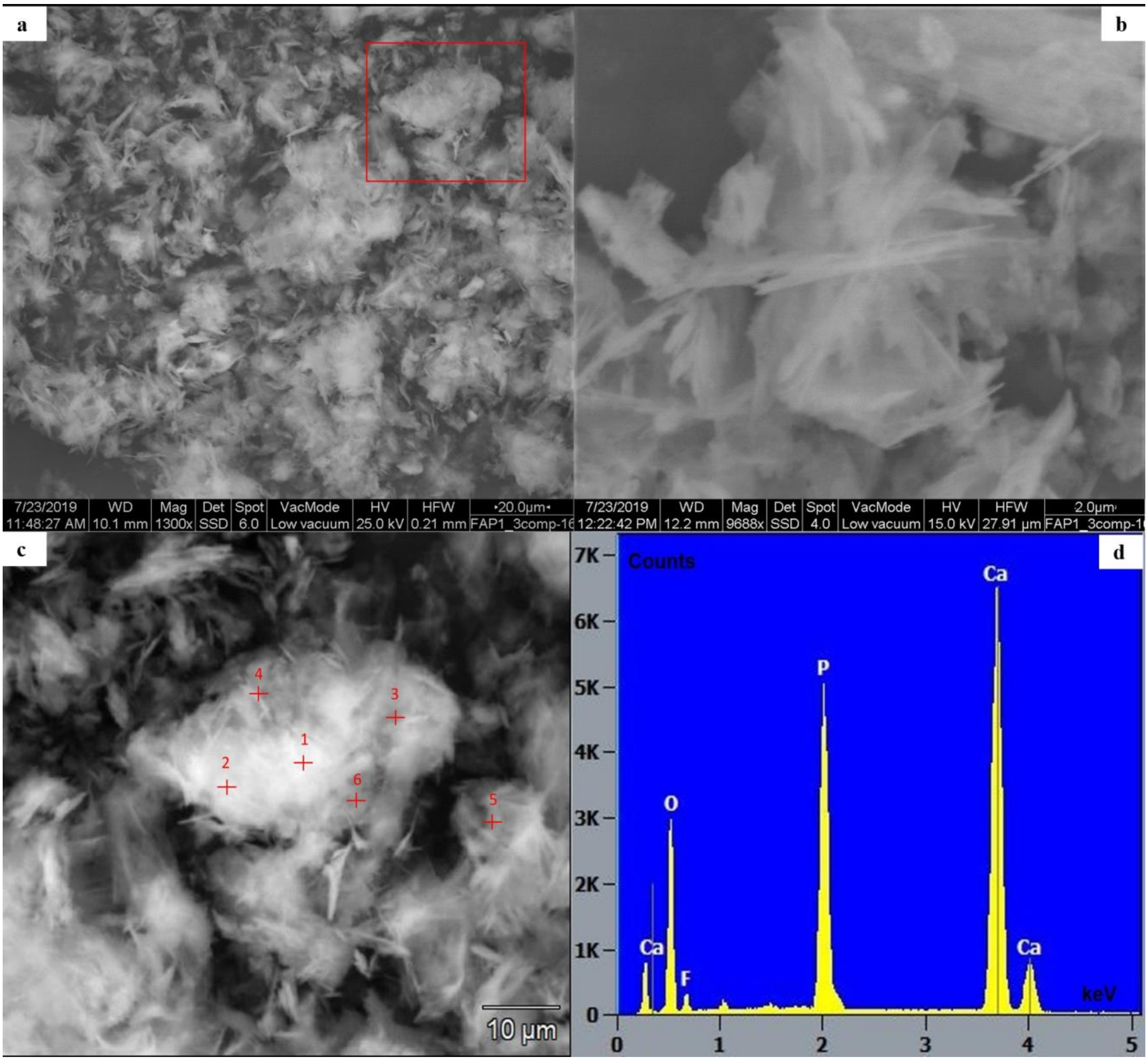

Fig. 6. ESEM images and EDS spectrum of the solid phase collected at the end of the anionic competition experiment Tot_Comp: a) aggregate of fluorapatite (FAp) acicular crystals, the red square is one of the areas analysed by EDS; b) magnification of FAp aggregates; c) magnification of FAp aggregates within the red square in a) with the EDS analysis spots; d) example of EDS spectrum with elemental identification.

3.4 Chemical analysis and mineral chemistry of solid phases

The wet chemical analysis of the solid phases collected at the end of the anionic competition experiments was performed after the acidic dissolution of 150 mg of each sample in 1 L of deionized water. The results (Table 6) have been interpreted on the basis of the following general crystallochemical formula for the apatite group minerals: $M_5(TO_4)_3X$, where M = Ca^{2+}, T = P^{5+}, X = F^-, Cl^-, OH^-.

The concentrations of Ca and P are quite similar in all solid phases (Ca = 58.81-59.13 mg/L; P = 26.67-27.57 mg/L). The low concentrations of Na (0.72-1.28 mg/L) measured in all samples are due to the possible Ca ⇆ Na substitution in the M site. All solid phases contain F^-, the highest concentration is in the No_Comp experiment sample (5.13 mg/L), the lowest one in the OH_Comp experiment sample (4.28 mg/L). Very low Cl^- concentrations were detected only in the solids of the Cl_Comp (0.92 mg/L) and Tot_Comp (0.53 mg/L) experiments.

The chemical composition expressed in wt. % of oxides and elements (Table 6) clearly converges towards the stoichiometric mineral chemistry of FAp. The calculation of the atoms per formula unit (a.p.f.u.), performed using the Apatite Calculation Sheet by ©Gabbrosoft 2011 and following the recommendations of [1], shows that there is a deficiency in the T site and an excess of positive charge (Table 6), even perfectly filling the X site up to the value of 1 with the addition of OH^-. In order to balance the excess of positive charge, it was assumed the contribution of the carbonate anion both from atmospheric CO_2 dissolved in water and from $NaHCO_3$ salt used in the Alk_Comp and Tot_Comp experiments. The possible PO_4^{3-} ⇆ CO_3^{2-} substitution [25] was considered at an extent sufficient to obtain a perfect charge balance, and the resulting calculation is close to the theoretical value of 3 for the T site. The M site, occupied by Ca^{2+} and Na^+, is close to the expected value of 5.

Table 6. Wet chemical analysis (concentrations in mg/L), chemical composition (concentrations in wt. %) and atom per formula unit (a.p.f.u.) calculation of the solid phases collected at the end of the anionic competition experiments. FAp$_{th}$ indicates the theoretical values for fluorapatite. The general crystallochemical formula used for the apatite group minerals is $M_5(TO_4)_3X$.

Wet chemical analysis (mg/L)

	No_Comp	Cl_Comp	OH_Comp	Alk_Comp	Tot_Comp
Ca	59.03	59.13	58.81	59.12	58.92
Na	1.28	1.20	1.38	0.93	0.72
P	27.07	26.95	27.57	26.67	26.95
Cl	0.00	0.92	0.00	0.00	0.53
F	5.13	4.73	4.28	5.00	4.56

Chemical composition (wt. %)

	No_Comp	Cl_Comp	OH_Comp	Alk_Comp	Tot_Comp	FAp$_{th}$
CaO	55.06	55.16	54.86	55.15	54.96	55.60
Na_2O	1.15	1.08	1.24	0.84	0.65	
P_2O_5	41.35	41.17	42.12	40.74	41.16	42.22
Cl	0.00	0.61	0.00	0.00	0.35	
F	3.42	3.15	2.85	3.33	2.64	3.77
Sub-Total	100.98	101.17	101.07	100.06	99.76	101.59
$-O=F_2,Cl_2$	1.44	1.46	1.20	1.40	1.19	1.59
Total	99.54	99.71	99.87	98.66	98.57	100

atom per formula unit (a.p.f.u.)

	No_Comp	Cl_Comp	OH_Comp	Alk_Comp	Tot_Comp	FAp$_{th}$
Ca	4.819	4.835	4.782	4.879	4.871	5
Na	0.182	0.171	0.196	0.134	0.104	
P	2.859	2.852	2.901	2.848	2.883	3
Cl	0.000	0.085	0.000	0.000	0.050	
F	0.883	0.815	0.733	0.843	0.691	1
OH	0.117	0.100	0.267	0.157	0.259	
Charge Balance	+0.243	+0.285	+0.057	+0.348	+0.197	
Charge Balance + (CO_3)	0	0	0	0	0	
M site (Ca + Na)	5.001	5.006	4.978	5.013	4.975	5
T site (P)	2.859	2.852	2.901	2.848	2.883	3
T site + (CO_3)	2.980	2.994	2.930	3.022	2.982	
X site (F + Cl + OH)	1.000	1.000	1.000	1.000	1.000	1

4. Experimental summary and discussion

The results of the No_Comp experiment show that OCP reacts in the presence of F^- to form FAp. The OCP → FAp reaction also occurs in the presence of single competing anions (i.e. OH^-, Cl^- or $HCO_3^- + CO_3^{2-}$) at the same dissolved concentration of F^- (respectively, OH_Comp, Cl_Comp and Alk_Comp experiments), and even when the competing anions are all simultaneously present in solution at the same concentration (Tot_Comp experiment) (Tables 2, 3 and 6). The possibility of precipitation of F-phases other than FAp (e.g. fluorite CaF_2, whose XRD pattern overlaps that of FAp) was excluded by observation of the crystal morphology from ESEM images and the semi-quantitative chemical analyses from EDS spectra (Figs. 3 and 6). The application of the Rietveld algorithm to the XRD patterns from the solid phases collected at the end of the anionic competition experiments confirms FAp as the main phase, followed by HAp, in every experiment (Table 4). The calculation of cell parameters for all solid phases provides very similar values (Table 5) that can be solved in the Hexagonal system and are close to the cell parameters of the apatite group end-members.

Considering the theoretical OCP → FAp transformation (reaction (1)), our results show two main, though not fundamental, differences. The first one concerns the amount of F^- removed from solution: in the No_Comp experiment, the amount of F^- removed is 0.30 mmol (Table 3), while the stoichiometry of the reaction indicates 0.357 mmol; the second difference concerns the presence of some Ca in solution (0.03-0.04 mmol) and the amount of dissolved P, that ranges from 0.30 to 0.33 mmol and is about 17.6% higher than the expected value of 0.267 mmol (Table 3). The excess of P and the presence of Ca in solution, that should be related to the solubility product (K_{sp}) of FAp at the experimental conditions, indicate that at least 0.01 mmol of FAp is missing from the theoretical expected value of 0.357 mmol and, consequently, 0.01 mmol of F^- was not removed. The other effect that affects the uptake of F^- is the occupancy of the X site of apatite by OH^-: the a.p.f.u. calculations indicate that OH^- occupies up to 11.7% of the X site in the No_Comp experiment solid, while in the OH_Comp experiment solid the percentage of occupancy reaches 26.7% (Table 6).

The Cl^- competition has a very limited effect on the uptake of F^- (93% of F^- removed in the Cl_Comp experiment, Table 3), but also the OH^- competition affects the Cl^- entry into the X site. In fact, the chemical analysis and the a.p.f.u. calculation of the Cl_Comp experiment solid show that the X site occupancy is 81.5% F^-, 8.5% Cl^- and 10% OH^- (Table 6). The poor affinity of Cl^- can be explained by two reasons: (i) FAp is thermodynamically more stable than ClAp [26] and (ii) F^- can occupy the same crystallographic position of Cl^- but not vice versa [27].

The effect of carbonate species on F^- uptake in the Alk_Comp experiment is very limited (97% of F^- removed, Table 3). Actually, the possible role of CO_3^{2-} concerns more the T site, due to the $PO_4^{3-} \rightleftharpoons CO_3^{2-}$ substitution, rather than the X site for a hypothetical $(F^-, Cl^-, OH^-) \rightleftharpoons CO_3^{2-}$ substitution, as discussed by [25].

In the Tot_Comp experiment, where all the competing anions are tested simultaneously, the F^- removed decreases to 80% (Table 3), and the a.p.f.u. calculation of the corresponding FAp shows that OH^- is always the main competitor of F^- (X site occupancy 26%, Table 6).

Another effect observed in the OCP → FAp reaction is that the final pH tends to circum-neutral values, regardless of the initial OH^- concentration (Table 2). The OH^- neutralization can be explained by a different mechanism other than the ingress of OH^- in the FAp structure: the OCP → FAp reaction releases H^+ and monohydrogenphosphate (HPO_4^{2-}) into solution. The dissociation constants of hydrogen phosphate species:

$H_2PO_4^{-} \rightleftharpoons HPO_4^{2-} + H^+$ pKa2 = 7.20 (3)

$HPO_4^{2-} \rightleftharpoons PO_4^{3-} + H^+$ pKa3 = 12.37 (4)

indicate that $H_2PO_4^-$ and HPO_4^{2-} are the main species present in solution at circum-neutral pH values such as those measured at the end of the anionic competition experiments (Table 2). Moreover, the stability of $H_2PO_4^-$ is strongly affected by the formation of the ion-pair $NaHPO_4^-$ (Na^+ is from NaF salt used to provide F^- in solution) that can bind up to 19% of dissolved HPO_4^{2-}, as in the case of apatite supersaturation condition. Consequently, the subtraction of HPO_4^{2-} by complexation with Na^+ moves reaction (3) to the right, generating more H^+ in solution [28].

As mentioned in the Introduction, the use of OCP as the precursor of FAp for removing F^- from groundwater has been documented. The experimental evidence suggests that the OCP can be used as a precursor of FAp also in the presence of strong anionic competitors other than F^-. Conversely, the release of P from the OCP → FAp reaction should be taken into account to avoid an environmental adverse effect. For instance, the addition of Ca^{2+}, using soluble Ca-salts such as CaO or $Ca(OH)_2$, could bind dissolved PO_4^{3-} and F^- (and/or OH^-), so triggering the precipitation of FAp thanks to its low K_{sp} [29].

Finally, on the basis of a.p.f.u. calculations (Table 6), the empirical formula of each experimental phase can be written as follows:

No_Comp = $Ca_{4.819}Na_{0.182}(PO_4)_{2.859}(CO_3)_{0.122}(F_{0.883},OH_{0.117})$

Cl_Comp = $Ca_{4.835}Na_{0.171}(PO_4)_{2.852}(CO_3)_{0.142}(F_{0.815},OH_{0.100},Cl_{0.085})$

OH_Comp = $Ca_{4.782}Na_{0.196}(PO_4)_{2.901}(CO_3)_{0.028}(F_{0.733},OH_{0.267})$

Alk_Comp = $Ca_{4.879}Na_{0.134}(PO_4)_{2.848}(CO_3)_{0.174}(F_{0.843},OH_{0.157})$

Tot_Comp = $Ca_{4.871}Na_{0.104}(PO_4)_{2.883}(CO_3)_{0.098}(F_{0.691},OH_{0.259},Cl_{0.050})$

5. Conclusions

The reactivity of 0.223 mmol of octacalcium phosphate (OCP, $Ca_8(HPO_4)_2(PO_4)_4 \cdot 5H_2O$) in 50 mL solution has been tested in the presence of 0.368 mmol of F^-, Cl^-, OH^- and HCO_3^- + CO_3^{2-}. The results of the anionic competition experiments indicate that dissolved F^- is the anion mostly removed from solution in every experiment, and the removal efficiency decreases by 20% when all the anions are present in solution simultaneously.

Crystallographic and crystal chemistry analyses point out to the reaction of OCP into fluorapatite (FAp, $Ca_5(PO_4)_3F$) as the main apatitic phase that is always formed. The crystallochemical analysis of the resulting FAp indicates that OH^- is the most important competitor of F^-, especially when the OCP → FAp reaction occurs at uncommon high pH values (pH ~ 12).

From experimental evidence, it can be said that OCP is a crystalline precursor of apatite and can be used to efficiently remove dissolved F^- from polluted water by forming FAp even in the presence of high concentrations of possible anionic competitors. These peculiar features of OCP could also contribute to the environmental research on the use of apatite for the uptake of toxic metals through the ion-exchange property of the M site (e.g. $Ca^{2+} \rightleftharpoons Pb^{2+}$, $Ca^{2+} \rightleftharpoons Cd^{2+}$, etc.).

Acknowledgments

The authors declare that no conflict of interest exists. This research is a part of the PhD project of Alfredo Idini, funded by MIUR (Ministry of University and Research, Italy) in the frame of the Italian National Program PON R&I 2014-2020 “Innovative doctorates with industrial characterization.” This research is also financially supported by the FLOWERED project (Coordinator Giorgio Ghiglieri, University of Cagliari, Italy), a Horizon2020 program funded by the European Commission (Grant Agreement N. 690378) (www.floweredproject.org). We wish to thank Francesca Podda and Dario Fancello from the University of Cagliari (Italy) for their helpful support with the ESEM and ICP-OES analyses.

References

[1] M. Pasero, A. R. Kampf, C. Ferraris, I. V. Pekov, J. Rakovan, and T. J. White, “Nomenclature of the apatite supergroup minerals,” *Eur. J. Mineral.*, vol. 22, no. 2, pp. 163–179, 2010.

[2] J. M. Hughes and J. F. Rakovan, “Structurally Robust, Chemically Diverse: Apatite and Apatite Supergroup Minerals,” *Elements*, vol. 11, no. 3, pp. 165–170, June 2015.

[3] I. Jarvis, “Phosphorite geochemistry: state-of-the-art and environmental concerns,” *Eclogae Geol. Helv.*, vol. 87, no. 3, pp. 643–700, 1994.

[4] J. F. Rakovan and J. D. Pasteris, “A technological gem: Materials, medical, and environmental mineralogy of apatite,” *Elements*, vol. 11, no. 3, pp. 195–200, June 2015.

[5] S. V. Dorozhkin, “Multiphasic calcium orthophosphate ($CaPO_4$) bioceramics and their biomedical applications,” *Ceram. Int.*, vol. 42, no. 6, pp. 6529–6554, 2016.

[6] T. Sakae, H. Nakada, and John P. LeGeros, “Historical Review of Biological Apatite Crystallography,” *J. Hard Tissue Biol.*, vol. 24, no. 2, pp. 111–122, 2015.

[7] B. Wopenka and J. D. Pasteris, “A mineralogical perspective on the apatite in bone,” *Materials Science*

and Engineering C, vol. 25, pp. 131–143, 2005.

[8] M. J. Arellano-Jiménez, R. García-García, and J. Reyes-Gasga, “Synthesis and hydrolysis of octacalcium phosphate and its characterization by electron microscopy and X-ray diffraction,” *J. Phys. Chem. Solids*, vol. 70, no. 2, pp. 390–395, 2009.

[9] O. Suzuki, “Octacalcium phosphate (OCP)-based bone substitute materials,” *Jpn. Dent. Sci. Rev.*, vol. 49, no. 2, pp. 58–71, 2013.

[10] R. Xin, Y. Leng, and N. Wang, “In situ TEM examinations of octacalcium phosphate to hydroxyapatite transformation,” *J. Cryst. Growth*, vol. 289, no. 1, pp. 339–344, 2006.

[11] A. Carino, C. Ludwig, A. Cervellino, E. Mueller, and A. Testino, “Formation and Transformation of Calcium Phosphate Phases under Biologically Relevant Conditions : Experiments and modelling,” *Acta Biomaterialia*, vol. 74, pp. 478-488, 2018.

[12] A. Idini, E. Dore, D. Fancello, G. Ghiglieri, and F. Frau, “Dissolved fluoride removal by OCP, a precursor of apatite,” *E3S Web Conf.*, vol. 98, pp. 4, 2019.

[13] E. T. Everett, “Critical reviews in oral biology & medecine: Fluoride’s effects on the formation of teeth and bones, and the influence of genetics,” *J. Dent. Res.*, vol. 90, no. 5, pp. 552–560, 2011.

[14] D. L. Ozsvath, “Fluoride and environmental health: A review,” *Rev. Environ. Sci. Biotechnol.*, vol. 8, no. 1, pp. 59–79, 2009.

[15] S. Ayoob and A. K. Gupta, “Fluoride in Drinking Water : A Review on the Status and Stress Effects Fluoride in Drinking Water : A Review,” *Crit. Rev. Environ. Sci. Technol.*, vol. 36, no. 6, pp. 433–487, 2006.

[16] World Health Organization, "Fluoride in drinking-water," WHO, pp. 17, 2004.

[17] A. Idini, E. Dore, D. Fancello, and F. Frau, “Defluoridation of water through the transformation of octacalcium phosphate into fluorapatite,” *Heliyon*, vol. 5, e02288, pp. 9, 2019.

[18] A. Idini, F. Frau, L. Gutierrez, E. Dore, G. Nocella, and G. Ghiglieri, "Application of octacalcium phosphate with an innovative household-scale defluoridator prototype and behavioral determinants of

its adoption in rural communities of the East African Rift Valley," I*ntegr. Environ. Assess. Manag.*, accepted on 6 March 2020, pp.15, 2020.

[19] W. E. Brown, “Octacalcium phosphate and hydroxyapatite,” *Nature*, vol. 196, pp. 1048–1050, 1962.

[20] A. W. Frazier *et al.*, “Crystallographic properties of fertilizer compounds,” *TVA Bulletin Y-217*, NFERC, United States, pp. 983, 1991.

[21] A. Boultif and D. Louër, “Powder pattern indexing with the dichotomy method,” *J. Appl. Crystallogr.*, vol. 37, no. 5, pp. 724–731, 2004.

[22] G. S. Smith and R. L. Snyder, “FN : A criterion for rating powder diffraction patterns and evaluating the reliability of powder-pattern indexing ,” *J. Appl. Crystallogr.*, vol. 12, no. 1, pp. 60–65, 1979.

[23] W. I. F. David, “Powder diffraction: Least-squares and beyond,” *J. Res. Natl. Inst. Stand. Technol.*, vol. 109, no. 1, pp. 107–123, 2004.

[24] A. Le Bail, “Monte Carlo indexing with McMaille,” *Powder Diffr.*, vol. 19, no. 3, pp. 249-254, 2004.

[25] A. Awonusi, M. D. Morris, and M. M. J. Tecklenburg, “Carbonate assignment and calibration in the Raman spectrum of apatite,” *Calcif. Tissue Int.*, vol. 81, no. 1, pp. 46–52, 2007.

[26] C. Drouet, “A comprehensive guide to experimental and predicted thermodynamic properties of phosphate apatite minerals in view of applicative purposes,” *J. Chem. Thermodyn.*, vol. 81, pp. 143–159, 2015.

[27] J. M. Hughes *et al.*, “Solid solution in the fluorapatite-chlorapatite binary system: High-precision crystal structure refinements of synthetic F-Cl apatite,” *Am. Mineral.*, vol. 99, no. 2–3, pp. 369–376, 2014.

[28] P. R. Patel, T. M. Gregory, and W. E. Brown, “Solubility of $CaHPO_4 \cdot 2H_2O$ in the quaternary system $Ca(OH)_2$-H_3PO_4-NaCl-H_2O at 25 °C,” *J. Res. Natl. Bur. Stand. Sect. A Phys. Chem.*, vol. 78A, no. 6, pp. 675-681, 1974.

[29] C. Wei, Y. Zhu, F. Yang, J. Li, Z. Zhu, and H. Zhu, “Dissolution and solubility of hydroxylapatite and fluorapatite at 25°C at different pH,” *Res. J. Chem. Environ.*, vol. 17, no. 11, pp. 57–61, 2013.

SUPPLEMENTAL DATA

Mineralogical-geochemical study of the anionic competition effect on the octacalcium phosphate reaction into apatite: implications on water defluoridation

Alfredo Idini, Franco Frau

Department of Chemical and Geological Sciences, University of Cagliari, 09042, Monserrato (CA), Italy

Table SD1. List of the 24 indexed reflections of the synthesized OCP used for the anionic competition experiments.

No.	Pos. [°2θ]	d-spacing [Å]	FWHM [°2θ]	Rel. Int. [%]	Backgr. [cts]	h	k	l
1	4.7407	18.62505	0.1224	100	1510	1	0	0
2	9.4451	9.35612	0.0612	8.43	1101.5	2	0	0
3	9.7606	9.05445	0.102	7.66	1071.39	0	1	0
4	16.0634	5.51312	0.1632	3.34	608.94	2	1	0
5	22.7354	3.90807	0.1428	3.46	334	3	-1	-1
6	24.3102	3.65836	0.1632	4.78	319	3	0	1
7	26.0654	3.41586	0.1632	8.85	304	1	-2	1
8	26.8079	3.3229	0.1224	3.79	298	0	2	-1
9	27.2249	3.27295	0.102	5.45	295	2	-3	0
10	27.6633	3.22206	0.1632	3.55	291	4	0	1
11	28.0123	3.18271	0.1224	3.97	288	1	-3	0
12	29.1839	3.05756	0.1632	3.49	278	5	1	0
13	31.405	2.84619	0.2448	10.92	260	5	0	1
14	31.7384	2.81705	0.1428	14.67	257	6	-1	-1
15	32.0787	2.78793	0.1428	7.82	254	4	1	1
16	32.505	2.75234	0.1632	5.48	250	4	2	0
17	33.5204	2.67125	0.102	16.07	242	7	0	0
18	33.8789	2.64379	0.1632	6.24	239	6	1	0
19	34.3864	2.60593	0.1428	3.93	235	1	-3	-1
20	35.0155	2.56054	0.1632	3.86	229	7	-3	0
21	40.7799	2.21091	0.1632	3.54	201	7	-4	0
22	42.7952	2.11135	0.1224	3.39	194	3	-2	-2
23	46.4035	1.95522	0.2448	3.28	183	5	-2	2
24	49.6988	1.83302	0.2448	3.02	172	3	2	2

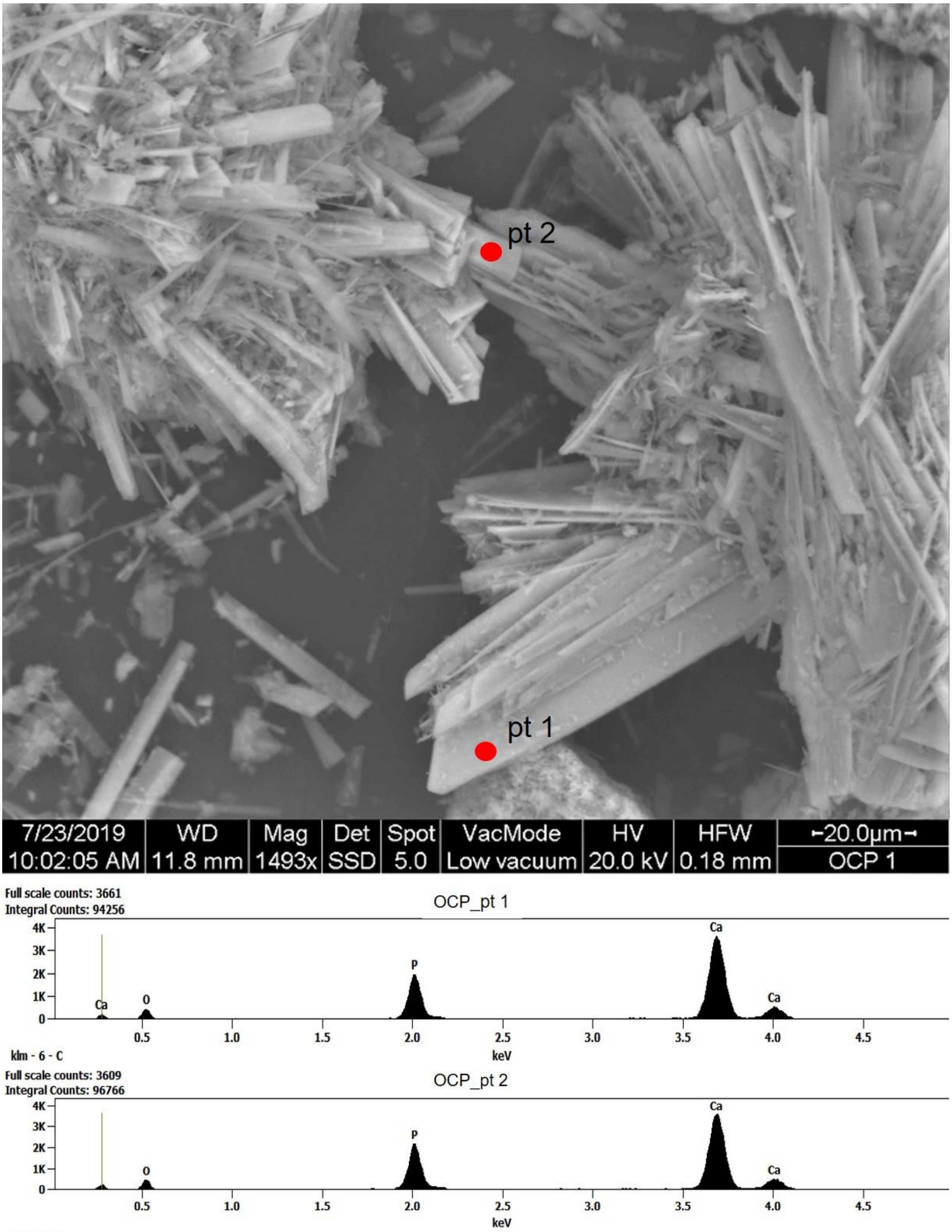

Figure SD2. ESEM image and EDS spectra of the synthesized OCP used for the anionic competition experiments.

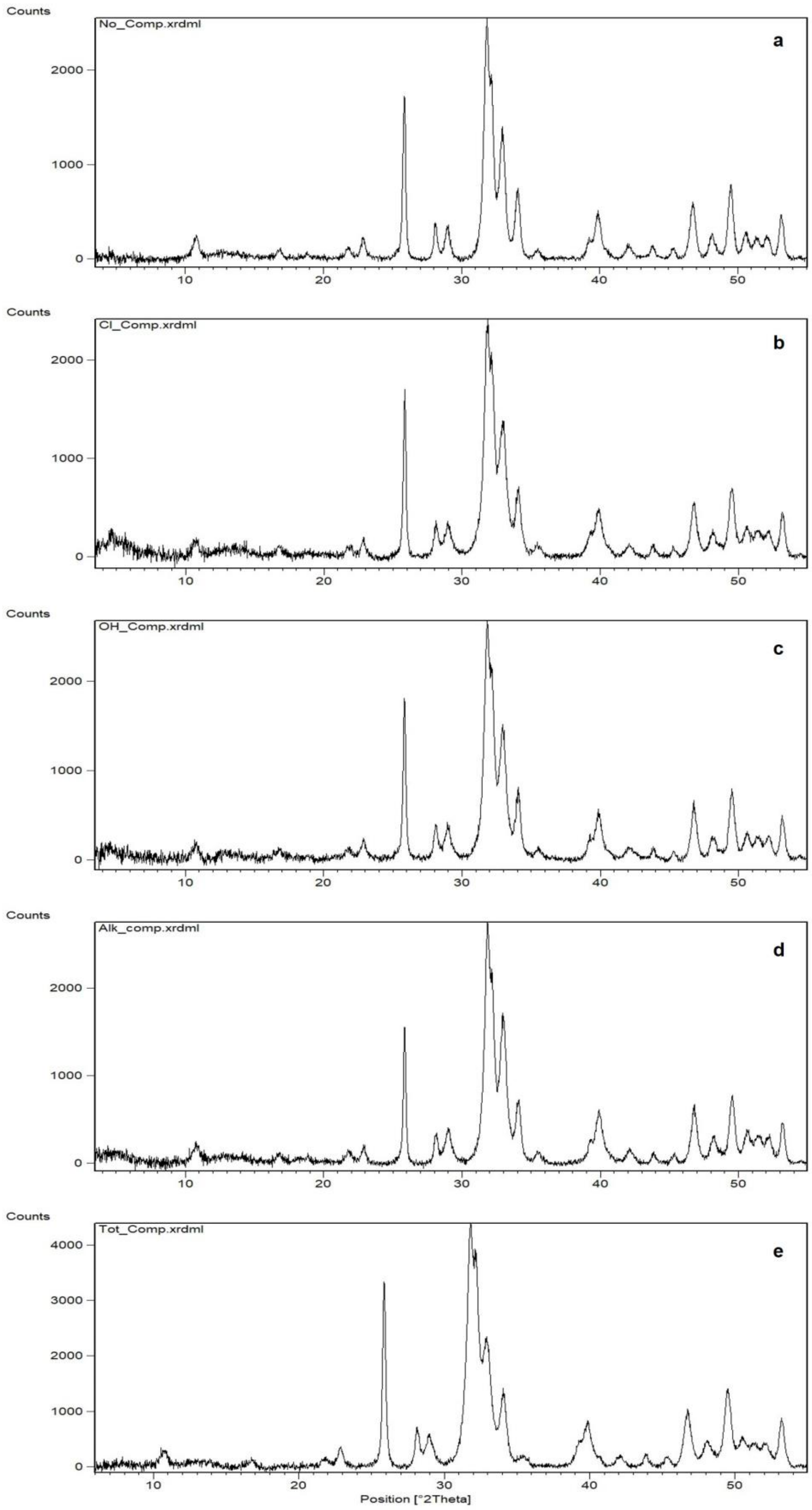

Figure SD3. XRD patterns of the fluorapatite (FAp) collected after the No_Comp (a), Cl_Comp (b), OH_Comp (c), Alk_Comp (d) and Tot_Comp (e) experiments.

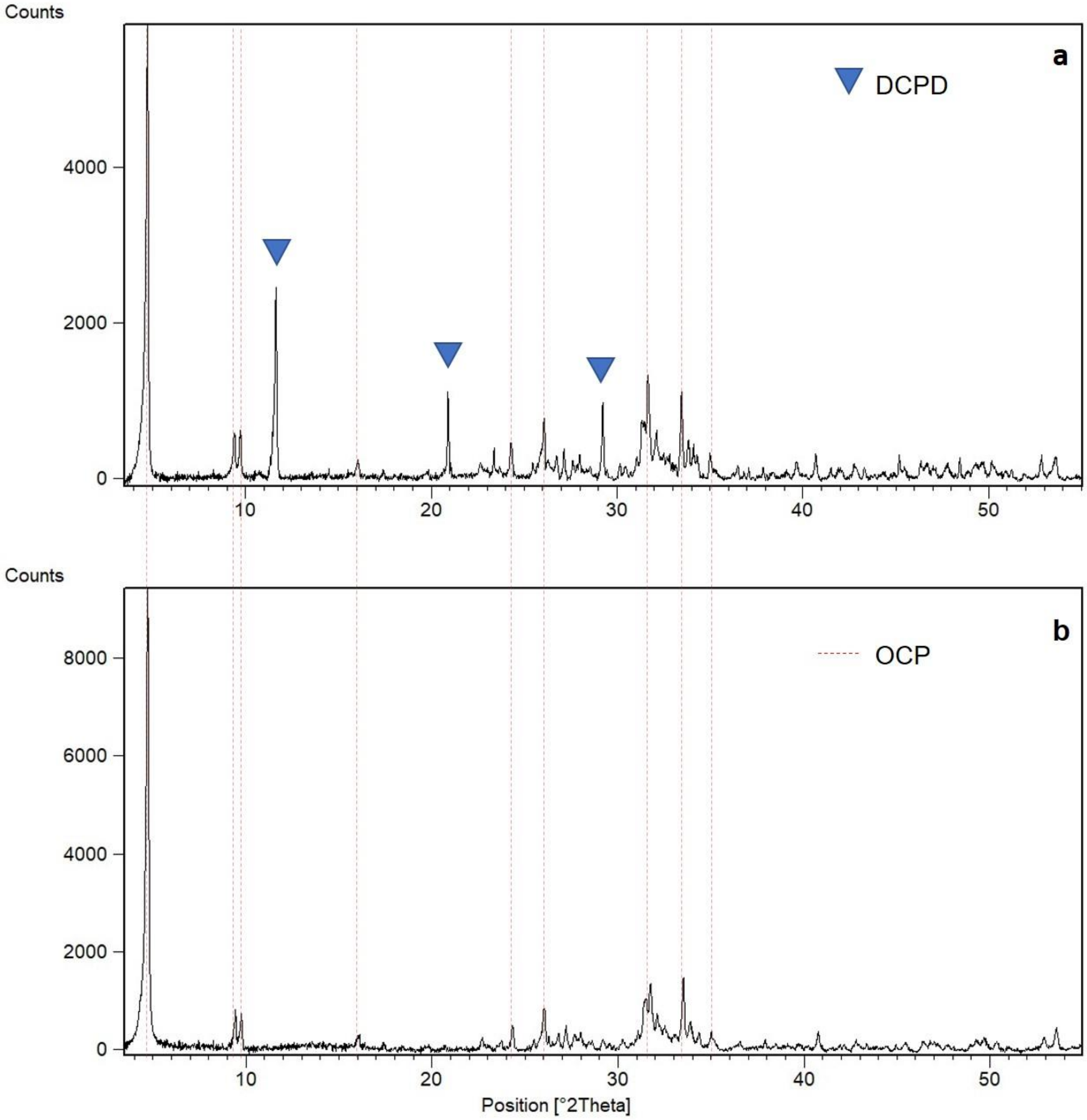

Figure SD4. XRD patterns of initial OCP (b) and final OCP (a) collected after immersion in deionized water in the absence of any of the competing anions (initial pH =7, final pH = 5.62). The dotted lines indicate the OCP peaks and the blue triangles identified the peaks of the DCPD phase, showing that OCP tends to retrocede to DCPD when other anions are not present in solution.

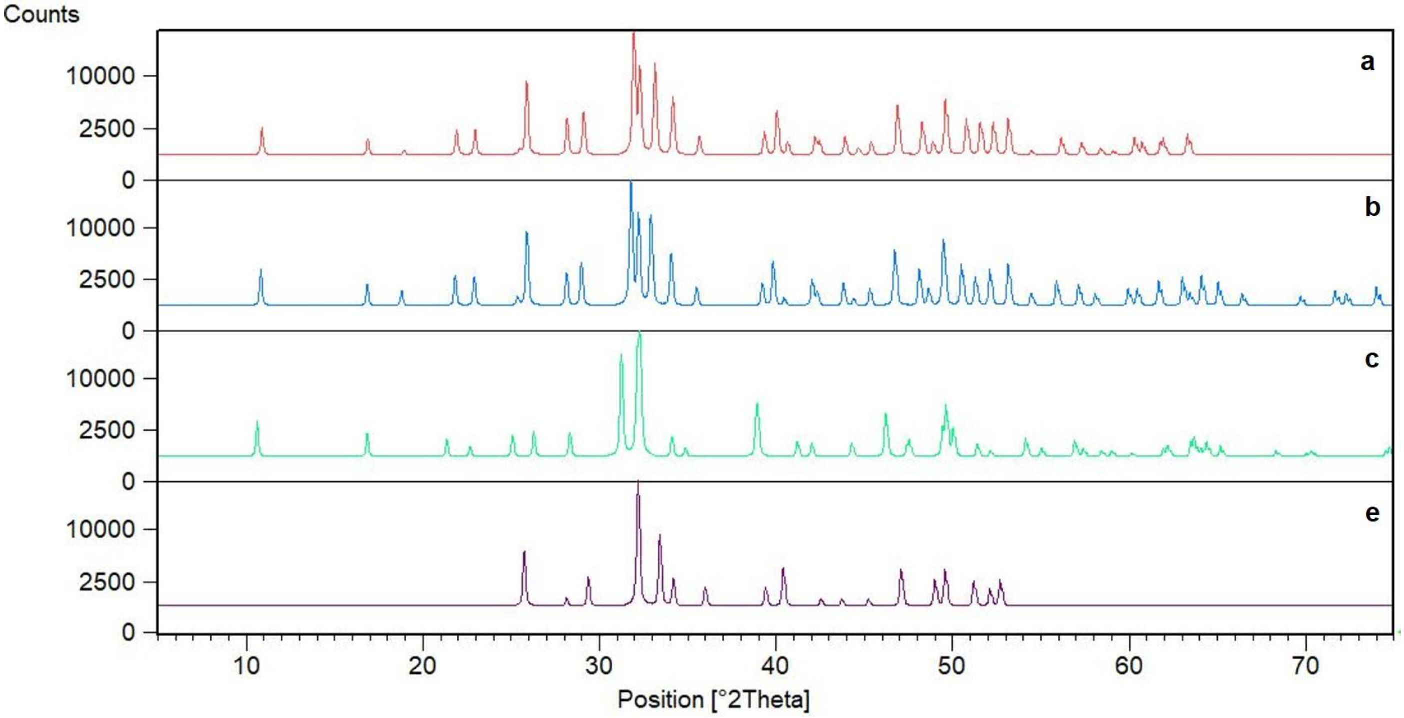

Figure SD5. Comparison of the XRD reference patterns of (a) fluorapatite (FAp, PDF code 00-015-0876); (b) hydroxyapatite (HAp, PDF code 00-009-0432); (c) chlorapatite (ClAp, PDF code 00-033-0271); (e) carbonate-apatite (CarbAp, PDF code 00-019-0272).

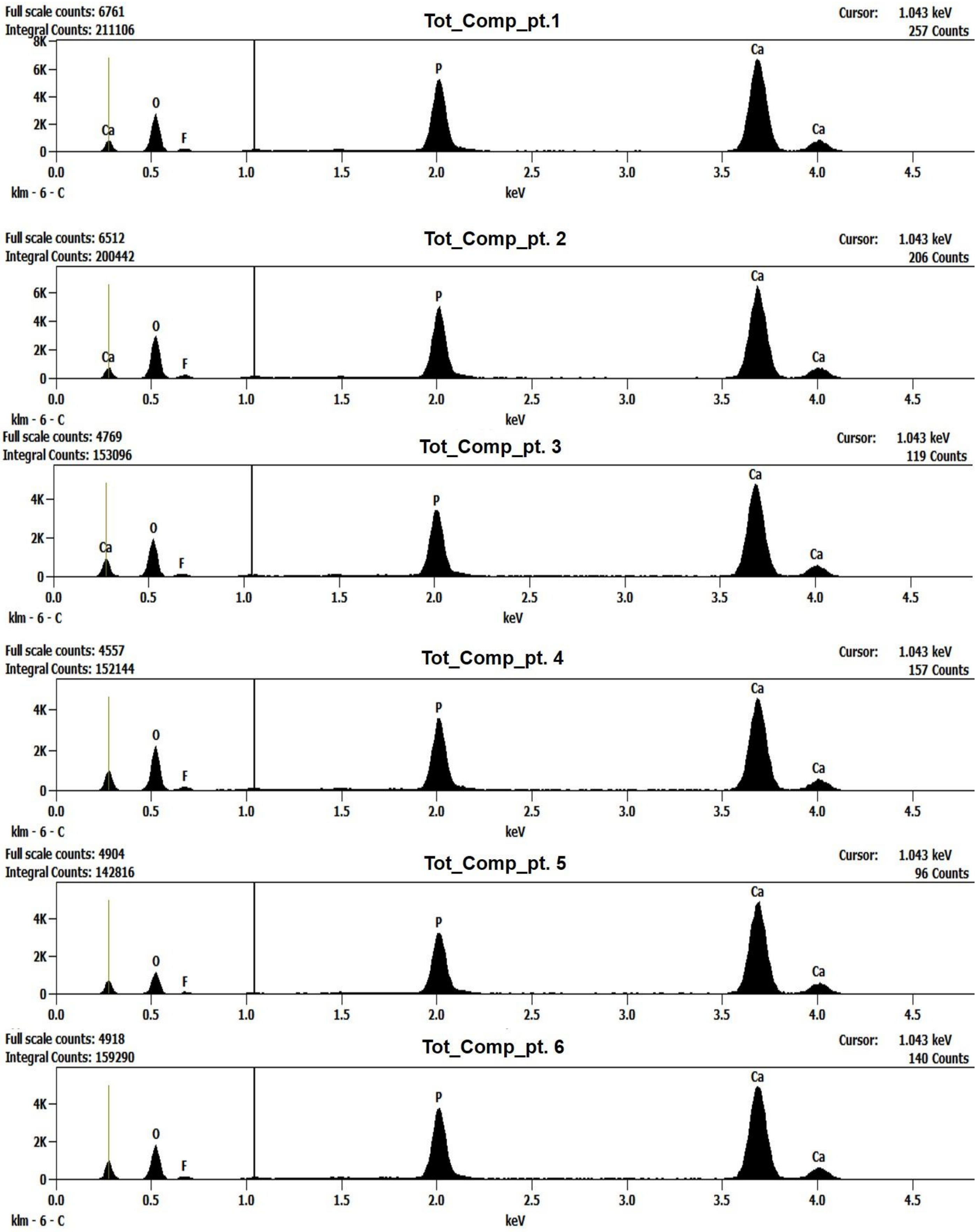

Figure SD6. EDS spectra of the spot analyses performed on FAp from the Tot_Comp experiment. The ESEM images of the analysed sample are visible in Fig. 6 of the manuscript.

CHAPTER III

Application of octacalcium phosphate with an innovative household-scale defluoridator prototype and behavioral determinants of its adoption in rural communities of the East African Rift Valley

Alfredo Idini,*† Franco Frau,† Luciano Gutierrez,‡ Elisabetta Dore,† Giuseppe Nocella,§ and Giorgio Ghiglieri†

†Department of Chemical and Geological Sciences, University of Cagliari, Cagliari, Italy ‡Department of Agricultural Sciences and Desertification Research Centre, University of Sassari, Sassari, Italy §School of Agriculture, Policy and Development, University of Reading, Reading, United Kingdom

Published 6 March 2020

By Integrated Environmental Assessment and Management- John **Wiley** & Sons, Inc.

Integrated Environmental Assessment and Management — Volume 00, Number 00—pp. 1–15
Received: 9 September 2019 | Returned for Revision: 14 November 2019 | Accepted: 6 March 2020

Special Series

Application of Octacalcium Phosphate with an Innovative Household-scale Defluoridator Prototype and Behavioral Determinants of its Adoption in Rural Communities of the East African Rift Valley

Alfredo Idini,† Franco Frau,† Luciano Gutierrez,‡ Elisabetta Dore,† Giuseppe Nocella,§ and Giorgio Ghiglieri†*

†Department of Chemical and Geological Sciences, University of Cagliari, Cagliari, Italy
‡Department of Agricultural Sciences and Desertification Research Centre, University of Sassari, Sassari, Italy
§School of Agriculture, Policy and Development, University of Reading, Reading, United Kingdom

EDITOR'S NOTE:

This article is part of the special series "Improving Water Security in Africa." The work is the culmination of 7 Horizon 2020 projects focused on the environmental and social challenges of improving water security in African countries.

ABSTRACT

Natural fluoride contamination of drinking water is a serious issue that affects several countries of the world. Its negative health impact is well documented in the East African Rift Valley, where water consumption with fluoride (F^-) concentration greater than 1.5 mg/L can cause fluorosis to people. Within the framework of the European Union (EU) Horizon 2020 FLOWERED project, we first designed an effective defluoridation device based on innovative application of octacalcium phosphate (OCP) and then explored its acceptance within rural communities. The prototype (FLOWERED Defluoridator Device [FDD]) essentially is composed of a 20-L tank and a recirculating pump that guarantees the interaction between water and OCP. The device is powered by a car battery for a fixed pumping working time using a fixed amount of OCP for every defluoridation cycle. The results of tests performed in the rural areas of Tanzania show that a standardized use of the prototype can lower the dissolved F^- from an initial concentration of 21 mg/L to below the World Health Organization (WHO) drinkable limit of 1.5 mg/L in 2 h without secondary negative effects on water quality. The approximate cost of this device is around US$220, whereas that of OCP is about $0.03/L of treated water. As with any device, acceptance requires a behavioral change on behalf of rural communities that needed to be investigated. To this end, we piloted a survey to explore how psychological and socioeconomic factors influence the consumption of fluoride-free water. Results show that the adoption of FDD and OCP is more appealing to members of the rural communities who are willing to pay more and have a high consumption of water. Moreover, we suggest that given the low level of knowledge about fluorosis diseases, the government should introduce educational programs to make rural communities aware of the negative health consequences. *Integr Environ Assess Manag* 2020;00:1–15. © 2020 The Authors. *Integrated Environmental Assessment and Management* published by Wiley Periodicals LLC on behalf of Society of Environmental Toxicology & Chemistry (SETAC)

Keywords: Octacalcium Phosphate (OCP)   Fluoride contamination of groundwater   Defluoridation method
RANAS behavioral model   Fluorosis

INTRODUCTION

Geogenic contamination of fluoride (F^-) in groundwater above the World Health Organization (WHO) limit of 1.5 mg/L (WHO 2017) is an issue that affects the health of about 260 million people in many countries worldwide (Amini et al. 2008; Biswas et al. 2017; Akuno et al. 2019; Chowdhury et al. 2019). Fluoride-rich drinking water is a primary source of dietary F^- that can overcome the tolerable upper intake level (UL) of 10 mg/d for adults and from 0.7 to 2.2 mg/d for infants and children (US Institute of Medicine 2006). High F^- intake causes different adverse health effects on teeth and bones, such as dental and skeletal fluorosis, and toxic effects on nonskeletal tissues, such as the nervous system, cardiovascular system, liver, kidney, reproductive system, thyroid, and the

This article contains online-only Supplemental Data.

* Address correspondence to alfredo.idini@gmail.com

DOI: 10.1002/ieam.4262

progeny, which have been extensively studied in the last few years (Ozsvath 2009; Barbier et al. 2010; Wei et al. 2019). Endemic fluorosis, both skeletal and nonskeletal, is still diagnosed in many countries (Tanzania, Kenya, Ethiopia, India, China, etc.) (Hunter et al. 2010) especially where rural communities are exposed to fluoride-rich groundwater.

Within the framework of the Horizon 2020 European-funded "de-FLuoridation technologies for imprOving quality of WatEr and agRo-animal products along the East African Rift Valley in the context of aDaptation to climate change" (FLOWERED) project (www.floweredproject.org), we focused our research on the development and acceptance of an innovative defluoridation method that can be effective for rural communities, which is mandatory to achieve one of the Sustainable Development Goals of United Nations, specifically Goal 6: Clean water and sanitation (https://sustainabledevelopment.un.org/sdg6).

An effective and frugal defluoridation method should be 1) low cost, to make even the poorest part of the population able to access to drinkable water; 2) low tech based, easy to use and distribute, to reach the population regardless of where people live; 3) highly efficient, to avoid waste of water resource; and 4) free of collateral effects on the overall water quality. Despite the great number of technologies and materials successfully tested at a laboratory scale, the challenge to find an effective and reliable in-situ method is still open (Ayoob et al. 2008; Yadav et al. 2018). There are several reasons why the defluoridation of water in rural contexts is an open challenge. Up to now, this seems to be determined by the lack of technology transfer to a feasible method in terms of overall cost and power supply (e.g., reverse osmosis), complexity of the method (e.g., electrocoagulation), cost of sorbent supply and management (e.g., most of synthetic compounds), or low F^- removal capacity (e.g., bone char [BC] and many natural materials) (Khairnar et al. 2015; Mumtaz et al. 2015; Velazquez-Jimenez et al. 2015). Furthermore, the acceptance of any new defluoridation method on behalf of rural communities is critical for policymakers and other stakeholders if they want to facilitate the adoption of the technology (Sorlini et al. 2011; Datturi et al. 2015). Therefore, the objectives of the present study are to conduct in-situ defluoridation tests with a new device loaded with octacalcium phosphate (OCP; $Ca_8(HPO_4)_2(PO_4)_4 \cdot 5H_2O$), and to explore rural communities' acceptance of this new technology. The abovementioned tests were performed in northern Tanzania to assess the applicability of this new technology in the same environmental conditions faced by potential adopters of these rural populations. The starting point for the development of the technology was based on the absorption and accumulation mechanisms of F^- in human tissues. The inorganic part of human bones and teeth consists of bioapatite, a mineral with a general formula similar to hydroxyapatite (HAP; $Ca_{5-x}(PO_4)_{3-y}OH_{1-z}$, where the most common substitutions are $x = Na^+$, Mg^{2+}; $y = CO_3^{2-}$, HPO_4^{2-}; $z = F^-$, Cl^-) (Wopenka and Pasteris 2005). The formation of bioapatite is subsequent to the formation of its precursor: the OCP (Markovic and Chow 2010; Carino et al. 2018). One of the processes of bioaccumulation of F^- into the hard tissue is the formation of fluorapatite (FAP; $Ca_5(PO_4)_3F$) instead of bioapatite (Everett 2011). The underpinning key concept of the method for water defluoridation is to transfer the mechanism of F^- absorption by the human body to a defluoridator device based on the same mineralogical principle. A previous research paper showed that OCP has empirical F^- removal capacity of 25.7 mg/g; the water treatment lasts a few hours and is free of collateral effects (Idini et al. 2019). To meet the requirement "easy to use" targeted for rural communities of the East African Rift Valley (EARV), a standardization of the defluoridation procedure and use of the prototype named "FLOWERED Defluoridator Device" (FDD) is presented. Importantly, the purpose of the standardized use is to guarantee the defluoridation of water regardless of a defined range of the initial F^- concentration.

However, the availability of a new efficient defluoridation method that allows EARV rural communities to drink fluoride-free water may not be enough to increase the consumption of safe water. Switching from untreated drinking water to safe defluoridated water can be challenging for individuals living in these rural communities. This is because the use of defluoridated water and the acceptance of any new device such as the OCP and FDD can be influenced by socioeconomic and psychological factors that may affect the adoption of the new healthy drinking behavior. Thus, we piloted a survey where the Risk, Attitude, Norm, Ability, Self-regulation (RANAS) model (Mosler 2012) was applied to explore how these factors can influence the consumption of fluoride-free water in EARV rural communities.

STUDY AREA

Tanzanian scenario: Fluoride, fluorosis, and its mitigation

In the last decades, several kinds of research have clarified that the geogenic origin of F^- contamination is strictly linked to the water interaction with the volcanic lithology of the EARV and that high F^- concentration is associated to sodium-bicarbonate water facies (Giaciri and Davies 1993; Gizaw 1996; D'Alessandro 2006; Rango et al. 2009; Ghiglieri et al. 2012; Olaka et al. 2016). It is important to emphasize that this hydrogeochemical feature is the same worldwide in the fluorotic belts (Chowdhury et al. 2019). Collecting 213 data from cited literature of EARV fluorotic areas (Giaciri and Davies 1993; Tekle-Haimanot et al. 2006; Ghiglieri et al. 2012; Olaka et al. 2016; Malago et al. 2017), it can be estimated that the range of geogenic contamination of waters by F^- is under 40 mg/L in 97% of water sources used for human consumption (Figure 1).

Tanzanian occurrence of F^- rich groundwater and its relationship with fluorosis has been documented since 1944 (Grech and Latham 1964). Current Tanzanian regulation and guideline for drinking water set the permissible F^- limit to

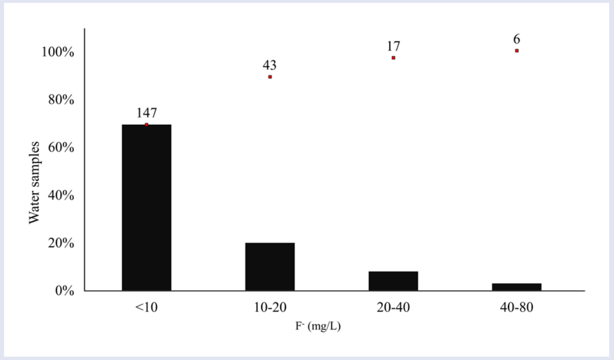

Figure 1. Range and distribution of F⁻ contamination in 213 samples of natural water of EARV (Giaciri and Davies 1993; Tekle-Haimanot et al. 2006; Ghiglieri et al. 2012; Olaka et al. 2016; Malago et al. 2017). Red squares represent the number of samples in each range. EARV = East African Rift Valley.

4 mg/L (Tanzania Bureau of Standard 2018). In 2010 the Ministry of Water and Irrigation (MoWI) issued the National Water Quality Management and Pollution Control Strategy 2010 (SMEC 2010) in which it explained that about 10.5 million people are exposed to drinking water with F⁻ concentration above the WHO limit; this population lives in the regions of Arusha, Manyara, Singido, and Shinyanga (Figure 2). Up to now, not only the rural communities have been exposed to fluorosis but also the urban population, as happens in the urban area of Arusha (Chacha et al. 2018). The MoWI document highlights that, despite successful research (Mbabaye et al. 2017), outcomes and development efforts have not been widely implemented, and many people still consume water containing F⁻ levels above the healthy limit.

MATERIALS AND METHODS

Synthesis of octacalcium phosphate (OCP)

The OCP was synthesized in 2 steps (Supplemental Data Table S1): 1) synthetic brushite (dicalcium phosphate dihydrate [DCPD]; $CaHPO_4 \cdot 2H_2O$) was synthesized at room temperature adding 0.366 moles of both H_3PO_4 and $CaCO_3$ in 2 L of tap water (Supplemental Data Table S2) acidified at pH 1.5 with HCl. After precipitation, the DCPD was recovered through filtration and dried at 40 °C; 2) 1.2 g of DCPD was added to 500 mL of tap water, and the solution was then heated in a stove at 60 °C for 65 h; the solid was recovered through filtration and dried at room temperature. The synthesized OCP is a white powder with particle size in

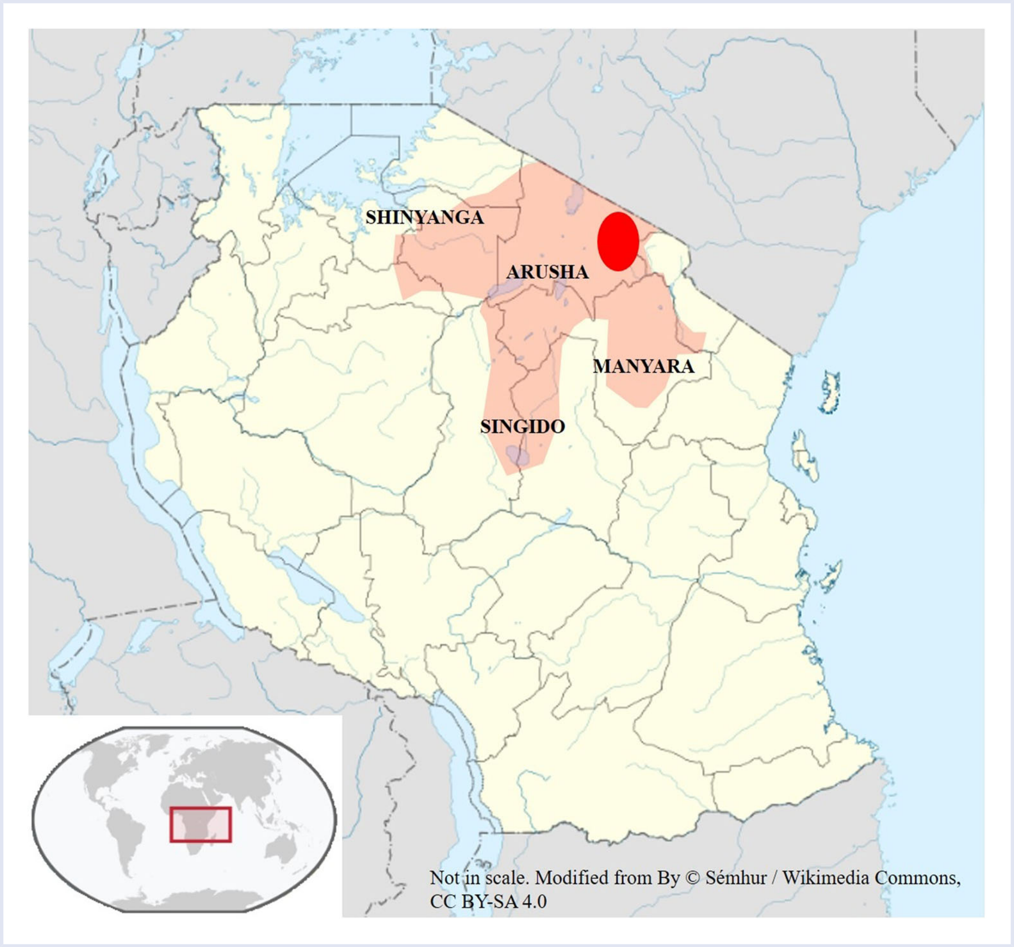

Not in scale. Modified from By © Sémhur / Wikimedia Commons, CC BY-SA 4.0

Figure 2. Sketch map of fluorotic regions of Tanzania, extrapolated from Malago et al. (2017). The red circle indicates the area of defluoridation tests and interviews.

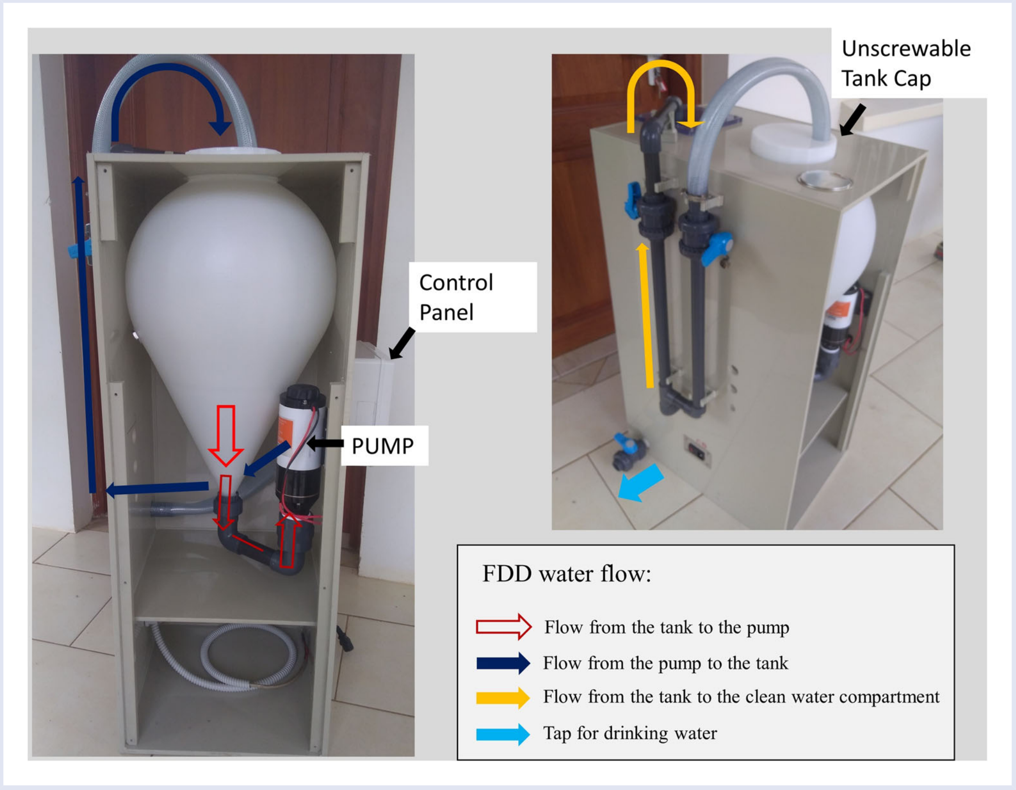

Figure 3. The FLOWERED Defluoridator Device (FDD) and its recirculating water circuit.

the range of 14 to 125 µm, determined using a mesh sieves. All the reagents were of analytical grade (Carlo Erba reagents ACS-for analysis) and used without further purification. The synthesis procedure was carried out in the laboratories of the Department of Chemical and Geological Sciences (DCGS), University of Cagliari, Italy.

FLOWERED Defluoridator Device (FDD)

The FDD is a conceptual reproduction of a laboratory batch experiment designed to meet the rural household application. It is composed of a 25-L polyethylene terephthalate (PET) drop-shape tank (where OCP and water interact) (Figure 3). An electric recirculating-macerator pump (model LIGHTEU-SEAFLO 12 V −12 A × h, nominal water volume flow rate 45 L/min; 32.2 × 15.3 × 10.9 cm; weight 2.6 kg) is necessary to maintain the mixing between OCP and water. The pump is powered by a car battery (locally bought, model FB 38B19L-MF, voltage 12 V and capacity 28 A × 5 h–35 A × 20 h, Furukawa Battery CO Ltd) to guarantee a recirculating flow rate of 22 L/min constant for 3 h. The FDD battery can be recharged by different power supplies (e.g., solar panel, power generator, electric grid). An elastic nylon net, located in a second compartment (clean water compartment), is necessary to separate exhausted sorbent from water and to collect the treated water. The pump, tank, and compartment for treated water are connected by pipes and faucets and are assembled in a 100 × 43 × 55−cm plastic case. The total weight is 23 kg. The FDD has been designed and assembled by the FLOWERED technological partner Hydro Technical Engineering (HTE) s.r.l. (Verona, Italy).

Defluoridation field tests

The defluoridation field tests (Figure 4; Supplemental Data Figures S1, S2, S3, and S4) were performed in different areas using 3 natural waters (labeled BUL for Bule Bule spring, NGO for Maji ya Chai spring, and KYU for Ngarenanyuki borehole) with different initial F^- concentrations (F^- i.c.) (Table 1). The reason for choosing those areas was because the geogenic contamination of F^- in the Arusha Region is well documented. Besides, the selected water points are representative of the range of F^- concentration of the water the rural population drinks. Another important criterion was the finding that in those areas a defluoridation method is not available at all.

All the defluoridation field tests were performed as follows: 20 L of natural water was collected directly from the spring or borehole, poured directly with 80 g of OCP into the FDD through the unscrewable cap of the tank, and the pump was turned on. The concentration of F^- in the water was measured during the FDD working time. After the F^- concentration had decreased below the WHO drinkable limit, the faucet of the flow from the pump to the tank was closed and the faucet of the flow from the pump to the treated water compartment was opened. In the second compartment, an elastic nylon net recovered the exhausted OCP powder. At the end of the process, the treated water was collected from the tap (Figure 3) and the exhausted OCP was recovered from the

Figure 4. Site of defluoridation experiment in rural areas around Mount Meru, Northern Tanzania. On the left side the FLOWERED Defluoridator Device (FDD) during defluoridation test and behind a typical water point used for human and animal consumptions.

recovery compartment. The FDD was carefully washed with the same water as the next experiment. Considering the OCP empirical removal F^- capacity of 25.7 mg/g, obtained during lab-scale batch experiments performed with the OCP synthesized with the same method (Idini et al. 2019), and the aim of obtaining the defluoridation in about 2 h of FDD working time, different dosages of OCP (solid-to-liquid ratio [S/L] equals to 1, 2, and 4 g/L) were tested using NGO water (F^- i.c. = 20.9 mg/L). The choice of 2 h as optimal FDD working time will be discussed in *Defluoridation tests*.

Chemical analyses and mineralogical characterization

At the field experiment sites, the pH and the F^- concentrations of both untreated and treated water were determined, respectively, using a portable pH meter (Hanna) and a potentiometer (HQ30d Portable meter, HACH) equipped with an ion-selective F^- electrode (IntelliCALTM ISEF121, HACH). Fluoride measurements were performed by adding the TISAB III solution (Total Ionic Strength Adjustment Buffer, concentrated for F^- analyses, HACH), in the recommended volume ratio 1:5 (v/v) between TISAB III and standard or sample solutions, to buffer the pH and avoid the interference of metal complexes. For each defluoridation test, portions of untreated water and water recovered at the end of reaction time were collected and stored in a polyethylene (PE) bottle at 4 °C to perform chemical analysis. Before chemical analysis, all water samples were filtered (0.4-μm pore size, OlimPeak, Teknokroma). The concentrations of major ions were determined through ion chromatography (IC; Dionex ICS3000) and inductively coupled plasma optical emission spectroscopy (ICP-OES; ARL Fisons 3520), and the total alkalinity was determined with the Gran method.

The mineralogical characterization of OCP, before and after the tests, was performed collecting X-ray diffraction (XRD) patterns in the 3.5° to 55° 2θ angular range on an automated PANalytical X'pert Pro diffractometer, with Ni-filtered Cu-Kα_1 radiation ($\lambda = 1.54060$ Å), operating at 40 kV and 40 mA, using the X'Celerator detector. The software used for mineralogical identification and analysis was X'Pert HighScore Plus version 2.1b (Degen et al. 2014). The percentage of crystallinity of the samples recovered after the experiments, defined by the intensity ratio (I_{net}) of the diffraction peaks on the sum of all measured intensities, was calculated according to Equation 1 subtracting from the total intensity (I_{tot}) the constant background intensity (Bgr_{const}) of OCP crystals 125 to 150 μm in size, used as external standard:

$$\text{Crystallinity [\%]} = 100 \times \Sigma I_{net} / (\Sigma I_{tot} - Bgr_{const}). \quad (1)$$

Semiquantitative mass fraction calculation [%w/w] was performed from diffraction data by normalized reference intensity ratio (RIR) algorithm (Chung 1974), using the RIR

Table 1. Water points and their initial F^- concentration used for defluoridation tests

Label sample	Location	Coordinates		Waterpoint type	F^- i.c. (mg/L)
BUL	Bule Bule spring, Uwiro village, Tanzania	3°10′39.66″S	36°51′10.68″E	Diffuse spring	8.4
NGO	Maji ya Chai spring, Ngurdoto village, Tanzania	3°17′36.60″S	36°52′43.32″E	Catch spring	20.9
KYU	Ngarenanyuki, secondary school, Tanzania	3°15′5.84″S	36°54′47.54″E	Borehole	37.2

i.c. = initial concentration.

DOI: 10.1002/ieam.4262

value of OCP and FAP from the International Centre of Diffraction Data (ICDD; http://www.icdd.com/).

The socioeconomic survey

To achieve the stated objective, a questionnaire was developed and piloted in rural communities of North Tanzania using the RANAS model (Mosler 2012). The RANAS model has been applied in a few similar studies (Huber et al. 2012; Huber and Mosler 2013), where researchers have attempted to evaluate how the psychological elements of this conceptual framework can influence the use of devices and/or the adoption of healthy drinking behavior, that is, defluoridated drinking and cooking water.

In the present study, the pilot questionnaire was divided into 3 sections, and information about questions, items, and values of measurement scales are reported in Supplemental Data Table S3. The first section (Supplemental Data Table S3) elicited information about water drinking habits and the 5 elements of the RANAS. The 9 risk items captured perceived vulnerability and perceived severity and factual knowledge of individuals toward dental and skeletal fluorosis. The 2 vulnerability items measured individuals' perceived probability of getting these 2 diseases, whereas severity items assessed the negative consequences of these diseases on health. The 5 factual knowledge items tested whether respondents knew how to prevent these diseases correctly by applying simple precautions (boiling water, brushing teeth, taking medicine, and drinking milk). Five attitude items evaluated both positive aspects of drinking defluoridated water concerning good health, reducing medical expenses, better taste, and feeling happy, and negative aspects in terms of time management. Three normative items elicited information about what respondents think other community members will do (descriptive norm), what other people think they should do (injunctive norm), and their commitment toward healthy drinking behavior (personal norm) if the rural community had the possibility of using these new OCP and FFD. The ability item measured the personal capacity of an individual to carry out healthy drinking behavior, whereas the 5 self-regulation items gathered information about plans regarding the use of these devices in terms of daily routine, disaster, and commitment. Other than vulnerability items evaluated on a 5-point scale ranging from very unlikely to very likely, factual knowledge is captured with yes/no answers, and all the other components of the RANAS model were measured on a Likert scale ranging from completely disagree to completely agree.

The second section collected information on the willingness to pay where participants were prompted with a hypothetical market scenario and asked to state the maximum amount that they were willing to pay for OCP. It was assessed following an open-ended format.

The third section gathered information about sociodemographic characteristics of respondents such as gender, age, education, assets of individuals, and household amenities such as main sources of drinking water and minutes necessary to collect drinking water on foot from home.

The pilot study was preceded by a training workshop where researchers in collaboration with the OIKOS East Africa, a nongovernmental organization in Tanzania, explained to interviewers the aim of the study, providing them with information about F^-, dental and skeletal fluorosis diseases, and use of FDD whose model was shown and tested in the same area where this study was conducted. Interviewers were also trained on how to collect data using tablets. The pilot survey was administered between May and June 2019, conducting 100 random face-to-face interviews in 7 villages near the city of Arusha: Oldonyowas, Uwiro, Lemanda, Engutukoit, Lemongo, Losinoni Juua, and Losinoni Kati (Figure 2 and Supplemental Data Figure S2). These hundred participants were water consumption decision makers of 5000 households living in an area of the world where collecting information is very challenging. The questionnaire was translated from English into Swahili by OIKOS East Africa and during data collection, the interviewers were supervised by 2 technicians from this nongovernmental agency.

Data analysis was conducted using STATA 15 (StataCorp 2017). For the multi-item components of the RANAS model, a Cronbach's alpha test of reliability was performed to evaluate their internal consistency as average aggregate scores. A logistic regression (2) was estimated to determine how the probability of consuming defluoridated water (CFW) is influenced by the sociodemographic characteristics of participants and the components of the RANAS models as follows:

$$\mathrm{P}(CFW_j \mid X_{1j},\ldots,X_{kj}) = \frac{1}{1+e^{-(\beta_0+\sum_{i=1}^{k}\beta_i X_{ij}+\epsilon_j)}}, \qquad (2)$$

where $\mathrm{P}(CFW_j \mid X_{1j},\ldots,X_{kj})$ is the conditional probability of consuming defluoridated water (i.e., adoption of healthy drinking and cooking behavior) given the set of psychological and sociodemographic variables (X_{ij} $i = 1, \ldots, k$); i is an index ranging from 1 to k, indicating the number of variables; j is an index ranging from 1 to N, indicating the number of individuals; β_0 is the intercept; β_i are the parameters; and ϵ_j is the error term. The adequacy of the model was evaluated by the pseudo coefficient of determination R^2 and the goodness-of-fit test for logistic regression proposed by Hosmer and Lemeshow (1980).

RESULTS

Defluoridation tests

Three different OCP dosages were tested with NGO water (F^- i.c. = 20.9 mg/L): 20, 40, and 80 g of OCP (S/L respectively equals of 1, 2, and 4 g/L in the tests NGOa, NGOb and NGOc). The results show that when starting with 20 L of natural water with 20.9 mg/L F^-, the FDD can reach the WHO limit of 1.5 mg/L F^- respectively in 12, 6, and 2 h as a function of the increasing OCP dosage (Table 2).

Considering the removal capacity of OCP of 25.7 mg/g, as mentioned in the *Introduction*, the theoretical minimum OCP dosage for effectively treating the NGO water is 0.82 g/L. This theoretical calculation is confirmed by the

Table 2. Effect of different solid-to-liquid ratio (S/L = 1, 2, and 4 g/L respectively in the tests NGOa, NGOb and NGOc) on time needed to decrease the F^- water concentration below the WHO limit of 1.5 mg/L

		F^- (mg/L)		
Label	OCP dosage (g/L)	Initial	Final	Time (h)
NGOa	1	20.9	1.28	12
NGOc	2	20.9	1.40	6
NGOb	4	20.9	1.32	2

NGO = Maji ya Chai spring, Tanzania; OCP = octacalcium phosphate; WHO = World Health Organization.

result of the NGOa test which uses a slightly higher dosage of 1 g/L. Increasing the OCP dosage from 1 to 4 g/L decreases the time required to reach the drinkable limit from 12 to 2 h (Table 2).

The dosage of 4 g/L of OCP was tested also with BUL (F^- i.c. = 8.4 mg/L) and KYU waters (F^- i.c. = 37.2 mg/L) (Figure 5). The results show that in 2 h FDD charged with 4 g/L of OCP decreases the dissolved F^- concentration below the WHO limit (1.5 mg/L) from the BUL water (Figure 5A). In the KYU test, after 6 h of treatment, the F^- concentration decreases from 37.2 to 7.2 mg/L, but as shown in Figure 5C, the reaction did not reach the equilibrium.

The main variations on NGO water after defluoridation treatment with different dosages of OCP (Table 3) indicate that the pH goes close to the neutrality; moreover, the decrease of HCO_3^- from 427 to 299 mg/L and the increase of P^{5+} up to 46.5 mg/L are observed. The increase of P^{5+} is explainable by the higher molar Ca-to-P ratio in FAP (1.67) to the starting molar Ca-to-P ratio in OCP (1.33). The small increase of Na^+, K^+, SO_4^{2-}, and Cl^- concentrations in treated water may be related to the tap water used for OCP synthesis. The behavior of Ca^{2+} can be linked to the OCP dissolution and precipitation of FAP: after 2 h (NGOb sample) FAP is not fully precipitated, whereas after 6 h (NGOc sample), where Ca^{2+} is less than the initial concentration, the precipitation of FAP is complete.

Effect on solid phase

The XRD patterns of sorbent (Figure 6), before and after the tests, point out the transformation of OCP into FAP:

$$Ca_8(HPO_4)_2(PO_4)_4 \cdot 5H_2O_{OCP} + 1.6F^- \rightarrow 1.6Ca_5(PO_4)_3F_{FAP} + 1.2HPO_4^{2-} + 5H_2O + 0.8H^+, \quad (3)$$

recognizable by its XRD peaks (100) (002) (202) (310) and (213). In the XRD patterns of the solid phase after the NGOb and BUL tests (Figures 6C and 6D) some residual OCP is clearly detectable by the presence of the characteristic peak (010) and/or twin peaks (020) (110) and (002) (−122) (−211). The XRD pattern from KYU test (F^- i.c. = 37.2 mg/L) shows more similar shape and peak position with FAP (Figure 6B) and the OCP characteristic peaks (010) (020) (110) are not visible but, because both OCP and FAP share similar XRD patterns in the range 20° to 40° 2θ (Iijima et al. 1996), the differences observed in the experimental XRD patterns in this angular range (Supplemental Data Figure S3) provide important information on secondary peaks and permit the OCP identification even from the KYU test. Phases other than OCP or FAP were not detected.

The crystallinity of the solids recovered after the tests decreases by 30% in BUL after 2.5 h, 31% in NGO after 2.5 h, and 22% in KYU after 6 h. Semiquantitative mass fractions analysis (%w/w) of detected phases calculated by RIR indicates a positive relationship with removed F^- from solution (Table 4) and OCP-to-FAP ratio in the solids recovered after the tests. In all tests reported in Table 4, characterized by an S/L ratio of 4 g/L, the amount of residual unreacted OCP is higher than the amount of formed FAP; this is because it is necessary to use more OCP than the stoichiometric amount to reduce the treatment from 12 to 2 h.

Preliminary results of the socioeconomic study

Descriptive statistics. Results of the pilot study show that 74% of *N* respondents (*N* = 100) were female with an

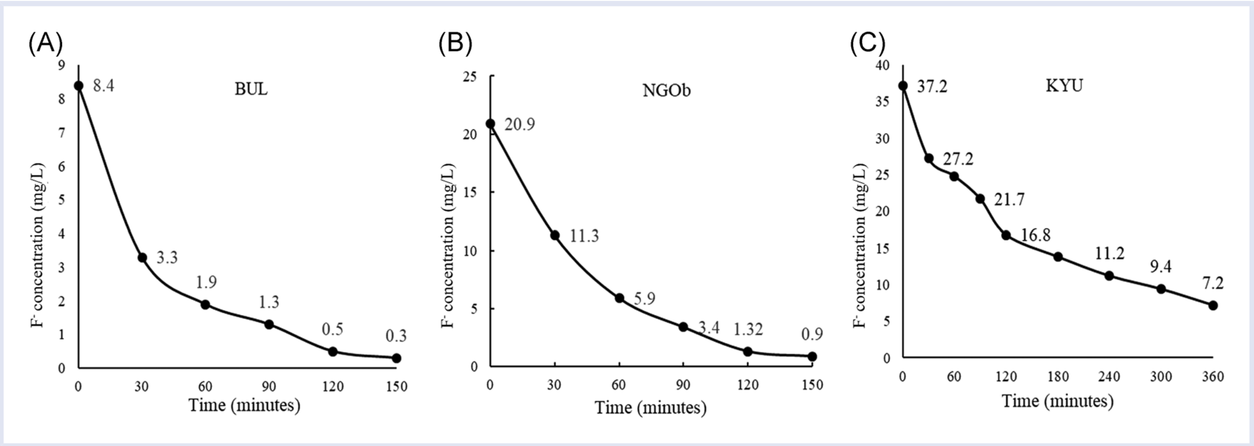

Figure 5. The plots show the removal trend of dissolved F^- by 80 g of OCP in 20 L (S/L = 4 g/L) of 3 different natural waters (**A** = BUL, **B** = NGOb, **C** = KYU) in different step times and different initial F concentrations. BUL = Bule Bule spring, Tanzania; KYU = Ngarenanyuki borehole, Tanzania; NGO = Maji ya Chai spring, Tanzania; OCP = octacalcium phosphate.

DOI: 10.1002/ieam.4262

Table 3. The compositional difference of natural water after defluoridation treatment with different dosage of OCP and different contact time

Sample	pH	Ca^{2+} mg/L	Mg^{2+} mg/L	Na^{+} mg/L	K^{+} mg/L	P^{5+} mg/L	SO_4^{2-} mg/L	Cl^{-} mg/L	HCO_3^{-} mg/L	F^{-} mg/L
NGO	8.45	4.2	<1.5	176	24.4	0.3	27.3	19.6	427	20.9
NGOb (4 g/L, 2 h)	6.96	8.1	<1.5	191	27.5	46.5	34.8	28.5	299	0.9
NGOc (2 g/L, 6 h)	7.18	2.5	<1.5	194	28.4	37.1	33.9	27.3	329	1.4

NGO = Maji ya Chai spring, Tanzania; OCP = octacalcium phosphate.

average age of 44.3 y (standard deviation [SD] = 14.5, median [Md] = 46.5) and an average household size of 5.6 (SD = 2.7, Md = 5). Regarding education, 35% of respondents were illiterate, 44% had completed primary education, and 21% had a level of education higher than primary school. Furthermore, 72% of respondents reported fetching a daily average of 2.5 (SD = 1.46, Md = 2) buckets (20 L) of drinking and cooking water, and only 52% declared to have consumed defluoridated water.

Table 5 presents the descriptive statistics of the variables used in the logistic regression analysis, the Cronbach's alpha values of the average aggregate scores of the RANAS components, and the results of the backward logistic regression analysis. Findings indicate that the Cronbach's

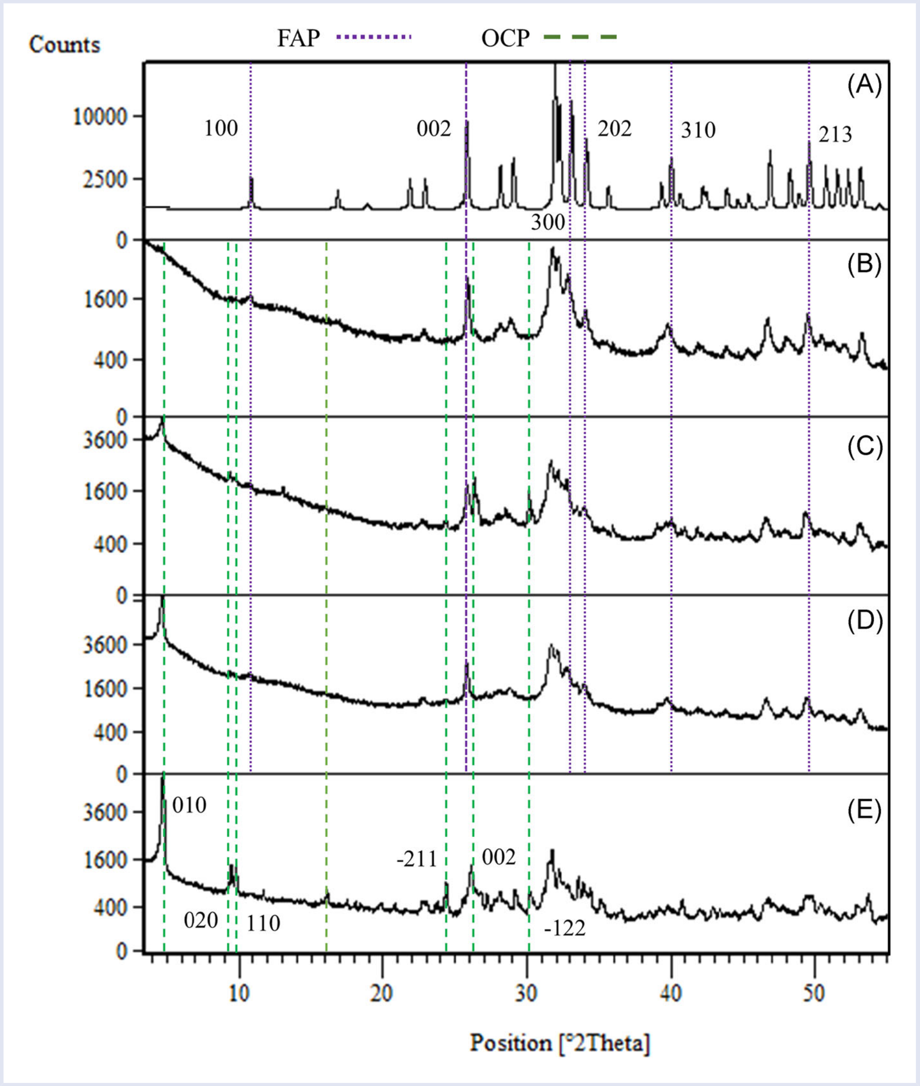

Figure 6. XRD patterns of standard FAP (reference ICSD pattern n. 00-015-0876) (A); sorbent recovered after KYU experiment (B); sorbent after NGOb experiment (C); sorbent after BUL experiment (D); OCP before experiment (E). BUL = Bule Bule spring, Tanzania; FAP = fluorapatite; ICSD = Inorganic Crystal Structure Database; KYU = Ngarenanyuki borehole, Tanzania; NGO = Maji ya Chai spring, Tanzania; OCP = octacalcium phosphate.

Table 4. Relationship between F^- removed by 80 g of OCP from 20 L of the solution and FAP in the solid phases after defluoridation tests determined by RIR of crystalline phases

	Solutions			Solids	
Sample	F^- i.c. (mg/L)	F^- f.c. (mg/L)	F^- removed (mg)	% w/w OCP	% w/w FAP
BUL	8.4	0.3	162	89	11
NGOb	20.9	0.9	400	82	18
KYU	37.2	7.2	600	68	32

BUL = Bule Bule spring, Tanzania; FAP = fluorapatite; F^- f.c. = fluoride concentration at the end of experiments; F^- i.c. = fluoride initial concentration; KYU = Ngarenanyuki borehole, Tanzania; NGO = Maji ya Chai spring, Tanzania; OCP = octacalcium phosphate; RIR = reference intensity ratio.

alpha test of the reliability of the multi-item components of the RANAS model is very good for the vulnerability (0.96), good for severity (0.73) and attitude (0.80), and barely acceptable for self-regulation (0.54). On the average, participants have a very low level of knowledge (Md = 0.48, SD = 0.25), feel moderately vulnerable (Md = 1.33; SD = 1.20) to dental and skeletal fluorosis, and believe that their health would be affected severely by these diseases (Md = 3.33, SD = 0.43). Furthermore, descriptive, injunctive, and personal norms mean values range from 1.19 to 1.33 and thus emphasize how important these norms are for EARV communities. Participants also scored very high on ability and self-regulation, and therefore they feel confident using and managing this new FDD. The average distance in minutes between the main source of water and respondents' homes was within 30 min, while the average willingness to pay for consuming 20 L of fluoride-free water was 89.92 Tanzanian shillings (TZS), equal to US$0.04 in January 2020, with high variability.

Logistic regression analysis. Results of the logistic regression (right side of Table 5) show that data fit the model quite well. The Hosmer-Lemeshow's goodness of fit test is not significant and therefore we reject the hypothesis that the model differs significantly from the observed data. Variables used in the model explain 34% of the total variance (pseudo $R^2 = 0.339$) in the consumption of defluoridated water, with factual knowledge, attitude, descriptive norm, injunctive norm, and self-regulation that turned out not to be significant. The significant and positive beta parameters of severity, personal norm, and ability indicate that participants who consume more defluoridated water are those concerned about the negative health consequences of these diseases, feeling strong obligations

Table 5. Descriptive statistics and results of the logistic regression analysis on the consumption of fluoride-free water ($N = 100$)

		Descriptive statistics regression results							
Factors/Covariates		Range	M	SD	α	β	SE β	Z	P>|Z|
Risk beliefs	Vulnerability	[0–4]	1.335	1.204	0.962	*−0.859***	0.363	−2.360	0.018
	Severity	[0–4]	3.330	0.428	0.735	*1.920**	0.913	2.100	0.036
	Factual knowledge	[0–1]	0.484	0.253		*−0.651*	1.775	−0.290	0.772
Attitudinal beliefs		[−2 to 2]	0.868	0.340	0.796	0.978	1.031	0.950	0.343
Normative beliefs	Descriptive	[−2 to 2]	1.330	0.513	—	−2.061	1.313	−1.570	0.122
	Injunctive	[−2 to 2]	1.190	0.734	—	−1.358	0.891	−1.520	0.135
	Personal	[−2 to 2]	1.290	0.477	—	2.222*	0.946	2.350	0.017
Ability beliefs		[−2 to 2]	1.230	0.736	—	2.074*	0.998	2.080	0.038
Self-regulation beliefs		[0–4]	2.964	0.435	0.539	−0.521	1.114	−0.460	0.649
Perceived distance		[0–5]	0.820	0.989	—	*0.970***	0.358	2.710	0.007
Willingness to pay for fluoride-free water		Open	188.1	1001.6	—	*0.007**	0.003	2.280	0.023
Age		Open	44.67	15.39		0.065**	0.024	2.700	0.007
Water consumption (number of 20 L buckets per week)		Open	15.480	9.070		0.122**	0.046	2.660	0.008
Constant						−11.620**	4.218	−2.760	0.006
The fit of the model						Log-likelihood = −45.779 LR χ (13) = 46.91 ($p < 0.000$) Pseudo $R^2 = 0.339$ Hosmer-Lemeshow χ (8) = 9.66 ($p = 0.289$)			

M stands for the mean values, α is the Cronbach (1951) measure, β are the logistic estimates, SE β their standard errors.
*, **Denote a significance value at 5% and 1% significance level respectively.

to adopt the same healthy drinking behavior of their rural community and being confident about the use of the new technology. For example, when all other variables are equal to their means, the severity beta parameter ($\beta = 1.92$) indicates that a marginal increment of its aggregate score will increase the probability of consuming defluoridated water by about 38%. By the same token, the beta parameter of the personal norm ($\beta = 2.22$) shows that a marginal increment of its score will increase the probability of consuming defluoridated water by nearly 45%. On the other hand, vulnerability shows a negative relationship with the dependent variable, that is, the higher the perceived likelihood of getting these diseases, the lower the consumption of defluoridated water. Even though the sign of this parameter was expected to be in the opposite direction, this behavior might be explained by the fact that when people feel extremely vulnerable, they do not believe or might not be motivated to adopt healthy drinking behavior. In this case, ceteris paribus, the vulnerability beta parameter ($\beta = 1.92$) indicates that a marginal increment of its aggregate score will decrease the probability of consuming defluoridated water by about 17%. The walking time of distance (0 indicates less than 14 min, 4 indicates more than 60 min) from the main source of water ($\beta = 0.97$) and the willingness to pay for fluoride-free water ($\beta = 0.03$) had a positive impact on the probability to consume defluoridated water. The first result implies that if the main source of water is distant from the participant's home, the probability of consuming fluoride-free water is higher than when this is close to them. This factor probably considers the implicit costs associated with the time spent in fetching water. Summing-up this implicit cost to the actual price reduces the relative price of consuming fluoride-free water and increases its demand.

Finally, the beta parameters of respondents' age ($\beta = 0.06$), perceived distance from the main source of water ($\beta = 0.97$), the weekly consumption of 20 L buckets of water ($\beta = 0.12$), and willingness to pay for fluoride-free water ($\beta = 0.03$) influenced positively the consumption of defluoridated water. Thus, keeping all other variables equal to their means, the probability of adopting healthy drinking behavior increases by 13% when participants are 10 y older, by 19% if perceived walking time of distance increases by 15 min, by about 2.5% for every extra bucket of water consumed, and by 1% for those who are willing to pay 100 TZS more for defluoridated water obtained using the new device.

DISCUSSION

Water defluoridation

The experimental data show that FDD charged with 80 g of OCP in 20 L (S/L = 4 g/L) of natural water can reduce the F^- content below the WHO limit for drinking water of 1.5 mg/L from initial concentrations of 8.4 mg/L (BUL water) and 20.9 mg/L (NGOb water) (Figures 5A and 5B) in 2 h. With F^- i.c. = 20.9 mg/L of NGOc and NGOa tests, the drinkable limit was reached in 6 and 12 h charging FDD with 2 g/L and 1 g/L of OCP, respectively.

In the test with F^- i.c. = 37.2 mg/L (KYU) the F^- concentration significantly decreases after 6 h of treatment (down to 7.2 mg/L). It is possible to note that, after 6 h of treatment, the equilibrium was not still reached (Figure 5C) and that about 68% w/w of OCP was still unreacted (Table 4). Failure to reach a final F^- concentration (F^- f.c.) below the drinkable limit of 1.5 mg/L was probably due to power loss of battery that occurred after about 2.5 h of working time, with consequent reduction of the flow to the pump that lowered the stirring rate and thus affected the reaction kinetics between OCP and water. On the other hand, the amount of residual unreacted OCP is always higher than the amount of formed FAP in the tests with S/L of 4 g/L (Table 4), and this is because the F^- i.c. in each test is far insufficient to transform all the OCP into FAP according to the stoichiometry of the reaction OCP → FAP (Supplemental Data Table S1). This excess of OCP favors a fast water treatment, a key feature for an effective and frugal defluoridation method. The seeming contradiction between XRD data (Figure 6) and semiquantitative calculation (Table 4) is because OCP tends to easily lose in crystallinity when in contact with water and its (010) peak dramatically decreases in intensity.

According to the Guidelines for Drinking Water (WHO 2017), it is worthwhile to underline that no deleterious collateral effects on the quality of treated water were produced during the defluoridation process; in fact, the solution pH slightly decreases but remains in the range suggested by WHO for drinking water (pH = 6.5–9.5) and the elements listed in Table 4 are within the drinkable limits. Moreover, the increase of dissolved P^{5+} (Table 3), which is not subject to limitations for drinking water (WHO 2017), can be considered a positive effect because it is an essential element for life with recommended dietary reference intake (DRI) of 100 mg/d for infants, 700 mg/d for pregnant women and adults, and 1250 mg/d for children and teenagers (US Institute of Medicine 2006).

Standardization of the use and procedure: Sorbent dose and optimum FDD working time

In order to meet the requirement for a disclosable method targeted to rural communities, some important considerations must be taken into account. Usually, rural people have a moderate knowledge of the F^- concentration in the water they drink daily, which can change in different areas and during the seasons and/or year by year. Without knowing this value, it is impossible to know how much sorbent and/or what contact time between sorbent and water is necessary to effectively defluoridate water. For instance, without a monitoring system, using a column-like method, it is impossible to know after how many liters of water the sorbent is exhausted and needs to be replaced. For these reasons, taking into account the use in a rural scenario, a standardization of the procedure regardless of the initial F^- concentrations is recommended. Also, a reasonable defluoridation time is another important factor. Reducing the sorbent amount per cycle at the minimum (1 g/L) implies to extend the working time of the FDD pump, which means more power consumption and battery wear. After these considerations, we suggest 2 h as an optimum FDD working time because we consider 2 h as a reasonable time for users and for saving the life of the battery. Up to now, the standard parameters are these: FDD loaded with 4 g of OCP per liter (20 L of water, 80 g of OCP), 2 h of mixing with a pump flow of 22 L/min. It is important to emphasize that this estimation is also based on the fact that about 89% of water for human consumption in the EARV has up to 20 mg/L F^-. Considering the results with F^- i.c. = 37.2 mg/L (KYU test) and the OCP removal F^- capacity, the next development will be focused on improving the FDD stirring process to guarantee the defluoridation of water with up to 40 mg/L F^- applying the above-reported standardized parameters. Moreover, in case of grid power supply and/or if the F^- i.c. is known and can be monitored, the amount of OCP necessary for defluoridation can be lowered to the minimum amount of 1 g/L instead of the standard S/L ratio of 4 g/L.

FLOWERED Defluoridator Device (FDD)

The key concept of FDD is to replicate a defluoridation batch process that needs mixing and stirring between sorbent (or a chemical reagent for F^- precipitation) and water. This means that FDD is not only OCP related but can be loaded with different compounds using sorbent reagent-related dose and mixing time. Every load of fluoride-rich water needs a dose of sorbent, and after every defluoridation cycle the exhausted sorbent can be recovered from the dedicated compartment. The FDD could also be used with an adsorbent material if the stirring system would significantly improve the defluoridation kinetics. The power supply through the battery is designed to be charged from different sources, such as solar panel, power generator, power grid, and so on. Finally, the FDD weight (23 kg), similar to the weight of water that can be treated per cycle (20 L), and the size 103 × 43 × 55 cm are targeted for household use.

Sustainability

Production of OCP. The synthesis of OCP requires calcium carbonate and phosphoric acid as sources for Ca^{2+} and P^{5+}. Considering industrial grade calcium carbonate and phosphoric acid, the reagent cost of 1 kg of OCP is about = \$6 to \$8, depending on the Tanzania marketplace. Considering the standardization of the use (4 g/L), 1 kg of OCP can treat 250 L of water, which means a cost of about \$0.024 to \$0.032/L of defluoridated water. The use of local georesources to synthesize the sorbent material can greatly improve its economic sustainability. Mineral sources of both Ca^{2+} and P^{5+} are already cultivated in Tanzania: Calcium carbonate is exploited for the cement industry from a limestone quarry in the eastern part of Tanzania, from Tanga to Dar Er Salaam (Stewart and Muhegi 1989; Nicholas et al. 2006; Jacob 2019), and P is one of the major elements of the phosphorite rock exploited in the central-northern part of Tanzania for fertilizer production (Msolla et al. 2005; Szilas et al. 2008). Further research will be focused on the use of local georesources and optimization of the OCP synthesis procedure.

Disposal of used sorbent. The solid phase recovered after the standardized defluoridation process is composed of OCP and FAP in variable percentages (Table 4). For the disposal of the OCP–FAP mix, different hypotheses can be formulated, first by using the OCP–FAP mix as a fertilizer in the same way in which natural FAP is already used in Tanzania (Msolla et al. 2005; Szilas et al. 2008). However, a focused study about the interaction of the OCP–FAP mix with soil and F^- from irrigation water is mandatory to understand if 1) the OCP–FAP mix can still immobilize F^- from soil and irrigation water or 2) the OCP–FAP mix can release F^- to the soil and or to the cultivation. The second hypothesis is based on different solubilities of OCP (8 mg/L) and FAP (0.2 mg/L) (Dorozhkin 2012): Adequate washing with water can dissolve only the OCP from the OCP–FAP mix to recover Ca^{2+} and P^{5+} and then restart the synthesis of new OCP. The residual FAP could be used as a source of P^{5+} to produce phosphate fertilizer and/or phosphoric acid (Schrödter et al. 2008; Kongshaug et al. 2014).

FLOWERED Defluoridator Device (FDD). Due to the simpleness of the components of the FDD and the possibility of a multichoice power supply source, the FDD meets the "low-tech" requirement for a disclosable method targeted for rural areas. Up to now, the overall cost of the FDD is about \$220; the most expensive components are the pump (about \$60) and the battery (about \$60–\$80). It is important to consider that the FDD is a prototype, and thus a subsequent industrial scale-up can improve all the technological aspects (i.e., maintenance aspect, different material instead of a plastic case, etc.) and costs. Theoretically, the FDD is designed to last for as many years as the life of the pump.

Comparison with other in situ household-scale defluoridation methods

As mentioned in the *Introduction*, in the last decade more than 800 different sorbent materials with a promising F^- removal capacity have been proposed in peer-reviewed literature. However, because the experimental laboratory conditions may differ greatly from natural field conditions, only the defluoridation methods effectively applied at household scale in rural contexts with natural water will be taken into consideration. Moreover, advanced treatment technologies, such as reverse osmosis, electrodialysis, and membrane distillation, have been excluded from the comparison because they cannot be used at household scale in rural areas of developing countries due to economic and technological limitations (e.g., power consumption, management of sludge water, maintenance cost) (Yadav et al. 2018).

The first defluoridation method applied in a rural context in India was the Nalgonda technique, involving the use of Al salts, lime, and bleaching powder, but it is no longer recommended due to the release of elements (i.e., Al, sulfate) above the drinkable limit into the defluoridated water and to the difficulty in managing the water treatment method (Ingle et al. 2014). Other defluoridation methods already in use at the village scale in some limited rural areas of developing countries are mainly based on BC (Ethiopia, Kenya, Tanzania, Senegal, South Africa, Thailand) (Kut et al. 2016) or activated alumina (India, Sri Lanka) (Fawell et al. 2006). However, both methods require a trained user for the management of the reagent and monitoring the water quality, whereas our main goal was to develop a very simple method that can be used directly by the population at household scale in rural contexts without any specific training. This is a very important aspect because the abandonment of a water treatment method in rural areas is often linked to the impossibility of finding one or more users with the ability and, above all, the will to manage the purification system constantly and correctly.

As far as we know, the only 2 methods already applied at household scale are based on a bucket–column type filter loaded with activated alumina, especially in India, or BC, especially in the EARV. The F^- removal capacity (Langmuir Q_{max}) of activated alumina is 2.40 mg/g (Ghorai and Pant 2005), whereas for OCP it is 26.8 mg/g (Idini et al. 2019). Moreover, the use of activated alumina, as reported in the literature (George et al. 2010; Jadhav et al. 2015; Yadav et al. 2018), can easily release Al into the treated water above the drinkable limit of 0.1 mg/L due to Al–F^- chemical complexes (e.g., AlF^{++}, AlF_2^+, AlF_3°, AlF_4^-) that are very stable in solution and subtract Al from precipitating as oxide or hydroxide, notably increasing Al solubility, and thus the health risk, given that Al is very toxic. Also, as recognized by the WHO (Fawell et al. 2006), the water treatment with activated alumina requires good operating conditions, mainly the use of optimum pH for the adsorption process and the avoidance of excessive Al dosage (this means that the concentration of F^- must be known before starting each treatment to correctly dose the reagent). Because of all these aspects, we have considered activated alumina a nonreliable reagent for household-scale application according to our goals.

Bone char is a calcium phosphate compound prepared by charring animal bones. The removal mechanism is based mainly on ion exchange between F^- and OH^- (Alkurdi et al. 2019):

$$Ca_5(PO_4)_3OH + F^- \rightarrow Ca_5(PO_4)_3F + OH^-. \qquad (4)$$

Charring the bones at the optimal temperature of 400 ° C, the calculated F^- removal capacity (Q_{max}) is 3.5 mg/g, whereas the empirical removal capacity using synthetic water with 21 mg/L F^- in a laboratory environment decreases to 0.985 mg/g (Mbabaye et al. 2017). That means that 19 g of BC are needed to reach the drinkable F^- WHO limit of 1.5 mg/L. For comparison, as reported in Table 2, starting from a F^- concentration of 20.9 mg/L, 1 g of OCP is more than enough to reach the drinkable limit. Very similar results about the BC removal capacity were obtained in Senegal (Sorlini et al. 2011), in Kenya (Korir et al. 2009), and in Ethiopia and Tanzania (Dahi 2016), where the BC method was implemented in small rural areas by governmental and nongovernmental organizations such as Nakuru defluoridation company, which is an initiative of the Catholic diocese of Nakuru, Kenya (https://nakurudefluoridation.co.ke/), and Oromo Self-Help Organization (OSHO) in Wayo Gabriel, Ethiopia. The data reported on these areas indicate that BC can work properly if the water to be treated has F^- content less than 8 mg/L (Albertus et al. 2000).

The cost of water treatment by sorbent reagent depends mainly on F^- concentration, or equally, how much F^- is to be removed from the water, given that the sorbent is consumed during the removal reactions. Because the concentration of F^- is highly variable site by site, and even varies during the seasons, it is not possible to compare the cost of 1 L of treated water for different methods, unless a standard F^- water concentration is assumed. Considering a removal capacity of 0.9 mg/g for the BC system (Albertus et al. 2000) and an average BC cost of \$0.30/kg, the approximate cost to remove 1 g of F^- from water is \$0.33. This value is very similar to the cost calculated for OCP: Taking into account the empirical removal capacity of 25.7 mg/g and an average OCP cost of \$7/kg, the approximate cost to remove 1 g of F^- is \$0.27.

Moreover, switching to the standardization of the method presented here (*Standardization of the use and procedure: Sorbent dose and optimum FDD working time*), with the advantage that water quality monitoring is not required and can treat the water regardless of its F^- concentration up to 21 mg/L, the cost of 20 L of treated water is \$0.28.

The cost of US\$220 for the FDD is more expensive than the bucket filter, which can range from \$19 to \$45, depending on the manufacturer. The difference between a batch system, as the FDD, and a bucket–column system, as in the BC method, consists in the use of the sorbent: In a batch system a single dose of the sorbent is poured into the water in every single cycle; in a bucket–column system the water passes through a fixed amount of sorbent, usually 8.5 kg of BC. In order to know when the BC load of 8.5 kg is exhausted, either constant monitoring of F^- concentration in raw water, due to its variability in space and time, or periodic monitoring of F^- concentration in treated water would be necessary. The monitoring of the bucket–column system at household scale is considered an important limitation for its effective use: The analysis of dissolved F^- concentration requires a specific chemical laboratory or expensive portable equipment to be used by a highly trained specialist. Up to now, a reliable, low-cost F^- detection method that can be used in situ by nonexpert users has not been developed, although some effort in this regard is ongoing (López-Alled et al. 2017).

Implications of the socioeconomic analysis

Preliminary results of the socioeconomic analysis indicate that respondents feel capable of employing the OCP and FDD regularly, supporting the idea that their use is a relatively easy activity to perform. This belief can facilitate the acceptance of the new device as a simple and efficient method for obtaining and consuming defluoridated drinking and cooking water. The adoption of healthy drinking behavior seems to be more appealing to members of the EARV rural communities, who are willing to pay more for the new technology and have a high consumption of water. However, findings also show that this is an area of the world dominated by a high degree of illiteracy, and people have a very low level of knowledge about dental and skeletal fluorosis. This indicates that the government should introduce educational programs to make EARV rural communities aware of the negative health consequences of these diseases. Educational programs should also motivate people to adopt healthy drinking behavior, making them aware that these new devices can reduce oral intake of water with elevated levels of F^-. Such approaches might reverse the observed negative relationship between perceived vulnerability and the safe drinking water. Furthermore, because personal norms are so important in the adoption of defluoridated safe water, stakeholders should consider how to change ingrained habits of unsafe water use in the EARV rural community. This could be achieved with demonstration fields having the scope first to unfreeze the bad ingrained habits of drinking untreated water and then changing people's attitudes with information related to how the new technology helps to reduce the risk of getting these diseases. Persuasion could start with older members of rural communities because they appear to be more susceptible to adopting healthy drinking behavior and then be propagated to younger members because of the positive impact of personal norms. The positive impact of moral obligation on the adoption of healthy behavior using a new defluoridator was also found in a study conducted by Huber et al. (2012).

SUMMARY

The present study employs a multidisciplinary approach to develop a defluoridator prototype for the EARV rural communities and to explore what socioeconomic and psychological factors can facilitate its acceptance within these rural populations. For this purpose, OCP, which has shown effective F^- removal capacity in previous batch tests, was used with a new defluoridator prototype, the FDD. The FDD is a new low-cost and low-tech device, designed to reproduce, in the field, the defluoridation laboratory process that requires mixing and stirring between the sorbent and the water. The FDD experimentation was carried out in the rural areas of northern Tanzania, at the same environmental conditions of its possible future use by rural populations, using 3 natural fluoride-rich waters with different F^- starting concentrations and testing different sorbent dosage. In agreement with our previous study, the results of the FDD field tests show that the OCP effectively removes the F^- from natural water by means of the transformation of OCP into FAP. Based on these results, a standardized use of FDD and dosage of OCP for the defluoridation of natural water has been presented: FDD loaded with 20 L of natural water with F^- concentration up to 21 mg/L, 80 g of OCP, and 2 h of FDD working time with constant mixing flow pump of 22 L/min. Further research will be focused on the sustainability of OCP production, using already available local georesources, and its green disposal after use.

Finally, preliminary results of the socioeconomic study are encouraging and support the proposed device as an easy activity to accomplish, as testified by the positive and significant coefficient of the ability variable in the logistic regression. However, from the analysis it emerges that, given the poor knowledge of the risk of dental and skeletal fluorosis, the government should introduce educational programs to make EARV rural communities aware of the negative health consequences of these diseases. Raising knowledge about the danger of consuming untreated water via educational campaigns can improve the consumption of fluoride-free water in the Rift Valley region. Increasing awareness can also reverse the sense of powerlessness observed for vulnerability in the logistic regression, making members of EARV rural communities more aware that the use of this device can reduce their vulnerability. Thus, the intervention of government agencies and donors seems to be an important aspect to consider mitigating the cost of defluoridation and to ensure access to clean and safe water for all communities as required by Goal 6 of the UN Sustainable Development Goals.

Acknowledgment—The authors declare that no conflict of interest exists. This research is a part of the PhD project of Alfredo Idini, funded by MIUR (Italian Ministry of Education, University and Research) in the frame of the Italian National Program PON R&I2014-2020 "Innovative doctorates with industrial characterization." This research is also financially supported by the FLOWERED project (Coordinator G Ghiglieri), a Horizon 2020 European-funded project (Grant Agreement—N. 690378) (www.floweredproject.org). We wish to thank OIKOS East Africa for logistical help during the field activities.

Data Availability Statement—We declare that all data are available by request to corresponding author Alfredo Idini (alfredo.idini@gmail.com).

SUPPLEMENTAL DATA

In the Supplemental Data, readers can find more information about the chemical reaction, behavior factors used in the analysis, and values used for the questionnaire and the map of the defluoridation experiments.

Figure S1. Site of defluoridation test and interview in the Uwiro village, Northern Tanzania.

Figure S2. Location of water point source used for defluoridation test (dotted circle) and interview (purple line is around the Engutukoit village; red line is around

Oldonyowas and Losinoni villages; yellow line is around Uwiro and Lemanda villages; Arusha Region, Northern Tanzania). Image © 2019 Digital Globe- Image © 2019 CNES/Airbus.

Figure S3. Configuration of the FLOWERED Defluoridator Device (FDD).

Figure S4. Step-by-step procedure for water treatment with the FLOWERED Defluoridator Device (FDD) and octacalcium phosphate powder (OCP).

Figure S5. Difference of XRD pattern between OCP before tests (black pattern), solids collected after KYU (blue pattern) and BUL (red pattern) defluoridation tests and FAP reference ICSD pattern n. 00-015-0876 (green lines). In the pattern of KYU experiment, where 600 mg of F^- was removed from solution, the residual peak of OCP is less detectable than BUL pattern where F^- removed was 162 mg. BUL = Bule Bule spring; FAP = fluorapatite; ICSD = Inorganic Crystal Structure Database; KYU = Ngarenanyuki borehole, Tanzania; OCP = octacalcium phosphate; XRD = X-ray diffraction.

Table S1. Chemical synthesis reactions of (I) dicalcium phosphate dihydrate (DCPD) and (II) octacalcium phosphate (OCP); (III) Chemical transformation of OCP into fluorapatite (FAP) in presence of dissolved F^-

Table S2. Chemical composition of the tap water used for OCP synthesis

Table S3. Example behavior factors used in the analysis, and values.

ORCID

Alfredo Idini http://orcid.org/0000-0002-9937-5149

REFERENCES

Akuno MH, Nocella G, Milia EP, Gutierrez L. 2019. Factors influencing the relationship between fluoride in drinking water and dental fluorosis: A ten-year systematic review and meta-analysis. *J Water Health* 17(6):845–862.

Albertus J, Bregnhøj H, Kongpun M. 2000. Bone char quality and defluoridation capacity in contact precipitation. In: Proceedings of 3rd International Workshop on Fluorosis Prevention and Defluoridation of Water; 2000 Nov 20–24; Chaing Mai, Thailand. Dunedin (NZ): ISFR, EnDeCo & ICOH. p 61–72.

Alkurdi SSA, Al-Juboori RA, Bundschuh J, Hamawand I. 2019. Bone char as a green sorbent for removing health threatening fluoride from drinking water. *Environ Int* 127:704–719.

Amini M, Mueller KIM, Abbaspour KC, Rosenberg T, Afyuni M, Møller KN, Sarr M. 2008. Statistical modeling of global geogenic fluoride contamination in groundwaters. *Environ Sci Technol* 42:3662–3668.

Ayoob S, Gupta AK, Bhat VT. 2008. A conceptual overview on sustainable technologies for the defluoridation of drinking water. *Crit Rev Environ Sci Technol* 38:401–470.

Barbier O, Arreola-Mendoza L, Del Razo LM. 2010. Molecular mechanisms of fluoride toxicity. *Chem Biol Interact* 188:319–333.

Biswas G, Kumari M, Adhikari K, Dutta S. 2017. A critical review on occurrence of fluoride and its removal through adsorption with an emphasis on natural minerals. *Curr Pollut Rep* 3:104–119.

Carino A, Ludwig C, Cervellino A, Müller E, Testino A. 2018. Formation and transformation of calcium phosphate phases under biologically relevant conditions: Experiments and modelling. *Acta Biomater* 74:478–488.

Chacha N, Njau KN, Lugomela GV, Muzuka ANN. 2018. Hydrogeochemical characteristics and spatial distribution of groundwater quality in Arusha well fields, Northern Tanzania. *Appl Water Sci* 8:1–23.

Chowdhury A, Adak MK, Mukherjee A, Dhak P, Khatun J. 2019. Review papers: A critical review on geochemical and geological aspects of fluoride belts, fluorosis and natural materials and other sources for alternatives to fluoride exposure. *J Hydrol* 574:333–359.

Chung FH. 1974. Quantitative interpretation of X-ray diffraction patterns, I. Matrix-flushing method of quantitative multicomponent analysis. *J Appl Crystallogr* 7:513–519.

Cronbach LJ. 1951. Coefficient alpha and the internal structure of tests. *Psychometrika* 16(3):297–334.

Dahi E. 2016. Africa's U-turn in defluoridation policy: From the Nalgonda technique to bone char. *Fluoride* 49:401–416.

D'Alessandro W. 2006. Human fluorosis related to volcanic activity: A review. *WIT Trans Biomed Health* 10:21–30.

Datturi S, Van Steenbergen F, Van Beusekom M, Kebede S, Ababa A. 2015. Comparing defluoridation and safe sourcing for fluorosis mitigation in the Ethiopian central Rift Valley. Research report. *Fluoride* 48(4):293–314.

Degen T, Sadki M, Bron E, König U, Nénert G. 2014. The HighScore suite. *Powder Diffr* 29(S2):S13–S18. https://doi.org/10.1017/S0885715614000840

Dorozhkin VS. 2012. Amorphous calcium orthophosphates: Nature, chemistry and biomedical applications. *Int J Mater Chem* 2:19–46.

Everett ET. 2011. Critical reviews in oral biology and medicine: Fluoride's effects on the formation of teeth and bones, and the influence of genetics. *J Dent Res* 90:552–560.

Fawell J, Bailey K, Chilton J, Dahi E, Fewtrell L, Magara Y. 2006. Fluoride in drinking-water. Geneva (CH): World Health Organization. 144 p. https://apps.who.int/iris/handle/10665/43514

George S, Pandit P, Gupta AB. 2010. Residual aluminium in water defluoridated using activated alumina adsorption—Modeling and simulation studies. *Water Res* 44:3055–3064.

Ghiglieri G, Pittalis D, Cerri G, Oggiano G. 2012. Hydrogeology and hydrogeochemistry of an alkaline volcanic area: The NE Mt. Meru slope (East African Rift-Northern Tanzania). *Hydrol Earth Syst Sci* 16:529–541.

Ghorai S, Pant KK. 2005. Equilibrium, kinetics and breakthrough studies for adsorption of fluoride on activated alumina. *Sep Purif Technol* 42:265–271.

Giaciri SJ, Davies TC. 1993. The occurrence and geochemistry of fluoride in some natural waters of Kenya. *J Hydrol* 143:395–412.

Gizaw B. 1996. The origin of high bicarbonate and fluoride concentrations in waters of the Main Ethiopian Rift Valley, East African Rift system. *J Afr Earth Sci* 22(4):391–402.

Grech P, Latham MC. 1964. Fluorosis in the northern region of Tanganyika. *Trans R Soc Trop Med Hyg* 58:566–574.

Hosmer DW, Lemeshow S. 1980. Goodness-of-fit tests for the multiple logistic regression model. *Comm Stat A—Theor* 9:1043–1069.

Huber AC, Bhend S, Mosler H-J. 2012. Determinants of exclusive consumption of fluoride-free water: A cross-sectional household study in rural Ethiopia. *J Public Health* 20:269–278.

Huber AC, Mosler H-J. 2013. Determining behavioral factors for interventions to increase safe water consumption: A cross-sectional field study in rural Ethiopia. *Int J Environ Health Res* 23(2):96–107.

Hunter PR, MacDonald AM, Carter RC. 2010. Water supply and health. *PLoS Med* 7(11).

Idini A, Dore E, Fancello D, Frau F. 2019. Defluoridation of water through the transformation of octacalcium phosphate into fluorapatite. *Heliyon* 5(8): e02288.

Iijima M, Nelson DGA, Pan Y, Kreinbrink AT, Adachi M, Goto T, Moriwaki Y. 1996. Fluoride analysis of apatite crystals with a central planar OCP inclusion: Concerning the role of F-ions on apatite/OCP/apatite structure formation. *Calcif Tissue Int* 59:377–384.

Ingle N, Dubey H, Kaur N, Sharma I. 2014. Defluoridation techniques: Which one to choose. *J Health Res Rev* 1:1.

Jacob T. 2019. When good intentions turn bad: The unintended consequences of the 2016 Tanzanian coal import ban. *Extr Ind Soc* [accessed 2019 Feb 28]. https://doi.org/10.1016/j.exis.2019.02.009

Jadhav SV, Bringas E, Yadav GD, Rathod VK, Ortiz I, Marathe KV. 2015. Arsenic and fluoride contaminated groundwaters: A review of current technologies for contaminants removal. *J Environ Manage* 162:306–325.

Khairnar MR, Dodamani AS, Jadhav HC, Naik RG, Deshmukh MA. 2015. Mitigation of fluorosis—A review. *J Clin Diagn Res* 9(6):ZE05–ZE09.

Kongshaug G, Brentnall BA, Chaney K, Gregersen J, Stokka P, Persson B, Kolmeijer NW, Conradsen A, Legard T, Munk H et al. 2014. Phosphate fertilizers. In: Ullmann's Encyclopedia of Industrial Chemistry. Weinheim (DE): Wiley-VCH. p 1–49.

Korir H, Mueller K, Korir L, Kubai J, Wanja E, Wanjiku N, Waweru J, Mattle MJ, Osterwalder L, Johnson CA. 2009. The development of bone char-based filters for the removal of fluoride from drinking water. In: Proceedings of the 34th WEDC International Conference—Water, Sanitation and Hygiene: Sustainable Development and Multisectoral Approaches; 2009 May 18–22; Addis Ababa, Ethiopia. Loughborough (UK): WEDC. p 418–423.

Kut KMK, Sarswat A, Srivastava A, Pittman CU, Mohan D. 2016. A review of fluoride in African groundwater and local remediation methods. *Groundw Sustain Dev* 2–3:190–212.

López-Alled CM, Sanchez-Fernandez A, Edler KJ, Sedgwick AC, Bull SD, McMullin CL, Kociok-Köhn G, James TD, Wenk J, Lewis SE. 2017. Azulene–boronate esters: Colorimetric indicators for fluoride in drinking water. *Chem Commun* 53:12580–12583.

Malago J, Makoba E, Muzuka ANN. 2017. Fluoride levels in surface and groundwater in Africa: A review 2. Sources of fluoride in surface and groundwater in Africa. *Am J Water Sci Eng* 3(1):3:1–17.

Markovic M, Chow LC. 2010. An octacalcium phosphate forming cement. *J Res Natl Inst Stand Technol* 115:257–265.

Mbabaye GK, Mtalo F, Minja RJA, Legonda I. 2017. Standardizing defluoridation of community waters using bone char. *J Water Supply Res Technol—AQUA* 66:131–139.

Mosler H-J. 2012. A systematic approach to behaviour change interventions for the water and sanitation sector in developing countries: A conceptual model, a review, and a guideline. *Int J Environ Health Res* 22(5):431–449.

Msolla MM, Semoka JMR, Borggaard OK. 2005. Hard Minjingu phosphate rock: An alternative P source for maize production on acid soils in Tanzania. *Nutr Cycling Agroecosyst* 72:299–308.

Mumtaz N, Pandey G, Labhasetwar PK. 2015. Global fluoride occurrence, available technologies for fluoride removal, and electrolytic defluoridation: A review. *Crit Rev Environ Sci Technol* 45:2357–2389.

Nicholas CJ, Pearson PN, Bown PR, Dunkley T, Huber BT, Karega A, Lees JA, Mcmillan IK, Halloran AO, Singano JM et al. 2006. Stratigraphy and sedimentology of the Upper Cretaceous to Paleogene Kilwa Group, southern coastal Tanzania. *J Afr Earth Sci* 45:431–466.

Olaka LA, Wilke FDH, Olago DO, Odada EO, Mulch A, Musolff A. 2016. Groundwater fluoride enrichment in an active rift setting: Central Kenya Rift case study. *Sci Total Environ* 545–546:641–653.

Ozsvath DL. 2009. Fluoride and environmental health: A review. *Rev Environ Sci Biotechnol* 8:59–79.

Rango T, Bianchini G, Beccaluva L, Ayenew T, Colombani N. 2009. Hydrogeochemical study in the Main Ethiopian Rift: New insights to the source and enrichment mechanism of fluoride. *Environ Geol* 58:109–118.

Schrödter K, Bettermann G, Staffel T, Wahl F, Klein T, Hofmann T. 2008. Phosphoric acid and phosphates. In: Ullmann's Encyclopedia of Industrial Chemistry. Weinheim (DE): Wiley-VCH. p 715–717.

SMEC. 2010. National water quality management and pollution control strategy. Dar er Salaam (TZ): Ministry of Water and Irrigation (MoWi). p 4–66.

Sorlini S, Palazzini D, Collivignarelli C. 2011. Fluoride removal from drinking water in Senegal: Laboratory and pilot experimentation on bone char-based treatment. *J Water Sanit Hyg Dev* 1:213–223.

StataCorp. 2017. Stata statistical software: Release 15. College Station (TX): StataCorp LLC.

Stewart DF, Muhegi B. 1989. Strategies for meeting Tanzania's future cement needs. *Nat Resour Forum* 13(4):294–302.

Szilas C, Koch CB, Msolla MM, Borggaard OK. 2008. The reactivity of Tanzanian Minjingu phosphate rock can be assessed from the chemical and mineralogical composition. *Geoderma* 147:172–177.

Tanzania Bureau of Standard. 2018. Tanzanian National Enviromental Standards Comependium (NESC) drinking specifications, TZS 789:2003. Dar er Salaam (TZ): Tanzania Bureau of Standard, Government in United Republic of Tanzania. p 23–29.

Tekle-Haimanot R, Melaku Z, Kloos H, Reimann C, Fantaye W, Zerihun L, Bjorvatn K. 2006. The geographic distribution of fluoride in surface and groundwater in Ethiopia with an emphasis on the Rift Valley. *Sci Total Environ* 367:182–190.

United Nations Development Group. 2003. Indicators for monitoring the millennium development goals. New York (NY). 115 p. ISBN 92-1-161467-8. http://mdgs.un.org/unsd/mdg/Resources/Attach/Indicators/HandbookEnglish.pdf

US Institute of Medicine. 2006. Dietary reference intakes: The essential guide to nutrient requirements. Washington (DC): National Acad. 1344 p. https://www.nap.edu/catalog/11537/dietary-reference-intakes-the-essential-guide-to-nutrient-requirements

Velazquez-Jimenez LH, Vences-Alvarez E, Flores-Arciniega JL, Flores-Zuñiga H, Rangel-Mendez JR. 2015. Water defluoridation with special emphasis on adsorbents-containing metal oxides and/or hydroxides: A review. *Sep Purif Technol* 150:292–307.

Wei W, Pang S, Sun D. 2019. The pathogenesis of endemic fluorosis: Research progress in the last 5 years F^-. *J Cell Mol Med* 23:2333–2342.

[WHO] World Health Organization. 2017. Guidelines for drinking-water quality. 4th ed. Geneva (CH). p 370–373. ISBN: 978-92-4-154995-0. https://www.who.int/water_sanitation_health/publications/drinking-water-quality-guidelines-4-including-1st-addendum/en/

Wopenka B, Pasteris JD. 2005. A mineralogical perspective on the apatite in bone. *Mater Sci Eng C* 25:131–143.

Yadav KK, Gupta N, Kumar V, Khan SA, Kumar A. 2018. A review of emerging adsorbents and current demand for defluoridation of water: Bright future in water sustainability. *Environ Int* 111:80–108.

DOI: 10.1002/ieam.4262

SUPPLEMENTAL DATA

Application of octacalcium phosphate with an innovative household-scale defluoridator prototype and behavioral determinants of its adoption in rural communities of the East African Rift Valley

Table S1. Chemical synthesis reactions of (I) dicalcium phosphate dihydrate (DCPD) and (II) octacalcium phosphate (OCP). (III) Chemical transformation of OCP into fluorapatite (FAP) in presence of dissolved F^-.

Chemical reactions		
DCPD synthesis	$CaCO_3 + H_3PO_4 + 2H_2O \rightarrow CaHPO_4 \cdot 2H_2O_{\mathit{DCPD}} + CO_2 + H_2O$	(I)
OCP synthesis	$CaHPO_4 \cdot 2H_2O \leftrightarrow 0.125Ca_8(HPO_4)_2(PO_4)_4 \cdot 5H_2O_{\mathit{OCP}} + 0.25HPO_4^{2-} + 1.375H_2O + 0.5H^+$	(II)
OCP → FAP	$Ca_8(HPO_4)_2(PO_4)_4 \cdot 5H_2O_{\mathit{OCP}} + 1.6F^- \rightarrow 1.6Ca_5(PO_4)_3F_{\mathit{FAP}} + 1.2HPO_4^{2-} + 5H_2O + 0.8H^+$	(III)

Table S2. Chemical composition of the tap water used for OCP synthesis.

	pH	K^+	Na^+	Ca^{2+}	Mg^{2+}	SO_4^{2-}	HCO_3^-	F^-
		mg/L	mg/L	mg/L	mg/L	mg/L	mg/L	mg/L
Tap Water	8.03	1.5	17	23	7.4	22	96	0.15

Table S3. Example behavior factors used in the analysis, and values

Factors	Values	Example items
Risk Factors		
Risk Vulnerability	0-4	How likely or unlikely is that you will develop dental fluorosis?
Risk Severity	0-4	If I had dental fluorosis this would affect my health severely
Risk Knowledge	0-1	Boiling water before consuming it
	0-1	Filtering water before consuming it
	0-1	Brushing teeth
Attitude Factors		
Overall Attitude	-2 - 2	Drinking filtered water from this new filter will be good for my health
	-2 - 2	Drinking filtered water from this new filter will reduce my medical expenditures
	-2 - 2	Obtaining drinking filtered water from this new filter will be time consuming
	-2 - 2	Drinking filtered water from this new filter will taste better than the water that I usually drink
	-2 – 2	Drinking filtered water from this new filter will make me feel happy
Norms Descriptive	-2 - 2	If your community had the possibility of using this new filter system, most people will be consuming filtered drinking water.
Norms Injunctive	-2 - 2	If your community had the possibility of using this new filter system, most of my neighbors will think that I should consume filtered drinking water
Norms Personal	-2 - 2	If your community had the possibility of using this new filter system, I would feel a strong personal obligation to consume filtered drinking water
Ability factor	-2 - 2	I believe I will have the ability to use this new filter system regularly
Self-regulation factors		
Self-regulation Action planning	0-4	I would have a detailed daily plan on how to use this new filter system
Self-regulation Copying planning	0-4	I would have a detailed plan on what to do if this new filter system breaks
Self-regulation Perceived habit	0-4	I feel that the use of this new filter system will become an ingrained habit
Self-regulation Commitment	0-4	I would feel committed to use this new filter system every day
Self-regulation Forgetting	0-4	I would never forget to prepare drinking water from this new filter system

Figure S1. Site of defluoridation test and interview in the Uwiro village, Northern Tanzania.

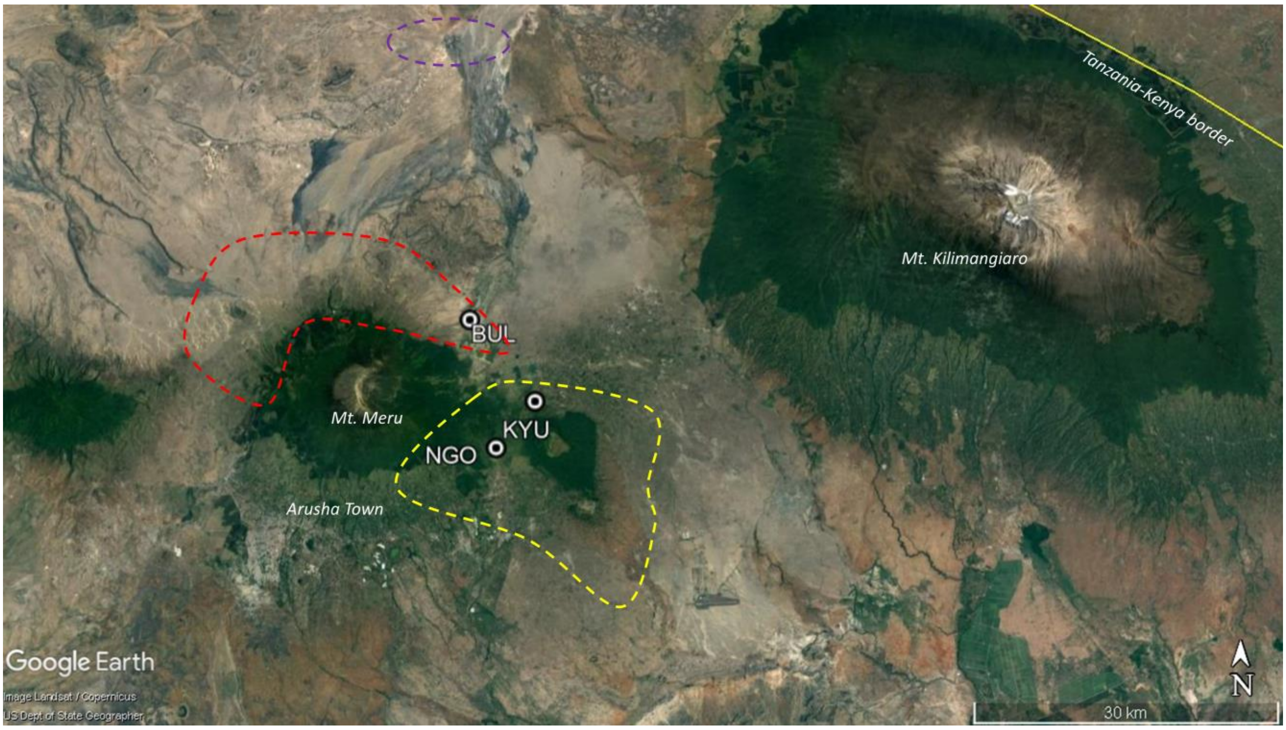

Figure S2. Location of water point source used for defluoridation test (dotted circle) and interview (purple line is around the Engutukoit village; red line is around Oldonyowas and Losinoni villages; yellow line is around Uwiro and Lemanda villages; Arusha Region, Northern Tanzania). Image © 2019 Digital Globe-Image © 2019 CNES/Airbus.

Figure S3. Configuration of the Flowered Defluoridator Device (FDD)

Flowered Defluoridator Device (FDD), how it works:

1. Add into the tank 20 L of water

2. Add 80 g of OCP

3. Switch on the pump for 2 hours to mix water and OCP

4. After 2 hours of mixing, turn on the tap to the filtration compartment to separate the exhausted OCP from water

5. Switch off the pump and open the output tap to collect the drinkable water

Figure S4. Step-by-step procedure for water treatment with the Flowered Defluoridator Device (FDD) and octacalcium phosphate powder (OCP)

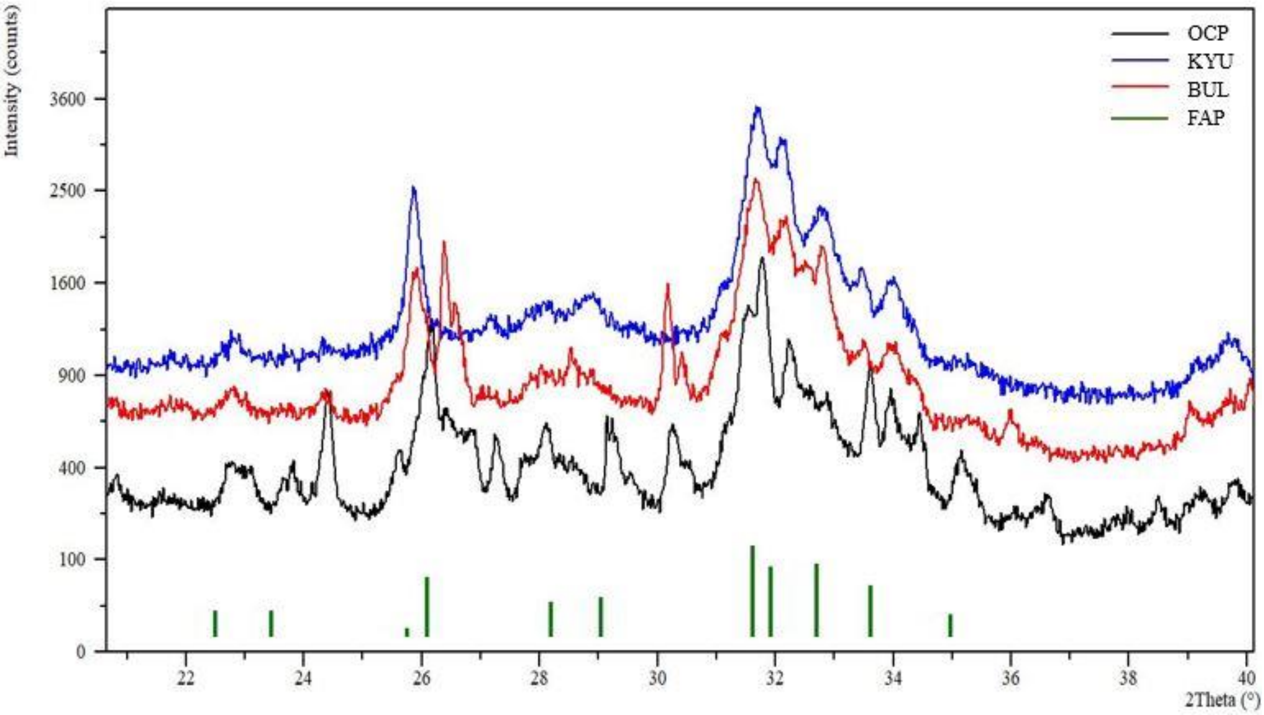

Figure S5. Difference of XRD pattern between OCP before tests (black pattern), solids collected after KYU (blue pattern) and BUL (red pattern) defluoridation tests and FAP reference ICSD pattern n. 00-015-0876 (green lines). In the pattern of KYU experiment, where 600 mg of F^- was removed from solution, the residual peak of OCP is less detectable than BUL pattern where F^- removed was 162 mg.

Conclusions

The use of octacalcium phosphate (OCP, $Ca_8(HPO_4)_2(PO_4)_4 \cdot 5H_2O$) has been tested for the removal of fluoride (F^-) from water in order to develop a simple, effective and low-cost defluoridation method suitable for rural communities affected by fluorosis in the East African Rift Valley (EARV) and in other parts of the world. The synthesis method of OCP has been successfully realized using calcium carbonate and phosphoric acid, in order to lower the production costs using non-expensive reagents and avoid any possible negative secondary effect in terms of water drinkability. The results of experiments indicate that OCP can act as an effective remover of F^- from water, obtaining experimental and calculated removal capacity of $Q_{exp} = 25.7$ mg/g and $Q_{max} = 26.8$ mg/g, respectively. The mechanism of F^- removal is represented by the transformation of OCP into fluorapatite (FAp, $Ca_5(PO_4)_3F$).

The reactivity of OCP was also tested in the presence of equal molar concentrations of F^-, Cl^-, OH^- and HCO_3^- + CO_3^{2-}. The results of the anionic competition experiments indicate that dissolved F^- is the anion mostly removed from solution in every experiment, and the F^- removal efficiency decreases by 20% when all the anions are present in solution simultaneously. Crystallographic and crystal chemistry analyses point out to FAp as the main apatitic phase that is always formed. The crystallochemical analysis of the resulting FAp indicates that OH^- is the most important competitor of F^-, especially when the OCP → FAp reaction occurs at uncommon high pH values (pH ~ 12). From experimental evidence, it can be said that OCP is a crystalline precursor of apatite and can be used to efficiently remove dissolved F^- from polluted water by forming FAp even in the presence of high concentrations of possible anionic competitors. Moreover, the release of some phosphorus to water during the transformation of OCP into FAp may be considered as an improvement of the quality of water after the treatment, because the minimum intake of phosphorus is 100 mg/day for infants, 700 mg/day for pregnant women, and 1250 mg/day for children and adults. Thus, drinking 2 L/day of water defluoridated with OCP can provide a significant percentage of phosphorus RDA (Recommended Dietary Allowance) to people living in rural areas in developing countries.

In order to scale up the use of OCP for the field experiments, a new device prototype has been designed: the FLOWERED Defluoridor Device (FDD). The FDD is a low-cost and low-tech device, designed to reproduce in the field the defluoridation laboratory process that requires mixing and stirring between the sorbent and the water. The FDD experimentation was carried out in the rural areas of northern Tanzania, at the same environmental conditions of its possible future use by rural populations, using three natural fluoride-rich waters with different F^- starting concentrations and testing different sorbent dosage. In agreement with the findings previously obtained at laboratory scale, the results of the FDD field tests show that the OCP effectively removes the F^- from natural water by means of the transformation of OCP into FAp. Based on these results, a standardized use of FDD and dosage of OCP for the defluoridation of natural water has been settled up: FDD loaded with 20 L of natural water with F^- concentration up to 21 mg/L, 80 g of OCP, and 2 h of FDD working time with constant mixing flow pump of 22 L/min. The preliminary results of the socioeconomic study are encouraging and support the proposed device as an easy activity to accomplish, as testified by the positive and significant coefficient of the ability variable in the logistic regression.

At the end of this dissertation, it is possible to say that OCP used with FDD meets the fours criteria adopted in the Introduction: (i) *Effective on F^- removal using natural groundwater; (ii) Free of collateral effects; (iii) Affordable and cost-effective; (iv) Easy to use directly by people at home.*

However, from the socioeconomic analysis it emerges that, given the poor knowledge of the risk of dental and skeletal fluorosis, the government should introduce educational programs to make the EARV rural communities aware of the negative health consequences of these diseases. Raising knowledge about the danger of consuming untreated water via educational campaigns can improve the consumption of fluoride-free water in the Rift Valley region. Increasing awareness can also reverse the sense of powerlessness observed for vulnerability in the logistic regression, making members of the EARV rural communities more aware that the use of the defluoridator device can reduce their vulnerability. Thus, the intervention of government agencies and donors seems an important aspect to be considered to mitigate the cost of defluoridation and ensure access to clean and safe water for all communities as required by Goal 6 of the UN Sustainable Development Goals.

APPENDIX I

Summary of the participation in the World Water Challenge 2018

September 13th, Daegu, Korea

World Water Challenge 2018

KOREA
INTERNATIONAL
WATERWEEK

This year, the World Water Challenge 2018 will be held as one of the signature programs of the KIWW 2018. Linking Problem Owners and Solution Providers, this 4th edition of World Water Challenge is expected to serve its role as an important platform to share the ideas and know-hows towards solving the global water challenges and to forge a broad network among experts and stakeholders in water sector, focusing on scientific and technological method that have contributed to the world's awareness on the importance of role of science and technology in solving the water challenges. The best solution out of 7 selected solutions to the 5 water challenges will be decided through the final presentation and winners will be awarded at the closing ceremony of KIWW 2018.

OBJECTIVES

- to share appropriate and innovative ideas and know-hows based on science and technology that are applicable to the real world by linking problem owners with solution providers
- to raise the world's awareness on the water issues as well as the importance of the role of science and technology in solving the water challenges
- to provide a networking opportunity among participants from the water-related corporations and organizations to create a business opportunity and make an inroad into the global market by presenting those innovative solutions

OVERVIEW

• **Date & Time**	September 13th, 2018 / 13:00 -17:30
• **Venue**	#315(3F), EXCO, Daegu, Korea
• **Participants**	Participants of final round, water-related organizations and corporations, Medias and other interested persons
• **Host/Organizer**	Ministry of Environment, Rep. of Korea / Korea Water Forum

World Water 2018 Challenge

KOREA
INTERNATIONAL
WATER WEEK

Challenge 4

Challenge

Problems Pertinent to Prevalence of Excessive Fluoride in Different Water Sources

Ms. Ruth Habte Hailemariam
Researcher and PhD Student, Korea Institute of Civil Engineering and Building Technology, Ethiopia

Solution

Low-cost and Low-tech Defluoridator Device based on Calcium Phosphate

Dr. Alfredo Idini, Ph.D.
Student, University Of Cagliari, Department of Chemical and Geological Sciences, Italy

Solution

Low-cost and Low-tech Defluoridator Device based on Calcium Phosphate

- Alfredo Idini

Natural fluoride contamination in waters is a serious issue that affects East African Rift Valley, especially the rural areas of Ethiopia, Kenya and Tanzania, resulting in a low quality of water and also in its scarcity given that many wells and springs are, up to now, too strongly contaminated to be used. Exposure to fluoride concentration > 1.5 mg/L via drinking water can cause deformities of hard tissue named skeletal and crippling fluorosis and, in the worst cases, neurological concerns. Furthermore, the scarcity of drinking water causes social-humanitarian issues, i.e. water conflict and migration flows, and prevents a normal community growth.

An effective defluoridation method should be: (i) low-cost to make even the poorest part of the population able to access to drinkable water; (ii) low-tech based, easy to use and distribute in order to reach the population regardless of where people live; (iii) highly efficient to avoid waste of water resources; (iv) free of collateral effects on water quality. Such a method has not yet been developed until now. These requirements are essential to enhance the quality of life and health of rural populations, the most susceptible to fluoride contamination. Furthermore, a decentralized distribution of cheap and simple defluoridators guarantees the population to exert a direct control on the local water resources leading to a mitigation of social problems and potential supply conflicts.

For these reasons we propose a very cheap, easy-to-produce, recyclable synthetic phase able to remove fluoride from water, and a simple, low-scale defluoridator device. The solid phase is a calcium phosphate composed of Octacalcium Phosphate (OCP), which is the precursor of apatite. The device essentially consists of a tank (in which water and the solid material are put inside) equipped with a tap on the bottom (for water recovery) and an overhead stirrer on the top that guarantees the better interaction between water and solid phase. A filter paper placed below the tap removes the solid residue after the fluoride uptake. Within the tank the OCP, in the presence of F^--rich water, transforms into fluorapatite removing fluoride from water; laboratory tests show that 1 g of Ca-phosphate can easily uptake more than 25 mg/L of fluoride in few hours. After the treatment the water is drinkable and the device can last indefinitely.

During the final round, each finalist presented his solution within its own "Challenge". At the end of each presentation, a jury of 10 international experts from the scientific, politics and industry world asked several questions and then proceeded to the final evaluation. The solution proposed by Dr. Idini, came first in its "Challenge" and second best among all the solutions presented to global problems of water management. Dr Idini's solution, awarded as "Outstanding", was chosen for being economic, efficient and based on very simple technologies, and therefore applicable in difficult environmental contexts, such as rural areas of the East African Rift Valley.

More details on:
https://kiww.org/home/2017/kiww/Files/WWCH%202018_Final%20Round_Problems%20and%20Solutions.pdf

APPENDIX II

Method of synthesis of the octacalcium phosphate molecule

Patent Application Number: 102019000009441

held by University of Cagliari

Inventors:

Alfredo Idini, Dario Fancello, Franco Frau, Elisabetta Dore, Giorgio Ghiglieri

Department of Chemical and Geological Sciences, University of Cagliari, 09042, Monserrato (CA), Italy

During the PhD project a novel route of the synthesis process of OCP has been designed. The main improvement of the new method consists to synthesises the OCP in a single step, thus avoiding the two-step passage as described in the thesis dissertation. The Patent Application has been submitted on 16/06/2019, and to guarantee its secrecy up to 18 months from the date of submission only the Patent Application Abstract can be shared in public documents.

Patent Application Abstract

The invention relates to a process for the production of octacalcium phosphate from calcium carbonate and orthophosphoric acid wherein the calcium carbonate and orthophosphoric acid are reacted in water according to a molar ratio in the range 1.25-1.41 and the mass of calcium carbonate ranges from 0.1 to20 g per litre of water. The reaction temperature ranges from 55 to 85 ° C and the reaction is carried out for a time interval between 3 and 16 hours. At the end of the reaction, the octacalcium phosphate is recovered from the aqueous suspension by filtration or settling.

La borsa di dottorato è stata cofinanziata con risorse del
Programma Operativo Nazionale Ricerca e Innovazione 2014-2020 (CCI 2014IT16M2OP005),
Fondo Sociale Europeo, Azione I.1 “Dottorati Innovativi con caratterizzazione Industriale”

UNIONE EUROPEA
Fondo Sociale Europeo

Ministero dell'Università
e della Ricerca

PON
RICERCA
E INNOVAZIONE
2014 - 2020

This research is also financially supported by the FLOWERED project
an Horizon2020 program funded by the European Commission
Grant Agreement - N. 690378

Coordinator Prof. Giorgio Ghiglieri, University of Cagliari, Italy

FLOWERED

An Horizon 2020 European Union project.